ENANTIOMERIC CHROMATOGRAPHIC SEPARATIONS AND IONIC LIQUIDS IN GAS CHROMATOGRAPHY

by

KE HUANG

Presented to the Faculty of the Graduate School of

The University of Texas at Arlington in Partial Fulfillment

of the Requirements

for the Degree of

DOCTOR OF PHILOSOPHY

THE UNIVERSITY OF TEXAS AT ARLINGTON

May 2010

This dissertation is dedicated to
My mother Ling Ma, uncle Jun Ma, and grandma Wanying Tang
who raised me, believed in me, surrounded me with love and made me the person I am

My love Xiaotong Zhang
who stood by me, supported me and inspired me in so many ways in life

ACKNOWLEDGEMENTS

My first and deepest acknowledgement must go to my major professor, Dr. Daniel Armstrong, who has been not only an erudite mentor in my research but also an inspiring teacher in so many aspects of my life. Without his guidance and persistent help this dissertation would not have been possible.

I would like to thank my committee members, Professor Richard Guan and Professor Kevin Schug. I am greatly honored to have them serve on my committee. I appreciate their precious time and research advice.

I would like to express my gratitude to the Department of Chemistry and Biochemistry for the financial aid and kind help. Also I thank the chemistry staff, especially Barbara for taking care of all my ordering and paperworks throughout the years.

Also, I would like to thank all my friends and coworkers at UTA. Special thanks to Xiaotong, Xinxin, Ye, Ping, Chunlei, and Violet, whose help and friendship have been tremendous support for me throughout my graduate studies.

Finally, I would like to express my heartful of appreciation to my mother, uncle, grandparents, and also Xiaotong for their endless support. Thank them for always standing by me and believing in me in whatever path I choose in life. Without their faith, help and generous love, I would not have been where I stand now.

April 15, 2010

ABSTRACT

ENANTIOMERIC CHROMATOGRAPHIC SEPARATIONS AND IONIC LIQUIDS IN GAS CHROMATOGRAPHY

Ke Huang, PhD

The University of Texas at Arlington, 2010

Supervising Professor: Dr. Daniel W. Armstrong

Due to the different therapeutic values of optical isomers, the production of enantiomerically pure drugs is of growing demand in pharmaceutical, biotechnology, and agrochemical industries. Today, gas chromatography (GC) and high performance liquid chromatography (HPLC) are the most prevalent analytical techniques for the enantiomeric separation of chiral molecules. Although the two techniques can have very different separation mechanisms, they are highly complementary to each other. Together, they can accomplish enantiomeric separations for large numbers of compounds of different functionalities. A great variety of chiral stationary phases (CSPs) have been developed over the years. However, since they are the heart of these enantiomeric separation processes, the development of new CSPs will continue to be of considerable academic and industrial interest.

In this dissertation, I present method development strategies, for enantiomeric and stereoisomeric separations using GC and HPLC. Also the development, characterization and application of novel ionic liquid-based GC stationary phases, and the development and evaluation of IL-based charge cyclodextrin GC-CSPs and dalbavancin-based HPLC-CSPs are discussed.

TABLE OF CONTENTS

ACKNOWLEDGEMENTS iv

ABSTRACT v

LIST OF ILLUSTRATIONS viii

LIST OF TABLES xi

Chapter Page

PART ONE ENANTIOSELECTIVE GAS AND LIQUID CHROMATOGRAPHY

1. INTRODUCTION 2

2. ENANTIOMERIC IMPURITIES IN CHIRAL SYNTHONS, CATALYSTS, AND AUXILIARIES 21

3. SEPARATION OF ENANTIOMERS AND CONTROL OF ELUTION ORDER OF *β*-LACTAMS BY USING CYCLODEXTRIN-BASED CHRIAL STATIONARY PHASES 41

4. GC/MS ANALYSIS OF CROCETANE, PHYTANE AND SOME OF THEIR STEREOISOMERS USING CYCLODEXTRIN-BASED STATIONARY PHASES 56

PART TWO IONIC LIQUIDS AS GC STATIONARY PHASES

5. OVERVIEW OF IONIC LIQUIDS IN ANALYTICAL CHEMISTRY 67

6. PEG-LINKED GEMINAL DICATIONIC IONIC LIQUIDS AS SELECTIVE, HIGH STABILITY GAS CHROMATOGRAPHIC STATIONARY PHASES 69

7. THE APPLICATION OF DICATIONIC ROOM TEMPERATURE DICATIONIC IONIC LIQUIDS IN THE GAS CHROMATOGRAPHIC ANALYSIS OF VOLATILE HERBAL ESSENCES 88

PART THREE DEVELOPMENT OF NEW CHIRAL STATIONARY PHASES FOR GAS AND LIQUID CHROMATOGRAPHY

8. IONIC CYCLODEXTRINS IN IONIC LIQUID MATRICES AS CHIRAL STATIONARY PHASES FOR GAS CHROMATOGRAPHY 102

9. EVALUATION OF DALBAVANCIN AS CHIRAL SELECTOR FOR HPLC AND COMPARISON WITH TEICOPLANIN BASED CIHRAL STATINARY PHASES 125

10. GENERAL CONCLUSIONS 150

APPENDIX

A. PUBLICATION INFORMATION 152

REFERENCES 154

BIOGRAPHICAL INFORMATION 164

LIST OF ILLUSTRATIONS

Figure Page

1.1 Scheme of Chirasil-Val 5

1.2 Structure of Chirasil-Metal 7

1.3 Structures of Chirasil-Dex™ stationary phase. 9

1.4 Scheme of forming bonded cyclodextrin through the reaction between cyclodextrin and organohydrosiloxane 10

1.5 N,N-dimethylephedrinium-bis(trifluoromethanesulfon)imidate based chiral IL GC-CSP 11

1.6 Structure of Whelk-O 1 stationary phase: 4-(3,5-dinitrobenzamido)-tetrahydrophenanthrene 12

1.7 Examples of commercial Cyclobond HPLC-CSPs. 15

1.8 Chemical Structures of macrocyclic glycopeptide molecules 17

1.9 Structure of Chiralcel OD and Chiralpak AD chiral stationary phases. 20

2.1 Examples of compounds with severe enantiomeric impurity contamination 24

2.2 GC enantiomeric separations of derivatized (A&B) and native (C&D) ethyl-4-chloro-3-hydroxybutyrate. 27

2.3 Comparison of results obtained in this study (2006) and results obtained in prior work (1998-99) 40

3.1 Summary of the total number of enantiomeric separations ($Rs \geq 0.3$) and the number of baseline separations ($Rs \geq 1.5$) achieved on different GC CSPs. 46

3.2 Examples of the best (A and B) and worst (C and D) enantiomeric separations for *β*-lactams obtained by GC CSPs 50

3.3 The influence of substituent ring size of *β*-lactams on the retention factor (k') selectivity (*α*), and resolution (Rs) of the enantioseparation. 53

4.1 Molecular structures of crocetane, phytane, and phytol 60

4.2 The best separation obtained for phytane and crocetane, and their stereoisomers 63

6.1 Structures of PEG functionalized RTILs 72

6.2 Thermal stability of PEG-functionalized dicationic RTILs 77

6.3 Separation of homologous alkane and alcohol mixture. 83

6.4 Separation of flavor and fragrance mixture 85

6.5 Separation of polar and nonpolar compound mixture. 86

7.1 Structures of PEG functionalized RTILs used 91

7.2 Separation for fennel. 94

7.3 Separation for cinnamon 95

7.4 Separation for nutmeg 96

7.5 Separation for Grob test mixture 98

8.1 Structures of ionic permethyl *β*-cyclodextrins used in this study 107

8.2 Structures of the ionic liquid matrices used for the dissolution of chiral selectors 108

8.3 Separation of *α*-ionone on: A. BIM-BPM-I plus MIM2PEG3-2NTf2
B.BIM-BPM-I plus TPP2C12-2NTf2
C. TPP-BPM-I plus MIM2PEG3-2NTf2
D. TPP-BPM-I plus TPP2C12-2NTf2. 110

8.4 Examples of separations achieved on BIM-BPM-I, BIM-BPM-TfO, and BIM-BPM-NTf2 containing columns 111

8.5 Examples of compounds showing improved separation on BIM-BPM-I column compared to on Chiraldex BPM column. 118

8.6 Comparison of compound peak shapes obtained on Chiraldex BPM column and the BIM-BPM-I column 119

8.7 Comparison of compound peak shapes obtained on neat polysiloxane column (Rtx-5) and neat MIM2PEG3-2NTf2 column 120

9.1 The structure of the macrocyclic antibiotic dalbavancin 129

9.2 The structure of the macrocyclic antibiotic teicoplanin 130

9.3 Representative chromatograms of two analytes on the T1 and D2 CSPs in the normal phase mode. 139

9.4 Representative chromatograms of two analytes on the T1 and D2 CSPs in the polar organic phase mode 147

9.5 Representative chromatograms of two analytes on the T2 and D2 CSPs in the reversed phase mode 149

LIST OF TABLES

Table Page

1.1 List of commercial GC-CSPs under the trade name Chiraldex and their maximum allowable operation temperatures (MAOTs) 8

2.1 Enantioselective methods by gas chromatography (GC)..... 25

2.2 Enantioselective methods by high performance liquid chromatography (HPLC). 25

2.3 The enantiomeric excess of the organic synthesis reagents 28

3.1 Enatiomeric separation of 19 *β*-Lactams with GC CSPs 47

3.2 Enatiomeric separation of 12 *β*-lactams with G-TA CSP under the same chromatographic conditions..... 52

4.1 Optimized separation achieved for crocetane, phytane and their stereoisomers. 62

4.2 Crocetane and phytane composition of branched/cyclic hydrocarbon fraction of Australian, North American and West African crude oils 64

6.1 Probe molecules employed in the RTILs characterizations, and their solute descriptors..... 75

6.2 Regression parameter coefficients of Series 1, Series 2 and Series 3 PEG linked RTILs 78

6.3 A comparison of the interaction parameters for analogous RTILs linked by PEG. versus hydrocarbons. 81

6.4 A comparison of the interaction parameters of PEG-linked RTILs with NTf_2 versus triflate anions 82

7.1 Temperature programs for the separation of essential oils..... 92

8.1 Performance improvement of the new IL CSP gained over its 2001 predecessor. 114

8.2 Performance comparison of neutral BPM stationary phases based on the monocationic IL (BMIM-Cl) and a dicationic IL (MIM2PEG3-2NTf2)..... 115

8.3 The separation of 56 compounds on BIM-PMBCD-I and Chiraldex BPM 122

9.1 Chromatographic data for he normal phase resolution of racemic compounds on D1, D2, T1 and T2 columns. 133

9.2 Chromatographic data for the polar organic phase resolution of racemic compounds on D1, D2, T1 and T2 columns 136

9.3 Chromatographic data for the reversed phase resolution of racemic compounds on D1, D2, T1 and T2 columns 140

PART ONE ENANTIOSELECTIVE GAS AND LIQUID CHROMATOGRAPHY

CHAPTER 1

INTRODUCTION

1.1 Overview of Enantiomeric Separations

Atoms such as carbon, sulphur, nitrogen, silicon are capable of forming four bonds, to different atoms or moieties, thus producing molecules with chirality. Such molecules have isomers known as enantiomers that are non-superimposable mirror images of each other. These isomers have identical physical and chemical properties except that they rotate plane polarized light in opposite directions. Therefore, these enantiomers have also been referred to as optical isomers.

The separation of enantiomers is of great importance in the pharmaceutical and biotechnology industries. The majority of biomolecules are chiral. Drugs of different chirality, when present in chiral environments (e.g. the human body), often have different pharmacokinetics /pharmacodyamics and thus have different therapeutic values.[2-4] The human body usually interacts differently with enantiomers. This phenomenon was first established in 1904 by Cushny when one enantiomer of hyoscyamine was discovered to possess greater anticholinergic activity than the other.[5] Another famous case is thalidomide, which was marketed as a sedative drug in the 1950s and early 1960s. In five years since the drug launch, thalidomide was reported to have caused teratogenicity and neuropathy in over 10,000 children all around the world. It was discovered later that the vicious side effects were caused by one enantiomer of the drug.

In 1992, the US Food and Drug Administration (FDA) issued guidelines regulating the marketing of new racemic drugs in a document entitled “FDA’s Policy Statement for the Development of New Stereoisomeric Drugs”.[6] Subsequently, companies were required to

conduct studies on the pharmacologic properties of both enantiomers. The marketing of racemic drug entities are also subjected to stringent toxicological criteria. As a result, the market share of single enantiomeric drug increased from 27% in 1996 to 39% in 2002. Although most of the new drugs are optically pure nowadays, a good number of racemic drugs are still available as the 1992 guidelines were exclusively for new drug candidates not existing ones.

Enantiomeric molecules are also import as pesticides in the agrochemical industry. Deltamethrin, one of the most widely applied insecticides for agricultural and home use, has three stereogenic centers (8 stereoisomers). Only one isomer was found to be active as an insecticide, while the other 7 are essentially inactive and serve only to increase the synthetic chemical and environmental loadings. In addition, chiral compounds are also widely employed in asymmetric synthesis. They constitute important reagents or substrate for the synthesis of optically pure compounds. They are also used in mechanistic studies for reaction pathways.

The most prevalent chromatographic methods for the separation of enantiomers are chiral gas chromatography (GC) and chiral high performance liquid chromatography (HPLC). GC is used for samples with low to moderate boiling points and high volatilities. It is fast, sensitive, efficient, cost effective, easy to handle, and with essentially universal detection capabilities. HPLC, on the other hand, has the advantage of greater versatility, since it can be used with thermally labile compounds, high boiling point compounds and solids. Also, a wider variety of stationary phases and mobile phases can be adopted in HPLC. Furthermore, HPLC possesses compatibility with chiroptical detection and preparative scale separations. As far as separation mechanisms are concerned, HPLC requires relatively strong analyte-stationary phase interactions, while GC in many cases needs only weak interactions for separation. The two techniques are complementary to each other and they are both widely employed for laboratory and industrial uses.

Chromatographically, enantiomeric separations can be achieved in two manners: indirect separation via the use of achiral stationary phases (which involves the derivatization of a racemate with a chiral agent to form diastereoisomers followed by cleavage and isolation), or direct separation on chiral stationary phases (CSPs). Over the years, numerous CSPs have been developed and proven to be broadly useful for the separation of enantiomers. In the following sections, an overview will be provided regarding the major types of chiral stationary phases in use for GC and HPLC.

1.2 Chiral Stationary Phases for Gas Chromatography

Gas chromatography, especially capillary gas chromatography or open tubular gas chromatography, gained popularity for its fast speed, high sensitivity and high efficiency. One unique feature of GC is that it can provide separations for compounds lacking polar functionalities. Separations of enantiomers and stereoisomers of isoprenoids, which are challenging for other chromatographic techniques, oftentimes have been reported using GC. The choice of stationary phase is the key to successful separations in gas chromatography. The historical evolution of GC stationary phase gives rise to a number of different types of GC columns. In the following sections of this chapter, the most important classes of chiral GC stationary phases will be described. They are amino acid-based CSPs, metal-ligand complexation CSPs and cyclodextrin derivative-based CSPs. Chiral ionic liquid-based CSPs are also briefly covered to indicate some new trends in GC-CSP development.

1.2.1 Amino Acid-Based Chiral Stationary Phases

In 1966, Gil-Av and coworkers demonstrated the enantiomeric separation of several N-trifluroacetyl amino acid esters on an N-trifluroacetyl (N-TFA)-L-isoleucine lauryl ester stationary phase.[7] It was the first case of successful direct chiral separation achieved by GC. It proved the feasibility of employing optically pure GC stationary phase for the separation of enantiomers. However, this stationary phase suffered from limited enantioselectivity and poor thermal stability.

The dominant interaction(s) for enantiomeric recognition on amino acid-based CSPs is hydrogen bonding interaction.

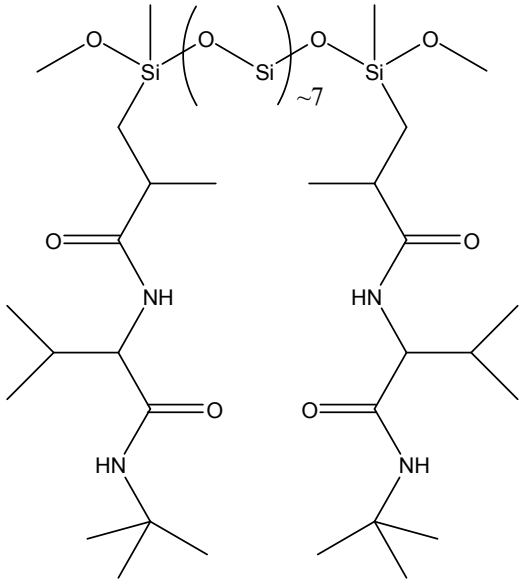

Figure 1.1 Scheme of Chirasil-Val[IM,8].

In 1977, Frank and coworkers produced a stationary phase with L-valine-tert-butylamide bonded to a polysiloxane copolymer of appropriate viscosity.[8-9] This column provided thermal stability up to 250°C and lower column bleed. Also, it was found to be especially suitable for the separation of derivatized amino acids, amino alcohols, and peptides. Due to these advantages, it became the first commercialized amino acid-based GC-CSP under the trade name Chirasil-Val[TM]. The structure of Chirasil-Val[TM] is shown in Figure 1.1. Stationary phases of both Chirasil-L-Val and Chirasil-D-Val are available from commercial sources. It is commonly observed that the Chirasil-L-Val usually retains D-amino acid derivatives longer while Chirasil-D-Val generally provides longer retention for L-amino acid derivatives.

To date, Chirasil-Val™ still constitutes an important CSP for the enantiomeric separation of chiral amino acids. However, it usually requires the pre-derivatization of the amino acids not only to afford more volatile GC amenable molecules, but also to introduce additional functionalities for hydrogen bonding association.

1.2.2 Metal-Ligand Complex Chiral Stationary Phases

After the discovery of amino acid-based CSPs by Gil-Av et al, Schurig and coworkers reported in 1971 the first successful enantiomeric separation of chiral olefin 3-methylcyclopentene on an optically active dicarbonylrhodium(I) 3-trifluoroacetyl-(1R)-camphorate stationary phase, which was the first abiotic selector-selectand system used for chiral recognition.[10] Since then, successive chiral transition metal based complexation GC stationary phases were reported by Schuig and his coworkers using manganese(II), cobalt(II) and nickel(II) bis[3-(heptafluorobutanoyl)-(1*R*)-camphorate].[11-13]

Metal-ligand CSPs, as is indicated by their name, operate on metal-ligand coordination. The enantioselectivity of this CSP results mainly from the different π-complexation energies between the stationary phase and the enantiomers. Pi and lone pair electron rich compounds, such as alkenes, alkynes, aromatics, as well as some sulfur, nitrogen and oxygen containing molecules are the major type of analytes suitable for this class of stationary phases.

Early metal-ligand complex CSPs possess narrow operating temperature ranges (25°C ~120°C). To increase the thermal stability, Chriasil-Metal™ is produced by coupling the metal-ligand complex onto the polysiloxane backbone.[14-15] The structure of Chriasil-Metal™ is shown in Figure 1.2. Nowadays, immobilization of the stationary phase on the capillary wall can also be practiced to effectively promote higher column stabilities. However, this class of stationary phases are still reported to suffer from poor efficiency (severe tailing) and insufficient enantioselectivity. Due to these drawbacks, metal-ligand complex GC-CSPs are currently of limited use for enantiomeric separation.

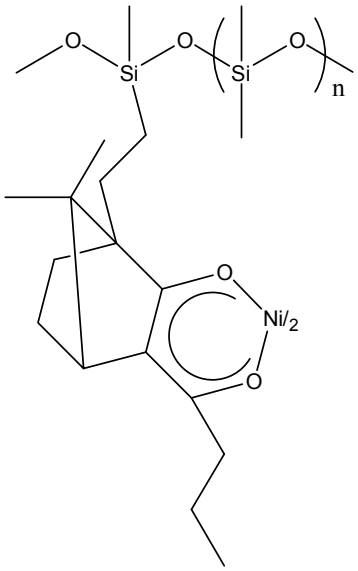

Figure 1.2 Structure of Chirasil-Metal^{TM}.[14]

1.2.3 Derivatized Cyclodextrin Chiral Stationary Phases

Cyclodextrin (CD) is a family of natural molecules produced from enzymatic treatment of starch. They are *α*-D-glucopyranoside units linked together in a ring structure by *α*-1,4 linkages. The most abundant and useful naturally occurring cyclodextrins are *α*-cyclodextrin (6-member ring), *β*-cyclodextrin (7-member ring), and *γ*-cyclodextrin (8-member ring). Cyclodextrins possess a toroidal shape with hydrophobic cavities and hydrophilic exteriors. In separation science, they have been widely used in different techniques such as HPLC, GC, SFC and CE. Native cyclodextrin based GC-CSPs was first introduced in the early 1980s.[16] Glass column was packed with celite, which was coated by native *α*- and *β*-cyclodextrin formamide solution. Separation of *α*- and *β*-pinene enantiomers was realized on this column. Few other molecules could be separated and selectivities and efficiencies on these polar cyclodextrin stationary phases were poor. After the discovery of the lowered melting points in some alkylated or acylated cyclodextrins by König et al,[17-19] different cyclodextrin derivatives were introduced as effective GC-CSPs and modified cyclodextrins gradually gained their dominant role among GC-CSPs.[20-22]

Unlike in liquid chromatography, native cyclodextrins are unlikely to be used in gas chromatography because they are poorly soluble in common matrices and their enantioselectivities are very limited. Modified cyclodextrins can be coated either as neat chiral stationary phases if they bare liquid forms at ambient temperature, or they can be dissolved in polysiloxanes to afford a coating mixture if they possess high melting points. It has been reported that the neat stationary phases usually provide broader enantioselectivities with shorter column lengths compared to the dissolved cyclodextrin phases.[23] Some commonly used commercial cyclodextrin GC-CSPs are listed in Table 1.1.[24]

Table 1.1 List of commercial GC-CSPs under the trade name Chiraldex and their maximum allowable operation temperatures (MAOTs).[24]

Name (Chiraldex)	Derivative	MAOT (°C)	
A-TA, B-TA, G-TA	2,6-di-O-pentyl-3-trifluoroacetyl	Isothermal	Programmed
B-DP, G-DP	2,3-di-O-propionyl-6-t-butyl silyl	180	180
G-PN	2,6-di-O-pentyl-3-propionyl	200	220
G-BP	2,6-di-O-pentyl-3-butyryl	200	220
B-DM, G-DM	2,3-di-O-methyl-6-t-butyl silyl	200	220
B-PM	2,3,6-tri-O-methyl	200	220
A-DA, B-DA, G-DA	2,6-di-O-pentyl-3-methoxy	200	220
B-PH	(S)-2-hydroxy propyl methyl ether	200	220

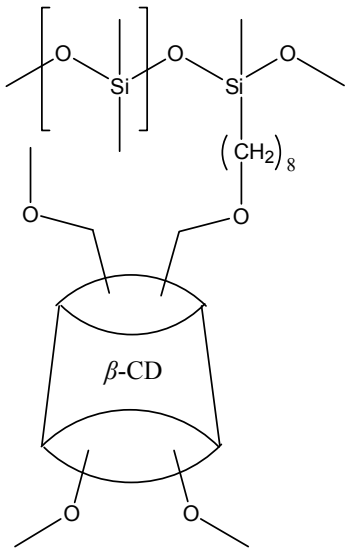

Figure 1.3 Structures of Chirasil-Dex™ stationary phase.[14]

Cyclodextrin derivatives can also be chemically bonded to support matrices, just like Chirasil-Val™. Chirasil-Dex™ is a stationary phase with permethylated cyclodextrin linked to dimethylpolysiloxane backbone via a mono-6-octamethylene spacer.[14] This version of bonded CSP has been reported to provide separations in the -20~220°C temperature range.[25] Moreover, Chirasil-Dex™ can be thermally immobilized on the inner surface of fused silica capillary column for use in chiral supercritical fluid chromatography (SFC), open-tubular electro-chromatography (OTCEC) and open-tubular liquid chromatography (OTLC). The structure of Chirasil-Dex™ is depicted in Figure 1.3.

Meanwhile, Armstrong and coworkers also introduced a method for the bonding of cyclodextrin on a polysiloxane backbone. The scheme of immobilization is shown in Figure 1.4. With the largely promoted physical resistance, this stationary phase could not be stripped off or washed away from the mobile phases or run buffers commonly used in liquid chromatography or capillary electrophoresis. This CSP was effectively used in capillary electrophoresis, capillary

gas chromatography and capillary supercritical fluid chromatography.[23] Later studies conducted by Armstrong, et al investigate the impact of different wall-immobilized cyclodextrins. It was discovered that while the wall-immobilization improved the stationary phase robustness, the column efficiency and enantioselectivity can be altered greatly. The bonded phases appeared to be more useful in resolving larger, bulkier chiral analytes with high boiling points and good hydrogen bonding groups[26]

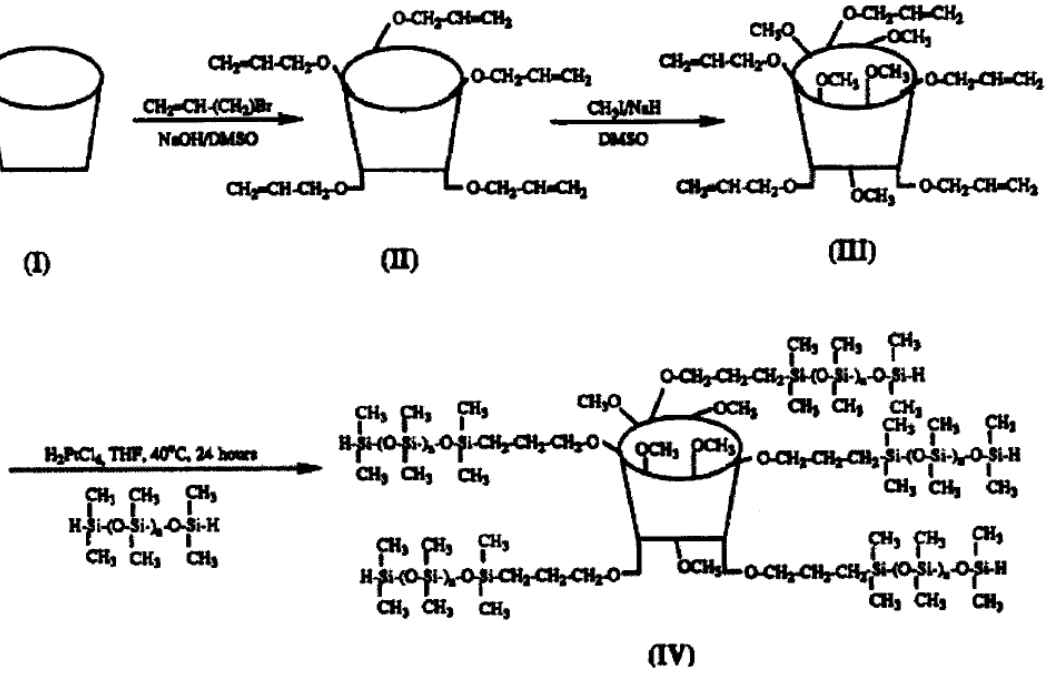

Figure 1.4 Scheme of forming bonded cyclodextrin through the reaction between cyclodextrin and organohydrosiloxane. Reprint with permission from Ref. 23

1.2.4 Chiral Ionic Liquid Chiral Stationary Phases

As mentioned previously, depending on the melting points of the chiral selectors, chiral stationary phases can be produced either by dissolving the chiral selector in a non-chiral matrix, or by directly utilizing the chiral selector as a neat stationary phase. Due to the range of favorable physicochemical properties possessed by ionic liquids, they constitute an ideal class

of GC stationary phase materials. Also due to their ease of preparation and structural engineering, it is reasonable to assume that optically pure chiral ionic liquids could make a new class of GC-CSPs. Although there have been reports on the application of chiral ILs in the enantiomeric separation in capillary electrophoresis (CE), the development of appropriate ionic liquid stationary phase for chiral GC has been extremely tricky. In 2004, N,N-dimethylephedrinium-bis(trifluoromethanesulfon)imidate-based ionic liquid CSP (see Figure 1.5) was developed by Armstrong, et al for the direct GC separation of several classes of chiral compounds: chiral alcohols, chiral sulfoxides, chiral epoxides and acetylate amines.[27] However, the stationary phase enantioselectivity and stability were still limited. The search for chiral IL GC stationary phase with high efficiencies and high enantioselectivities is ongoing.

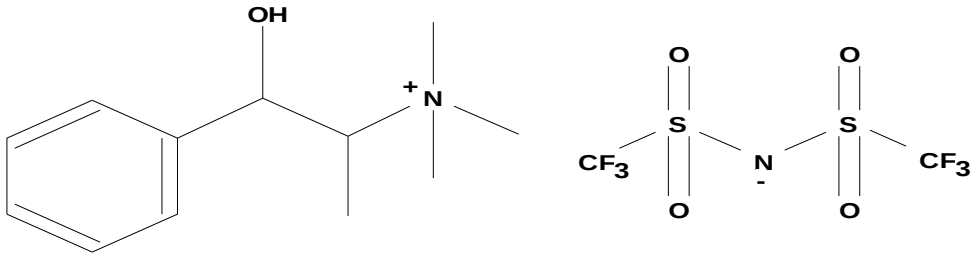

Figure 1.5 N,N-dimethylephedrinium-bis(trifluoromethanesulfon)imidate based chiral IL GC-CSP.[27]

1.2.5 Summary

Other types of chiral stationary phases have also emerged over the years, such as Chirasil-Crown and Chirasil-Calix.[28-29] However, up to date, the dominate class of GC-CSPs remain modified cyclodextrins, which account for more than 95% of all GC enantiomeric separations.

1.3 Chiral Stationary Phases for High Performance Liquid Chromatography

HPLC is an important complementary separation technique to GC. It has broader applicability in that it provides separation for thermally labile analytical samples. Also, it is easy to work on preparative scale especially when used in the normal phase mode in which the mobile phase solvents are easy to remove. In this section, a brief overview will be given on the different classes of HPLC stationary phases in use nowadays.

1.3.1 π-Complex Chiral Stationary Phases

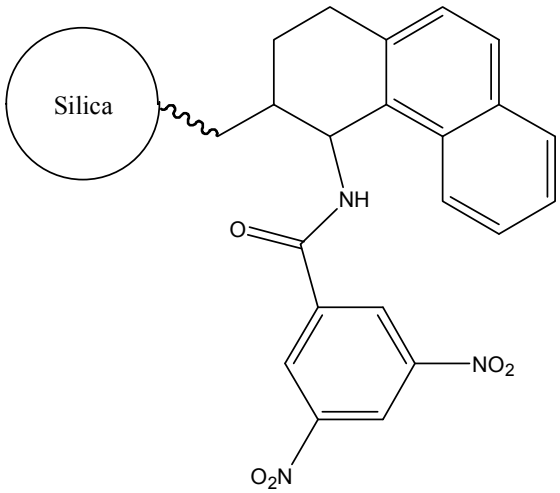

Figure 1.6 Structure of Whelk-O 1 stationary phase: 4-(3,5-dinitrobenzamido)-tetrahydrophenanthrene.[33]

Originally, π-complex chiral stationary phases were called charge transfer stationary phases. Separations on these chiral stationary phases result predominantly from π-π acceptor-

donor interactions, assisted by simultaneous dipolar interactions, hydrogen bonding, or steric repulsion interactions. They are basically normal phase stationary phases due to the more pronounced π-π interaction and hydrogen bonding interactions in nonpolar solvents. The π-acid (π-electron accepting) and π-basic (π-electron donating) HPLC stationary phases were introduced by Mikeš, et al in the 1970s, with the π-acid or π-basic moiety containing stationary phases coated on or bonded to a silica gel support.[30-32] Later on, newer versions of CSPs were developed with both π-acid and π-basic moieties, which broadened the applicability of π-complex CSPs over their earlier versions.[33]

Now, the π-complex CSPs are commercially available, such as Whelk-O 1 (see Figure 1.6). The limitation of this class of CSPs is that π-acidic compounds can only be resolved on π-basic CSPs, and π-basic compounds can only be separated on π-acidic CSPs. Otherwise, compounds will need to be derivatized so as to provide the needed "interaction groups".

1.3.2 Macrocyclic Chiral Stationary Phases

There are three important types of macrocyclic stationary phases that are popular in chiral HPLC: crown ether CSPs, cyclodextrin-based CSPs, and macrocyclic glycopeptide CSPs.

1.3.2.1 Crown Ether Chiral Stationary Phases

Chiral crown ether CSPs are a class of 18-crown-6-polyether based CSPs. They were first developed by Cram, et al in 1974 by immobilizing bis-(1,1-binaphthyl)-22-crown-6 on polystyrene or silica gel.[34] Enantiomeric separations for *α*-amino acids and their derivatives were accomplished using this CSP.[34] Subsequently, several different chiral crown ether derivatives were synthesized and employed as HPLC-CSPs. There are three subclasses of crown ether type CSPs based on their incorporated chiral functional units: binaphthyl types, tartaric acid types and sugar types. A type of binaphthyl functionalized crown ether stationary

phase has been commercialized under the trade name Crownpak-CR. Also, Crownpak-CR is available in both enantiomeric forms.

Due to the size and inclusion complexation mechanism of the 18-crown-6-polyether, this class of CSPs only forms inclusion complexes with ions the size of ammonium and potassium. For this reason, crown based-CSPs are only effective for the separation of chiral primary amines. When 18-crown-6-polyether-based CSPs are used, the mobile phase needs to be acidic to ensure ammonium ion formation from the amine analyte. Also potassium containing reagents or solvents should be avoided to preclude their competition with the analytes.

1.3.2.2 Cyclodextrin-Based Chiral Stationary Phases

As in gas chromatography, cyclodextrin also constitutes an important class of CSPs in HPLC. In fact the development of cyclodextrin HPLC stationary phases by Armstrong, et al predicted that of the GC work. Also, unlike in GC, both native and derivatized cyclodextrins can be used directly in HPLC. Figure 1.7 shows some important commercial derivatized cyclodextrin CSPs currently available on the market.[35]

Different modified cyclodextrin stationary phases excel in different operation modes, because the separation mechanisms between different modes are intrinsically distinct from each other. For example, native cyclodextrins are especially effective in reverse phase HPLC, in which inclusion complexation is the driving force in the enantiomeric separation process. All cyclodextrins can be used in the polar organic mode, in which analytes interact exclusively with the exterior hydroxyl groups or pendant functionalities due to the occupation of the cavity by the mobile phase organic solvent molecules used. For this reason, compounds elute in polar

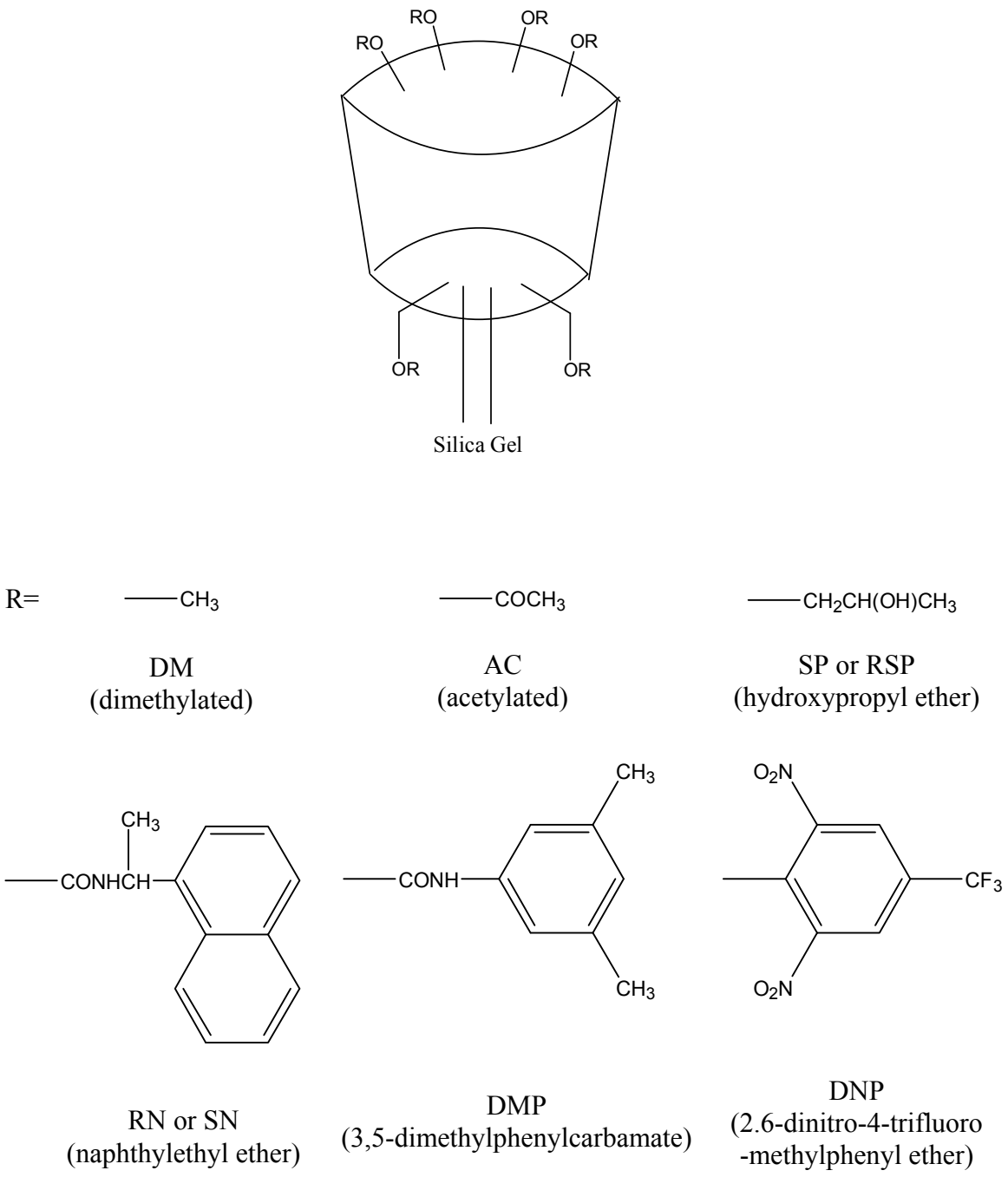

Figure 1.7 Examples of commercial Cyclobond HPLC-CSPs.[35]

organic mode usually presents shorter retention times and sharp, efficient peaks. Several cyclodextrin derivatives modified with aromatic moieties are good for normal phase separations, where π-π interactions make essential contributions to enantioselectivity.

1.3.2.3 Macrocyclic Glycopeptide Chiral Stationary Phases

Macrocyclic glycopeptide-based CSPs were first reported by Armstrong and coworkers in the mid-1990s.[36-39] So far, there are four subclasses of commercially available macrocyclic glycopeptide-based CSPs: vancomycin (Chirobiotic V and V2), teicoplanin (Chirobiotic T and T2), teicoplanin aglycone (Chirobiotic TAG), and ristocetin A (Chirobiotic R). The structures of macrocyclic glycopeptide molecules are illustrated in Figure 1.8.[40] All these macrocyclic antibiotics are produced by a fermentation process except for the TAG, which is formed by the removal of sugar groups from the teicoplanin structure.

These stationary phases contain abundant groups of various functionalities that can serve as interaction sites for chiral interactions. Therefore broad selectivity can be obtained on these chiral selectors. Also, the glycopeptide CSPs can be operated effectively in all operation modes. In other words, they are multimodal. Chiral amino acids are a class of compounds known to be best separated by this type of CSPs. They can be directly separated in their native form (without derivatization). In particular, no buffer additive is needed for the separation, which not only simplifies the separation procedures, but also facilitates preparative scale separation. According to practical experience, these CSPs possess complementary selectivity to each other. That is, when partial separation is achieved on one stationary phase, a baseline separation often can be obtained by directly switching to another structurally related Chirobiotic stationary phase using the same mobile phase conditions.[41]

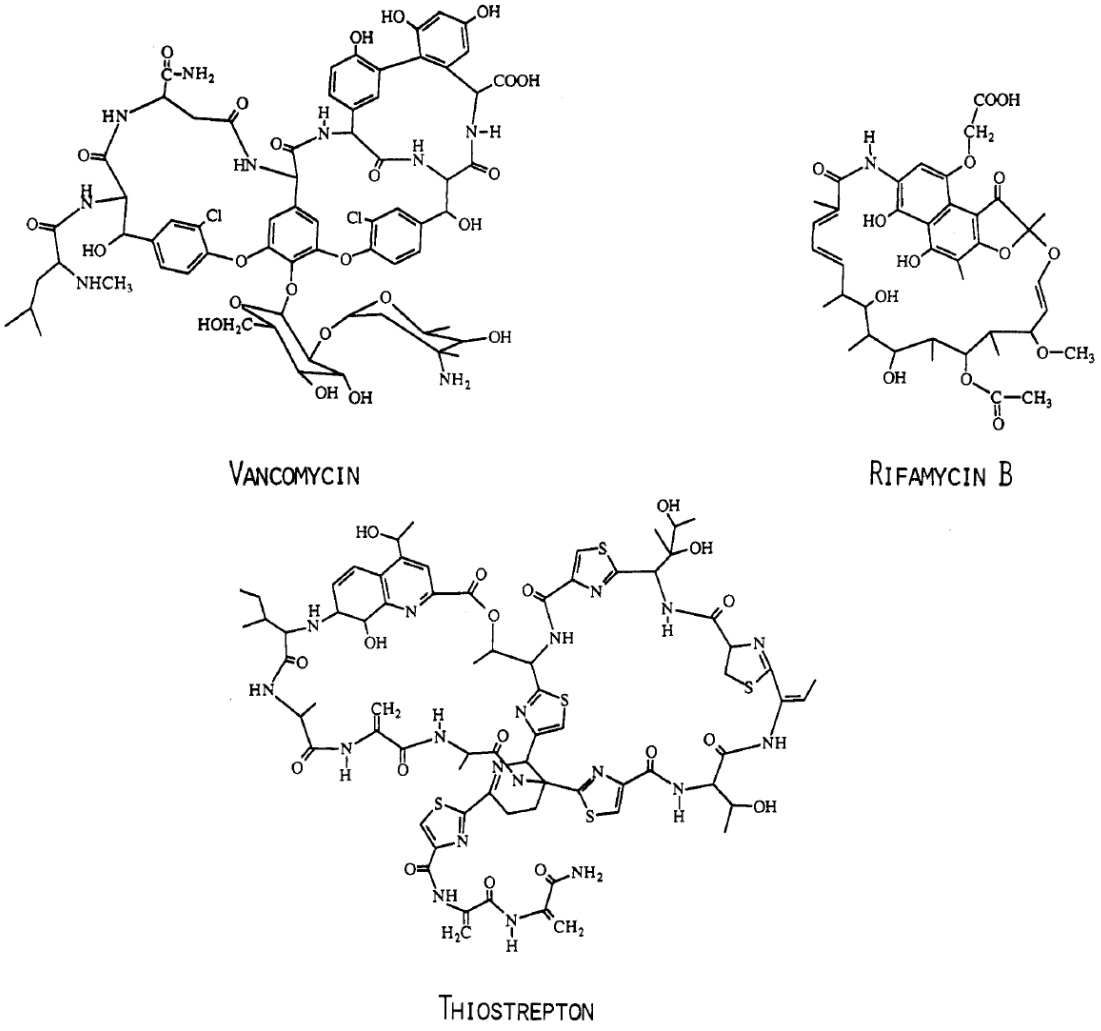

Figure 1.8 Chemical Structures of macrocyclic glycopeptide molecules. Reprint with permission from Ref.40

1.3.3 Polymeric Chiral Stationary Phases

Polymeric chiral stationary phases are based on chiral polymers that either occur naturally or are produced synthetically. They constitute a significant class of chiral stationary phases for

liquid chromatography. Since the impact of synthetic polymers in chiral HPLC is still relatively limited, only the two naturally occurring polymeric CSPs, i.e. protein-based CSPs and polysaccharide-based CSPs, will be discussed in this section.

1.3.3.1 Protein-Based Chiral Stationary Phases

Proteins, or polypeptides, are naturally occurring macromolecules composed of amino acids linked together through amide bonds in a linear structure. Protein molecules possess numerous stereogenic centers and make an effective class of chiral stationary phases for efficient resolution of many classes of racemates. Protein-based CSPs are usually produced from binding natural proteins to silica gel matrices. However, the unique structures of proteins limits this type of CSPs to reverse phase HPLC, where the secondary and tertiary structures of proteins can remain intact. Also special care needs to be taken with the mobile phase composition to prevent the denaturation of the protein molecules. The large size of proteins (40,000~70,000 Dalton) restricts the number of these chiral selectors that can be attached to the surface of the support. Also because of their size, relatively large pore size silica gel must be used. Consequently, the lowest sample capacities are found on the protein CSPs, which makes them unfavorable for large-scale separations. Due to these limitations and the advent of newer CSPs (e.g. the Chirobiotic series), the protein-based CSPs have only a minor role in enantiomeric HPLC separations today.

1.3.3.2 Polysaccharide-Based Chiral Stationary Phases

Polysaccharides are among the most common naturally occurring chiral macromolecules. Polysaccharide based HPLC-CSPs can be divided into two major categories: cellulose and amylose-based CSPs. Cellulose and amylose are formed by D-(+) glucose units linked by glycosidic bonds with β-1,4 and α-1,4 linkages, respectively. Although they were first used as LC-CSPs by German scientists in the 1970s,[42] polysaccharide CSPs only started to attract true worldwide attention after the mid-1980s when Okamoto developed a series of derivatized

cellulose and amylose stationary phases with good enantioselectivities and wide applicabilities.[43-44]

Today, cellulose and amylose are derivatized with carbamate and ester functionalities and coated on solid supports to produce HPLC stationary phases. The 3,5-dimethylphenylcarbamate derivatives have been the most effective CSPs of this class to date. They are able to separate a wide variety of compounds. They are commercialized under the trade names Chiralcel OD and Chiralpak AD (see Figure 1.9), respectively. However, since the chiral selectors are soluble in some solvents, caution should be taken when choosing mobile phases. For this reason, they are mainly used as normal phase stationary phases. This makes them highly amenable for use in preparative separations. In the meantime, some derivatives, such as Chiralcel OD-R, can also be used on a limited basis in the reverse phase mode, and Chiralcel OJ-R. Three bonded types of polysaccharide CSPs became commercially available after 2004 (Chiralpak IA, IB, IC). Although better column durability was obtained with these immobilized CSPs, the enantioselectivity of these CSPs were found to be inferior to that of their coated analogs.

1.4 Summary

In the case of chiral separation, it takes expertise and experience to choose the right path for method development. Based on the nature of the target compound, correct choice of separation technique, followed by proper selection of stationary phases and operation modes are crucial for the success of separation. The comprehensive knowledge of different chromatographic techniques should be of tremendous help in this process.

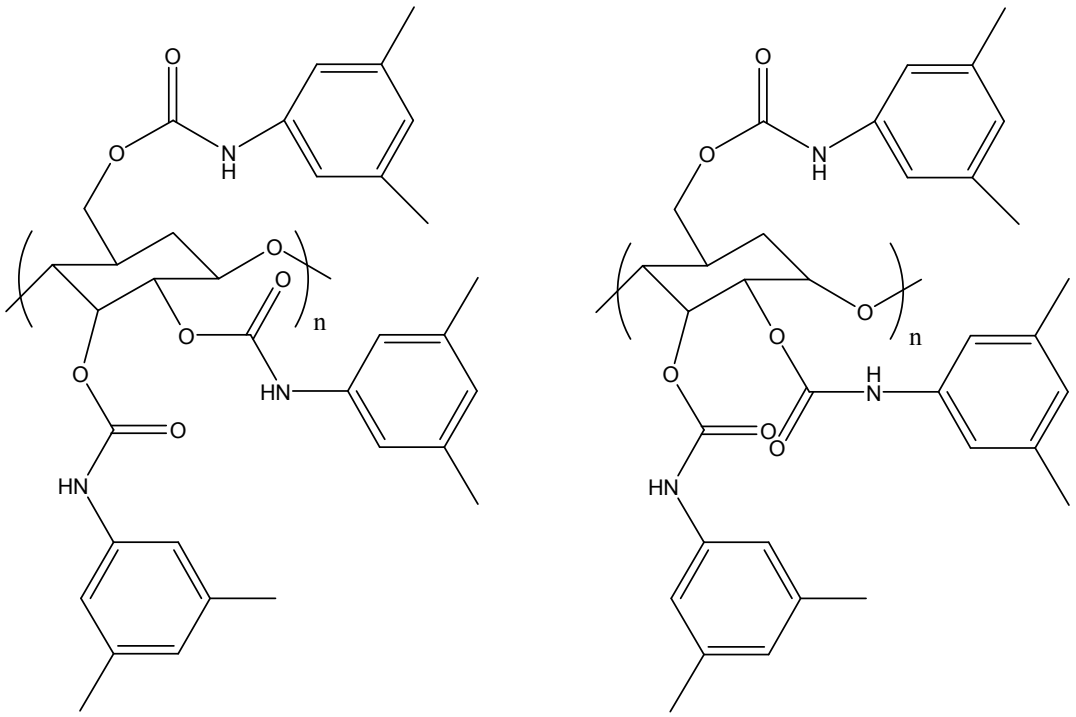

Figure 1.9 Structure of Chiralcel OD and Chiralpak AD chiral stationary phases. (a). cellulose tris(3,5-dimethylphenylcarbamate) (b) amylose tris(3,5-dimethylphenylcarbamate).

1.5 Dissertation Organization

This manuscript presents research in three areas: 1) enantiomeric and isomeric separation using GC and HPLC; 2) the development, characterization, and application of novel ionic liquids as GLC stationary phases; 3) the development and evaluation of new IL-based GC-CSPs and new macrocyclic glycopeptides-based HPLC-CSPs.

CHAPTER 2

ENANTIOMERIC IMPURITIES IN CHIRAL SYNTHONS, CATALYSTS, AND AUXILIARIES

2.1 Abstract

The enantiomeric purity of chiral reagents used in asymmetric syntheses directly affects the reaction selectivity and product purity. In this work, 84 of the more recently available chiral compounds were evaluated to determine their actual enantiomeric composition. These compounds are widely used in asymmetric syntheses as chiral synthons, catalysts, and auxiliaries. They include chiral alcohols, amines, amino alcohols, amides, carboxylic acids, epoxides, esters, ketones, and oxolanes among other classes of compounds. All enantiomeric test results were categorized within five purity levels (i.e. <0.01%, 0.01% to 0.1%, 0.1% to 1%, 1% to 10%, and >10%). The majority of the tested reagents were determined to have enantiomeric impurities over 0.01%, and two of them were found to contain enantiomeric impurities exceeding the 10% level. The most effective enantioselective analysis method was a GC approach using a Chiraldex GTA chiral stationary phase (CSP). This method worked exceedingly well with chiral amines and alcohols.

2.2 Introduction

Enantioselective reactions are of great importance to chemists involved in asymmetric synthesis. The enantiomeric purity of a product is affected by 3 factors: 1) the enantioselectivity of the reaction; 2) the optical purity of the starting material and/or the catalyst/auxiliary used; and 3) the susceptibility for the desired product to racemize, especially during work-up or storage. Previously, we found detectable amounts of enantiomeric impurities in 192 commercial chiral compounds.[45-46]

These compounds are widely employed in asymmetric syntheses as chiral catalysts/catalyst ligands, synthons/synthetic building blocks, chiral auxiliaries, and chiral

resolving agents. New chiral compounds, catalysts, auxiliaries, and synthons are continually being developed, and the most useful of them are made available commercially. In this work, we examine the new chiral compounds that have not been assayed previously and/or have been introduced after 1999, when the last comprehensive evaluation of commercial chiral compounds was reported.[46] When enantiomerically impure compounds are employed in asymmetric synthesis, especially in the pharmaceutical industry, the underestimated contaminants will introduce various amounts of optical impurities in the "single-enantiomer" reaction and products. In biological processes, these undesired enantiomeric byproducts usually show different effects and/or different pharmacokinetics/pharmacodynamics and thus have different therapeutic values.[47] Although the stereoselectivity of asymmetric synthetic processes continue to improve, an awareness of the enantiomeric composition of chiral reagents being used remains essential.

2.3 Experimental

2.3.1 Materials

All HPLC columns (25 cm x 4.6 mm i. d.) and GC columns (10 m x 0.25 mm, 20 m x 0.25 mm, 30 m x 0.25 mm) were obtained from Advanced Separation Technologies, Inc. (Whippany, NJ). The LC columns used were Cyclobond I 2000 AC (acetylated-β-cyclodextrin), Cyclobond I 2000 DM (dimethylated-β-cyclodextrin), Chirobiotic T_2 (teicoplanin), and Poly-DPEDA (poly N,N'-[(1R, 2R)-1,2-diphenyl-1,2-ethanediyl] bis-2-propenamide).[48] GC analysis was performed using Chiraldex B-DM (di-O-methyl-β-cyclodextrin), Chiraldex G-PN (2, 6-di-O-pentyl-3-propionyl-γ-cyclodextrin), Chiraldex G-BP (2, 6-di-O-pentyl- 3-butyryl-γ-cyclodextrin), Chiraldex G-TA (2, 6-di-O-pentyl-3-trifluoroacetyl-γ-cyclodextrin) columns and Chiraldex B-TA(2, 6-di-O-pentyl-3-trifluoroacetyl- β -cyclodextrin).

Trifluoroacetic anhydride (99+ %) was from Aldrich (Milwaukee, WI). Trifluoroacetic acid was obtained from Fisher Scientific (St Louis, MO). The water used was deionized and purified with a Synery 185, Millipore filter. All the mobile phases were degassed with a VWR Model

250HT sonicator before HPLC analyses. All the chiral compounds examined in this paper were obtained from Aldrich.

2.3.2 Apparatus and methods

All HPLC separations were performed on the following Shimadzu (Columbia, MD) instrumentation: two LC-6A pumps; a SPD-6A UV spectrophotometric detector; a SCL-10A system controller; and a CR 601 Chromatopac integrator. All compounds were dissolved in acetonitrile and the wavelength of detection was 254 nm. Most of the compounds were tested with the flow rate of 1 ml/min at ambient temperature (25ºC). Lower flow rate was used for 2-(Anilinomethyl) pyrrolidine, 6-hydroxy-2, 5, 7, 8- tetramethyl-chroman-2-carboxylic acid and 1-(2-methoxybenzoyl)-2-pyrrolidinemethanol to increase peak efficiency through decreasing the band broadening effect of mass transfer of analyte. Also, 2-(Anilinomethyl) pyrrolidine was chromatographed at 0ºC on order to optimize the selectivity of separation.

The GC equipment used was Shimadzu (Columbia, MD) model GC-17A gas chromatograph equipped with a flame ionization detector and EZStart 7.2.1 SP1 data acquisition software. All analyses were performed with a helium carrier gas flow rate of 1 ml/min and a split ratio of 100/1. The injector and detector temperature was set at 250ºC and 280ºC, respectively. In all GC analyses, chiral compounds with amino and/or hydroxyl groups were derivatized with excess trifluoroacetic anhydride, an achiral reagent that does not induce any change of analyte configuration.[49]

Typical enantiomeric separations on HPLC and GC are shown in Figure 2.1. All the results were calculated from at least 3 parallel measurements of sample with different concentrations. Each pair of enantiomers were separated with resolution greater than 1.5, so that when an excessive amount of a single enantiomer was injected, its broadening baseline width would not cause a co-elution of the single enantiomer being tested and the enantiomeric impurity.

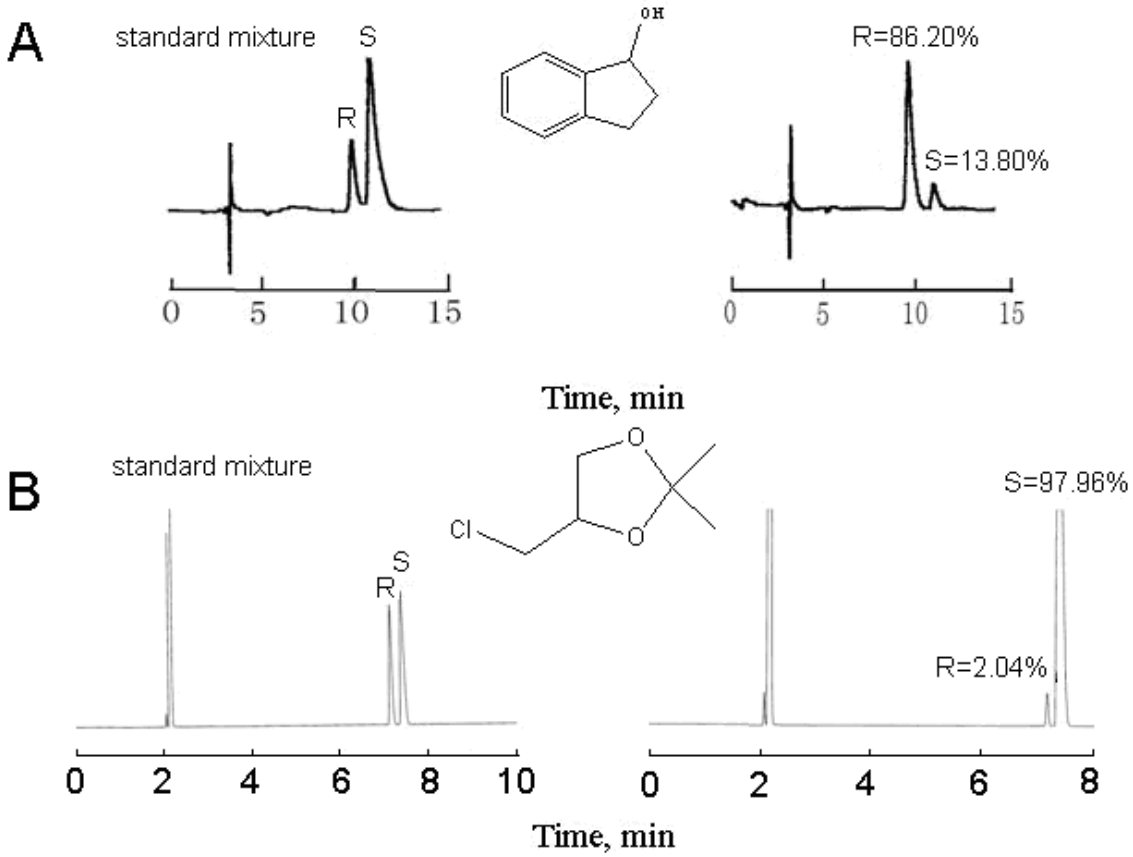

Figure 2.1 Examples of compounds with severe enantiomeric impurity contamination. Chromatograms A show the enantiomeric separation of 1-indanol on HPLC and the impurity tested in the R enantiomer purchased from Aldrich. Chromatograms B show the enantiomeric separation of 4-(chloromethyl)-2, 2-dimethyl-1, 3-dioxolane on GC and the assay of the S enantiomer obtained from Aldrich. The separation methods for A and B are listed in Table 3 as LC-7 and GC-11, respectively.

2.4 Results and Discussion

Of the 84 chiral compounds tested, 85 % of them were separated via enantioselective GC, and of these, 54 % were best separated on the Chiraldex GTA column. This is due to the fact that many of the compounds in this study were chiral amines and alcohols, which when trifluoroacetylated, gained distinct enantioselective interactions with the trifluoroacetylated chiral stationary phase of the GTA column.[22] Also, the GTA chiral stationary phase showed impressive separating capabilities for ketones, epoxides, and halogenated acids. Examples of

these include the separations of 3-methylcyclopentanone, epoxybutane, and chloropropionic acid, respectively.

Table 2.1 Enantioselective methods by gas chromatography (GC).

GC method number[a]	Column[b]	Length (m)	Temperature (°C)	Flow rate (ml/min)
GC-1	Chiraldex G-PN	20	110	1
GC-2	Chiraldex G-TA	30	110	1
GC-3	Chiraldex G-PN	20	100	1
GC-4	Chiraldex G-TA	30	115	1
GC-5	Chiraldex G-TA	30	100	1
GC-6	Chiraldex G-TA	30	130	1
GC-7	Chiraldex B-DM	20	130	1
GC-8	Chiraldex G-TA	30	95	1
GC-9	Chiraldex B-DM	20	150	1
GC-10	Chiraldex G-BP	20	135	1
GC-11	Chiraldex B-DM	20	90	1
GC-12	Chiraldex B-DM	20	140	1
GC-13	Chiraldex G-TA	30	60	1
GC-14	Chiraldex G-TA	30	140	1
GC-15	Chiraldex G-TA	30	120	1
GC-16	Chiraldex G-TA	30	65	1
GC-17	Chiraldex G-TA	30	50	1
GC-18	Chiraldex G-TA	30	160	1
GC-19	Chiraldex B-DM	20	80	1
GC-20	Chiraldex G-TA	30	150	1
GC-21	Chiraldex B-TA	20	100	1
GC-22	Chiraldex G-BP	20	140	1
GC-23	Chiraldex G-TA	30	35	1
GC-24	Chiraldex B-DM	20	125	1
GC-25	Chiraldex G-TA	30	80	1

[a] is used to identify the Seperation techniques in Table 2.3. Every analyte with amino or hydroxyl functional groups was derivatized with trifluoroacetic anhydride to help with the selectivity of separation and the volatility of analytes (see experimental section).
[b] is the abbreviation for the GC columns used. All the full names can be looked up in the experimental section.

Table 2.2 Enantioselective methods by high performance liquid chromatography (HPLC).

HPLC method number[a]	Column[b]	Mobile phase[c] (%, v/v)	Flow rate (ml/min)
LC-1	Chirobiotic T_2	H_2O:TEAA = 100:0.1, pH 4.1	0.25
LC-2	Chirobiotic T_2	ACN:HOAc:TEA = 100:0.15:0.15	1
LC-3	Poly-DPEDA	Heptane:IPA:TFA = 95:5:0.1	0.25
LC-4	Cyclobond I 2000 AC	H_2O:TEAA = 100:0.1, pH 4.1	1
LC-5	Cyclobond I 2000 AC	H_2O:TEAA = 100:0.1, pH 4.1	1
LC-6	Cyclobond I 2000 AC	H_2O:TEAA = 100:0.3, pH 4.1 (0 °C)	0.25
LC-7	Cyclobond I 2000 DM	H_2O:TEAA:CH_3OH = 97:0.1:3, pH = 7.1	1

[a] is notation is used to identify the Seperation techniques in Table 2.3.
[b] is the abbreviation for the HPLC columns used. All the full names can be looked up in the experimental section.
[c] Mobile phase: ACN=acetonenitrile; TEAA=triethylamine acetate; HOAc=acetic acid

Other effects of trifluoroacetylation of free alcohols and amines include altered enantioselectivity, increased analyte volatility, faster analysis time, improved peak shape, and increased efficiency. Figure 1 illustrates some of these properties in the GC enantiomeric separations of derivitized (Figure 2.2 A&B) and native (Figure 2.2 C&D) ethyl-4-chloro-3-hydroxybutyrate. Peaks A and D represent the (S)-(-) enantiomer and peaks B and C represent the (R)-(+) enantiomer. Both enantiomeric separations have comparable baseline separations with resolutions greater than two. However, a comparison of the separation of the native analyte versus its trifluoroacetyl derivative (Figure 2.2) shows that the analysis time for the derivative is shorter and the peaks are sharper (which makes the detection and quantitation of enantiomeric impurities much easier). Also, the reversal of elution order of the two enantiomers prior to and after derivatization indicates that the introduction of the trifluoroacetyl group alters the separation mechanism. It has also been reported that acetic anhydride, chloroacetic anhydride, dichloroacetic anhydride, and trichloroacetic anhydride may be used for this same purpose.[20]

Table 2.3 lists all chiral compounds examined in this study, as well as, references describing their use in asymmetric syntheses. The separation conditions for each compound assayed are listed in Table 2.1 and Table 2.2. Also, Table 3 indicates the actual enantiomeric composition of each compound and the technique used to determine this composition. As shown in Figure 2.2, 82% of the compounds analyzed were found to contain enantiomeric impurities over 0.01%. Only 8% of the compounds contained enantiomeric impurities between 0.01%-0.1%, whereas, 46% of the samples had enantiomeric impurities in the level 0.1%-1%, and 25% of the samples displayed enantiomeric impurities in the range of 1%-10%. Two compounds were found with enantiomeric contaminants over 10%.

Figure 2.3 also shows a direct comparison of the level of enantiomeric contaminants found in the chiral compounds assayed in this study with those that were tested in 1998-99. In both studies, 2% of the chiral compounds tested contained enantiomeric impurities greater than 10%. However, the greatest enantiomeric impurity for any chiral compound was found in the 1998

analysis of (R)-tert-butyl-4-formyl-2, 2-dimethyl-3-oxazolidine, which was determined to contain 15.11% of the S enantiomer. This is just slightly higher than the 13.80% maximum enantiomeric impurity found in (R)-1-indanol during this study. Figure 2.2 also shows that within the enantiomeric impurity ranges of 1-10% and 0.1-1%, the results of the two studies are fairly comparable with the abundances in this study being just slightly higher. The major difference in reagent purity in the studies is in the 0.01-1% and <0.01% ranges. The number of very high enantiomeric excess compounds found in this study approached 20%, whereas few, if any, chiral compounds of these purities were available prior to 1998-99. However, there were a higher percentage of compounds in the 0.01-1% range in previous studies.

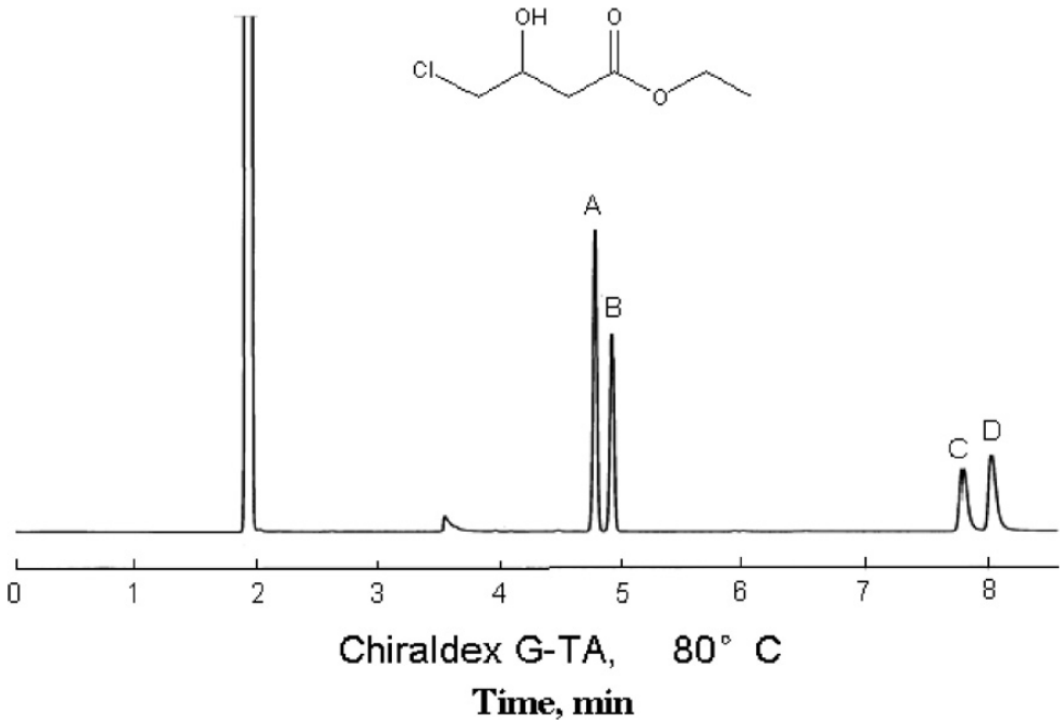

Figure 2.2 GC enantiomeric separations of derivatized (A&B) and native (C&D) ethyl-4-chloro-3-hydroxybutyrate. Peaks A and D represent the (S)-(-) enantiomer and peaks B and C represent the (R)-(+) enantiomer. Helium carrier gas, G-TA column, 120°C, FID.

Table 2.3 The enantiomeric excess of the organic synthesis reagents.

Use in Asymmetric Synthesis and References	Name and Structure of Chiral Compound	Enantiomeric Composition		Method Number[b]
		%enantiomeric contaminant	enantiomeric excess (e. e.)[a]	
Synthons or Chiral building blocks				
1) Development and synthesis of 2-*o*-methylcytidine[50] 2) Synthesis of amide analogs of the cannabinoid CB1 receptor antagonist[51]	2-Aminoheptane 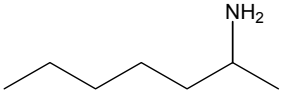	S=0.09	*99.83 (R)	GC-1
		R=0.35	99.31 (S)	
1) Synthesis of hydroxy perylenediimides[52] 2) Preparation of 4, 5-dialkylsubstutited 2-amino-3-thiazolidine derivatives as nitric oxide synthase inhibitors[53-54]	2-Amino-1-hexanol 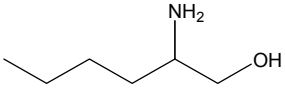	S=0.07	*99.87 (R)	GC-2
		R=0.09	99.82 (S)	
1) Enantioselective acylation[55] 2) Synthesis of a new class of nitric oxide synthase inhibitor, 4, 5 disubstituted-1,3-oxazolidin-2-imine derivatives[56]	2-Amino-1-pentanol 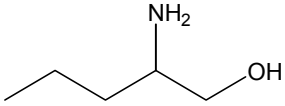	S<0.01	*>99.99 (R)	GC-3
		R<0.01	>99.99 (S)	
1) Synthesis of crystalline chellates[57] 2) Preparation of imidazo[1,2-b]pyridazines under Swern oxidative conditions[58]	2-Amino-1-phenyl-1, 3-propanediol 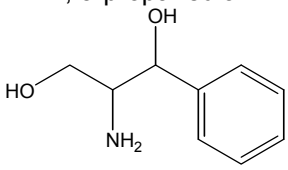	(S, S)=0.52	*98.97 (R, R)	GC-4
		(R, R)=0.06	>99.89 (S, S)	

Table 2.3 *Continued*

1) Stucture –activity relationship study of 1H-imidazo [4,5-c]quinolines that induce interferon production[59] 2) Preparation of 2'-aldehyde oligonucleotides for chemoselective ligation study[60]	3-Amino-1, 2-propanediol 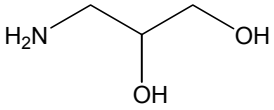	S=0.28 R=0.93	99.44 (R) *98.14 (S)	GC-5
Synthesis of antitumor agent[61-62]	3-Aminopyrrolidine 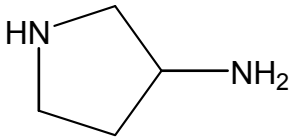	S=0.66 R=0.17	98.67 (R) *99.67 (S)	GC-5
Potential human dopamine D4 antagonists synthesis[63]	1-Benzyl-3-aminopyrrolidine 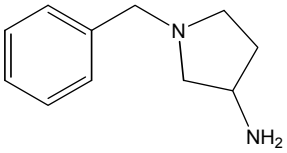	S=0.17 R<0.01	*99.67 (R) >99.99 (S)	GC-6
1) Preparation of Evans Auxiliary[64-65] 2) Chemoenzymatic synthesis of the polyketide macrolactone 10-deoxymethynolide[66] 3) Asymmetric total synthesis of (+)-migrastatin, a potent cell migration inhibitor[67]	4-Benzyl-3-propionyl-2-oxazolidinone 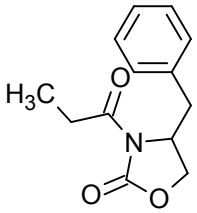	S=0.37 R<0.01	99.26 (R) *>99.99 (S)	GC-7
Ring-closing metathesis to cyclic sulfamide peptidomimetics[68]	*Bis* (α-methylbenzyl)sulfamide 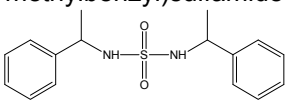	S=6.49 R=3.29	* 87.03 (R, R) 93.43 (S, S)	GC-8

Table 2.3 *Continued*

1) Starting material of chiral diamine-chelated aryllithiums[69] 2) Synthesis of a novel arylpiperazine as potent and selective agonist of the melanocortin subtype-4- receptor[70] 3) Fast microwave promoted palladium-catalyzed synthesis of Phthalides[71]	2-Bromo-α-methylbenzyl-alcohol 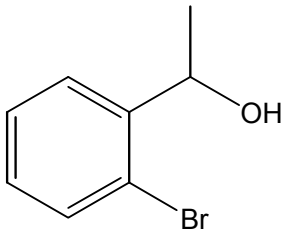	S=0.36 R=0.14	*99.29 (R) 99.73 (S)	GC-9
1) Synthesis of 2, 3-diminopyridine bradykinin B1 receptor antagonists[72] 2) Preparation of substituted N-(arylmethyl)aryloxy arylcarboxamide antagonists for the PGE2 receptor EP4	1-(4-Bromophenyl)ethylamine 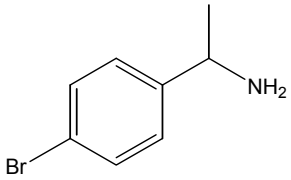	S=0.24 R=0.42	*99.53 (R) 99.16 (S)	GC-10
1) Total synthesis of 17,18,19,20-d4-iPF2a-III 32, for animal metabolism studies[73] 2) Synthesis of kinsenoside and goodyeroside A[74] 3) Control of regioselectivity of the pivalaldehyde acetalization[75]	1,2,4-Butanetriol 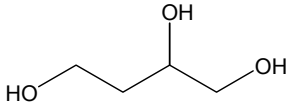	S=0.84 R<0.01	*98.33 (R) >99.99 (S)	GC-5
Synthesis of 1,2-dihdroxyimino-3,7-di-aza-9,10-O-iso-propylidene decane, a vic-dioxime derivative for its metal complex study[76]	4-(Chloromethyl)-2,2-dimethyl-1,3-dioxolane 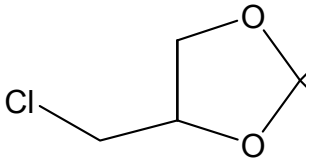	S=0.12 R=0.28	99.76 (R) *99.45 (S)	GC-11

Table 2.3 *Continued*

1) Used as substrates in transesterification of vinyl esters[77] 2) Lanthanide (III) triflate-catalyzed thermal and microwave-assisted synthesis of benzyl ethers[78] 3) Synthesis of 3-phenoxypropyl piperidine analogues as ORL1 receptor agonists[79] 4) Preparation of fluoxetine analogues, a novel class of anti-candida agents[80]	3-Chloro-1-phenyl-1-propanol 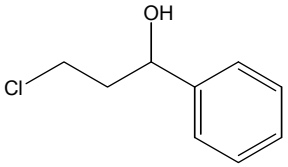 	S=0.39 R=0.24	*99.22 (R) 99.53 (S)	GC-12
1) Synthesis and structure-activity relationship study of ethacrynic acid analogues on glutathione-s-tranferase P1-1 inhibition[81] 2) Synthesis of a peroxime proliferator activated receptor (PPAR) α/γ agonist[82]	Chloropropionic acid 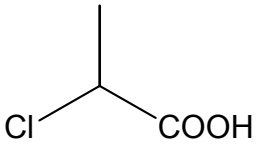 	S=2.79 R=0.38	*94.42 (R) 99.25 (S)	GC-5
1) Synthesis of C_1–C_{11} fragment of bafilomycin A1[83] 2) Used in DMF promoted xylosylation of terpenols[84] 3) Total synthesis of brasoside and littoralisone[85] 4)Synthesis of marine sponge alkaloid hachijodine B[86] 5) Stereoselective synthesis of Fusarium toxin equisetin, a	β-Citronellol 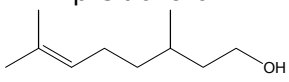 	S=1.38 R=0.29	*99.42 (R) 97.25 (S)	GC-13

Table 2.3 *Continued*

1) Study of a new method to oxidize primary alcohols to carboxylic acids[88] 2) Study of the influence of the nature of chiral auxiliaries on the diastereoselective hydrogenation of o-methoxy benzoic acid[89] 3) Used in the study of reductive alkylation of aromatic carboxylic acid derivatives[90]	1-(2-Methoxybenzoyl)-2-pyrrolidinemethanol 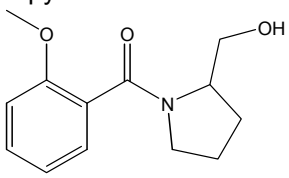	S<0.01	>99.99 (R)	LC-1
		R<0.01	>*99.99 (S)	
1) Preparation of chiral crown ethers[91-93] 2) Starting material for the synthesis of (3R, 4S)-3,4-dihydroxy-5-oxohexylphosphonic acid[94] 3) Synthesis through Mitsunobu reacion of chiral diesters and chiral diamines as macrocylic frameworks[95]	2,3-O-Benzylidene-D-threitol 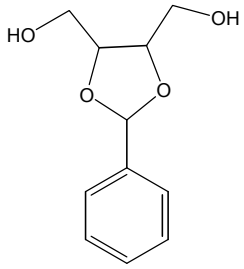	(-)=0.20	*99.60 (+)	GC-14
		(+)=7.42	85.16 (-)	
Synthesis of lower alkyl 4-cyano-3-hydroxybutyrates	Ethyl-4-bromo-3-hydroxybutyrate 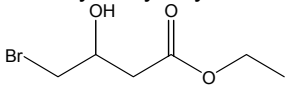	S=0.37	99.26 (R)	GC-15
		R=0.36	*99.29 (S)	

Table 2.3 *Continued*

1) Substrate for enzymatic ammonolysis[96] 2) Synthesis of 4-cyano-3-hydroxybutyric acid esters 3) Preparation of epoxybutanoic acid esters	Ethyl-4-chloro-3-hydroxybutyrate 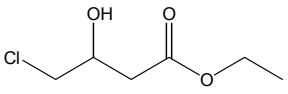 	S=0.49 R=0.04	*99.02 (R) 99.93 (S)	GC-15
1) Alkanol absolute configuration study with cyclopenta[b]furan derivative[97] 2）Ruthenium-catalyzed quinoline synthesis through 2-aminobenzyl alcohol cyclization with secondary alcohols[98] 3) Parallel carbonylation of aryl halides[99] 4) Palladium-catalyzed heteroannulation of bromobenzylaldehyde[100] 5) Enzymatic synthesis of aroma compound xylosides via transfer reaction[101]	2-Heptanol 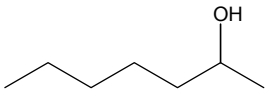 	S=0.12 R=1.32	*99.77 (R) 97.36 (S)	GC-16

Table 2.3 *Continued*

Synthesis of analogs of antitumor agents for action mechanism study of XK469 and SH80[102-103]	2-(4-Hydroxyphenoxy) propionic acid 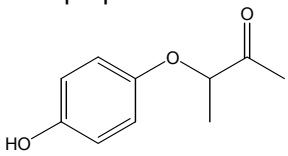	S<0.01	>99.99 (R)[c]	LC-2
1) Starting material for the synthesis of a new class of antiatherosclerosis agents, the NO-donor antioxidants[104] 2) Buiding block for novel potent inhibitors of lipid peroxidation with protective effects against reperfusion arrhythmias[105] 3) Synthesis of CX-659S and its related compounds for the study of their effects on hypersensitivity reaction[106] 4) Vitamin E precursor[107]	6-Hydroxy-2,5,7,8-tetramethyl-chroman-2-carboxylic acid 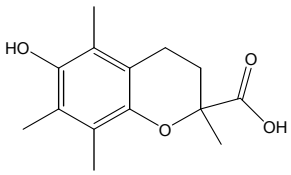	S<0.01	>99.99 (R)	LC-3
		R<0.01	>*99.99 (S)	
1) Substrate for optically pure 4 or 5 substituted lactones[108] 2) Study of oxidation of cyclic ketones by CH_3ReO_3/H_2O_2 catalytic system in room temperature ionic liquids through Baeyer–Villiger reaction[109] 3) Synthesis of 3,4-bridged 1, 6, 6aλ4-trithiapentalenes[110]	3-Methylcyclopentanone 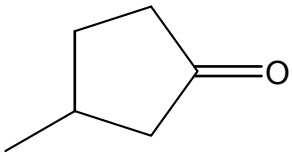	S=0.10	99.80 (R)[c]	GC-17

Table 2.3 *Continued*

1) Synthesis of the 5-HT_3 receptor probe[111] 2) Fullerene substitution with piperazine[112] 3) Preparation of 1, 4-benzothiazine analogues, thymocyte apoptosis and thymus inducers[113]	2-Methylpiperazine 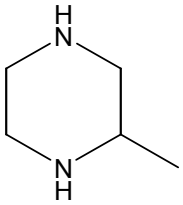	S=0.13 R=0.15	*99.75 (R) 99.71 (S)	GC-6
Synthesis of 10-azaprostaglandin E_1[114]	5-Oxo-3-pyrrolidinecarboxylic acid ethyl ester 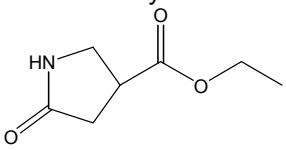	S<0.01 R=0.62	*>99.99 (R) 98.76 (S)	GC-18
Efficient Synthesis of Cyclopentenones from Enynyl Acetates[115]	1-Octyn-3-ol 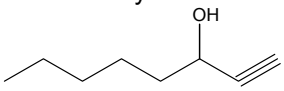	S=0.20 R=0.17	*99.61 (R) 99.77 (S)	GC-19
1) Preparation of prochiral phosphinic acid derivatives for the synthesis of P-Stereogenic phosphinates[116] 2) Synthesis of methyl ketone as substrate for samarium (II)-promoted aromatic ring spirocyclization[117]	4-Penten-2-ol 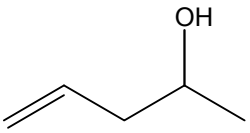	S=1.11 R=0.39	*97.79 (R) 99.22 (S)	GC-13

Table 2.3 *Continued*

1) Starting material for the synthesis of 1-arylmethyl-3-(1-methyl-2-amino)ethyl-5-aryl-6-methyluracils, a new class of small molecule GnRH antagonists[118] 2) Preperation of tri- and tetra-substituted ureas as a novel class of steroid mimics[119]	3-Pyrrolidinol 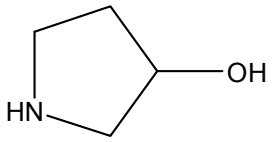 	S=0.04 R=0.54	99.92 (R) *98.92 (S)	GC-20
Used in the study of enantioselective palladium(II)-catalyzed aerobic Alcohol oxidations with (-)-sparteine[120-121]	α-(Trifluoromethyl) benzyl alcohol 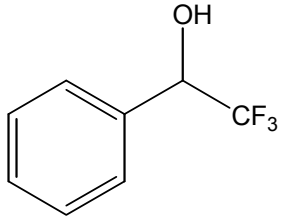 	S=1.06 R=1.32	97.88 (R) *97.36 (S)	GC-2
Important synthetic component of ferroelectric liquid crystals[122]	1,1,1-Trifluorooctan-2-ol 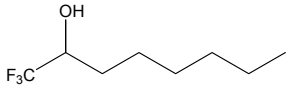 	S=0.90 R=0.56	98.20 (R) *98.88 (S)	GC-21
Catalyst/catalyst ligands				
Solid support catalysis for hydrosilylation of ketones[123]	2-Amino-1, 2-diphenylethanol 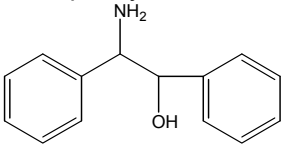 	1S, 2R<0.01 1R, 2S<0.01	*>99.99 (1R2S) 99.60 (1S, 2R)	GC-22

Table 2.3 *Continued*

Solid support catalysis for hydrosilylation of ketones[123]	2-Amino-3-methyl-1-butanol 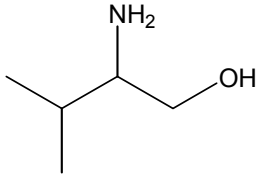	S=0.23 R=0.74	*99.54 (R) 98.52 (S)	GC-3
Solid support catalysis for hydrosilylation of ketones[123]	2-Amino-1-phenylethanol 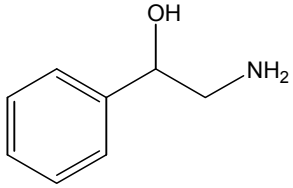	S=2.15 R=3.17	*95.70 (R) 93.66 (S)	GC-20
1) High throughput ruthenacycle-catalyzed asymmetric transfer hydrogenation[124] 2) Nantiotopic lithiation of prochiral benzamide chromium complex[125] 3) Used in asymmetric addition of silane to cyclohexanone[104] 4) asymmetric synthesis of (+)-anatoxina[126]	*Bis* (α-methylbenzyl)amine 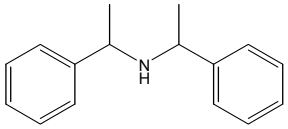	S<0.01 S=0.61	*>99.99 (R) 98.79 (S)	LC-4

Table 2.3 *Continued*

1) HBr scavenger to increase the yield of photoinduced addiction reaction product of 1,4-dibromo-2,5-piperazinedione and 1-alkenes[127] 2) Exchange reactions of ethylene oxides and Et_2CH_2CHROH[128]	Epoxybutane 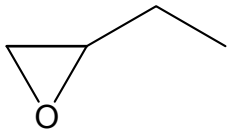	S=0.13 R=0.01	99.74 (R) *99.98 (S)	GC-23
Accelerators for hydrosilation of unsaturated organic compounds[129]	1-Phenyl-2-propyn-1-ol 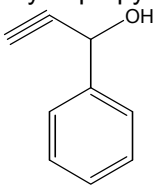	S=2.02 R=0.15	95.96 (R) *99.70 (S)	GC-24
Chiral auxiliaries				
Asymmetric alkynylation of aromatic ketones[130]	2-Amino-1,1-diphenyl-1-propanol 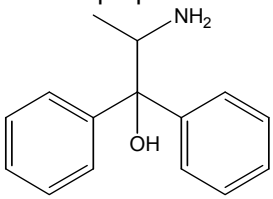	S=1.26 R<0.01	*97.49 (R) >99.99 (S)	LC-5
1) Synthesis of (S)-fontalin and its antipode[131] 2) Synthesis of malyngolide, a marine antibiotic[132] 3) Synthesis of sarcophytol A, an anticarcinogenic marine cembranoid[133]	2-(Anilinomethyl)pyrrolidine 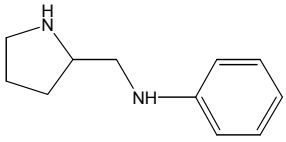	S=9.18 R=4.98	*81.64 (R) 90.04 (S)	LC-6

Table 2.3 *Continued*

Schoellkopf chiral auxiliary[134-138]	2,5-Dihydro-3,6-dimethoxy-2-isopropylpyrazine 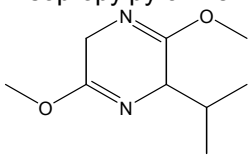	S=4.59 R=2.37	*90.83 (R) 95.26 (S)	GC-11
1) Synthesis of α-(1-methylethyl)-α-(3-oxopropyl)benzeneacetonitriles [139] 2) Chiral resolution of 6-phenyl-4-phenylethynyl-1,4-dihydropyridines, A3 adenosine receptor antagonists[140]	2,2-Dimethyl-1,3-dioxolane-4-methanol 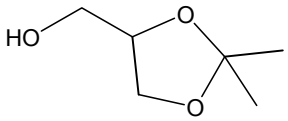	S=2.23 R=2.40	95.55 (R) *95.21 (S)	GC-25
NMR configuration assignment of α-carboxylic acids[141]	1-Indanol 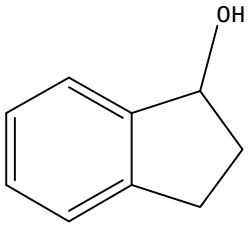	S=13.8 R=11.1	*72.50 (S) 77.80 (R)	LC-7
Dynamic kinetic resolution of α bromoesters[142]	Lactamide 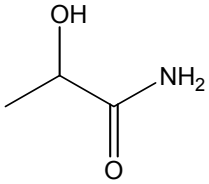	S=1.10	*97.80 (R)	GC-15

[a] The first eluted peaks are indicated with the sign *.
[b] GC=gas chromatography, LC=liquid chromatography (here high pressure chromatography). Each method is taken from Table 1 and Table 2 where the specific condition for each separation is listed
[c] For these two compounds, only one enantiomer is tested because the other enantiomer is commercially unavailable.

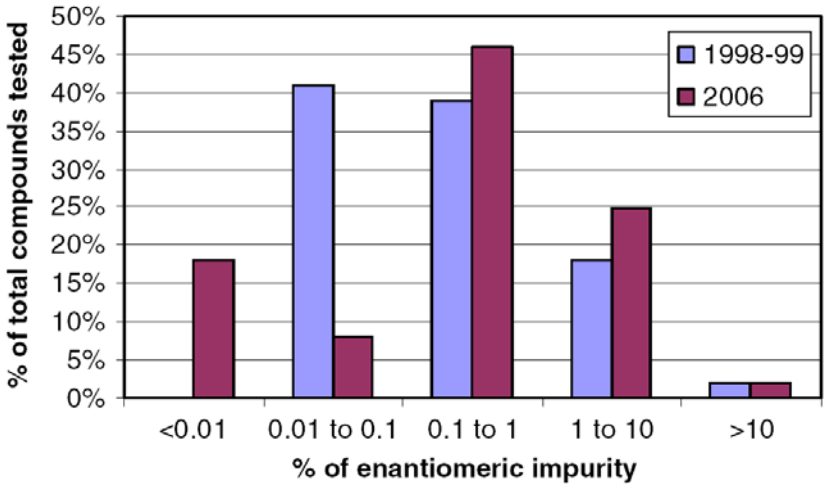

Figure 2.3 Comparison of results obtained in this study (2006) and results obtained in prior work (1998-99).

It was also observed that two enantiomeric compounds will not necessarily contain comparable amounts of enantiomeric impurities. This trend is best observed with the assay of 2, 3-O-benzylidene-D-threitol. The (+) enantiomer had an enantiomeric excess of 85.16%, while the much more pure (-) enantiomer had an enantiomeric excess of 99.60%. This determination is consistent with findings in other studies.[1, 2]

Given the results of this and previous studies, it is apparent that further improvements in the enantiomeric purities of reagents used in asymmetric synthesis would be beneficial. This can be achieved through further refinements in the manufacture and purification of most of these chiral reagents. Since novel chiral compounds are constantly being developed and added to the repertoire of synthetic organic chemists,[143-157] some knowledge as to their enantiomeric composition and the availability of facile methods for their analysis will remain important.

CHAPTER 3

SEPARATION OF ENANTIOMERS AND CONTROL OF ELUTION ORDER OF β-LACTAMS BY USING CYCLODEXTRIN-BASED CHRIAL STATIONARY PHASES

3.1 Abstract

Enantiomers of 19 racemic b-lactams, with 3 and 4-position substitutions, were separated using gas chromatography. Excellent results were achieved on derivatized cyclodextrinbased GC chiral stationary phases (CSPs). All 19 compounds were baseline separated, most with high resolution factors. The Chiraldex G-TA was found to be the most powerful CSP with the broadest enantioselectivity, while Chiraldex B-DM produced the fastest separations for most of the compounds assayed. Results obtained in this work suggest that GC can serve as a potential method for the enantiomeric separation of sufficiently volatile solid β-lactams.

3.2 Introduction

β-Lactams or penams have been widely used in a variety of applications in several scientific areas, especially in medicinal and synthetic chemistry. As the most commonly used group of antibiotics available nowadays, b-lactams function as lethal inhibitants for the growth of pathogenic bacteria cell walls.[158-159] They constitute an important class of antibacterial agents of penicillins, cephalosporins, carbapenems, monobactams, and others. Typically, these antibiotics either occur naturally or are semi-synthetic heterocyclic four membered rings that are amenable to a variety of transformations.[160] In addition, they have been employed as chiral building blocks and reaction intermediates for the stereoselective synthesis of more complex chiral structures of biological and medicinal interest, such as b-amino acids,[161] alkaloids,[162-163] short chain peptides,[164-165] and a variety of different nitrogen containing heterocyclic compounds.[166]

The stereochemistry of these chiral compounds greatly affects their pharmaceutical and biological properties. While one enantiomer can be the product having the desired biological properties, the other enantiomer is often considered a byproduct that can have different pharmaceutical effects or therapeutical values.[167] Therefore, an efficient and effective way is needed to investigate the stereochemistry of lactams so that their enantiomeric purity can be determined. Most reported methods for separating lactam enantiomers utilize liquid chromatography (LC) with an appropriate chiral stationary phase (CSP). Previously, a derivatized amino acid-based chiral stationary phase was used to separate a series of 3- or 4-position substituted *β*-lactams.[168] Huang et al. separated water soluble *β*-lactam enantiomers on *β*-cyclodextrinbonded HPLC stationary phases in 1991.[169] Peter et al. investigated the separation of aryl-substituted b-lactams, tricyclic *β*-lactams, and bicyclic b-amino acids on macrocyclic glycopeptide antibiotic CSPs.[170-172] Polysaccharide derivatives have also been employed in the separation of some *β*- and *γ*-lactam stereoisomers.[160, 173-174]

The 19 b-lactams investigated in this work can be divided into four categories, bicyclic (compounds 1–7), aromatic tricyclic (compounds 8–10), aliphatic tricyclic (compounds 11–12), and aryl-substituted (compounds 13–19). Compounds 1 through 12 had been previously separated by Peter et al. in 2005 with cellulose-tris-3,5-dimethylphenyl carbamate (Chiralcel OD-RH and ODH) and macrocyclic teicoplanin/teicoplanin aglycone CSPs.[160] The next year, Sun et al. used aromatically derivatized cyclodextrin CSPs for the separation of the same group of samples. They achieved seven baseline and five partial separations for this group of 12 compounds.[175] In 2007, the separation of the 12 *β*-lactams was reported usingcapillary electrophoresis (CE) with sulfated α-cyclodextrin as the most effective chiral run buffer additive.[176] In 2006, Peter et al. reported enantiomeric separation of aryl-substituted *β*-lactams (compounds 13–19) with macrocyclic teicoplanin and teicoplanin aglycone CSPs.[171] Although reports on the synthesis Of *β*-lactams have appeared which used gas chromatography (GC) as a means of reaction monitoring and product purity determination,[177-181] there has been no

systematic GC studies on the chiral recognition, separation optimization and elution order determination of these compounds. In this work, different functionalized enantioselective GC stationary phases were used to separate the entire group of 19 *β*-lactams and to investigate their enantiomeric selectivities. The performance of different stationary phases is compared and the influence of the compounds' features on their chiral recognition is evaluated. The high efficiency and fast analysis times of GC for these sufficiently volatile compounds, which are the advantages of this separation technique, were fully demonstrated in this work.

3.3 Experimental

3.3.1 Materials

The first 12 racemic b-lactams cis-6-azabicyclo[3.2.0]heptan-7-one (1), cis-7-azabicyclo[4.2.0]octan-8-one (2), cis-7-azabicyclo[4.2.0]oct-3-en-8-one (3), cis-7-azabicyclo[4.2.0]oct-4-en-8-one (4), cis-8-azabicyclo[5.2.0]nonan-9-one (5), cis-9-azabicyclo[6.2.0]decan-10-one (6), cis-9-azabicyclo[6.2.0]dec-4-en-10-one (7), cis-3,4-benzo-6-azabicyclo[3.2.0]heptan-7-one (8), cis-4,5-benzo-7-azabicyclo[4.2.0]octan-8-one (9), cis-5,6-benzo-8-azabicyclo[5.2.0]nonan-9-one (10), exo-3-azatricyclo[4.2.1.02.5]nonan-4-one (11) and exo-3-azatricyclo[4.2.1.02.5]non-7-en-4-one (12) were prepared by cycloaddition of chlorosulfonyl isocyanate to the corresponding cycloalkenes and cycloalkadienes.[160] 4-phenyl-2-azetidinone (13), 4-(p-tolyl)-2-azetidinone (14), 4-(p-fluorophenyl)-2-azetidinone (15), 4-(p-chlorophenyl)-2-azetidinone (16), 4-(p-bromophenyl)-2-azetidinone (17), 4-(o-chlorophenyl)-2-azetidinone (18), and 4-(mchlorophenyl)-2-azetidinone (19) were prepared according to the methods from published literature.[171] All 19 samples are in their racemic forms. They are all dissolved in high purity OmniSolv dichloromethane which was obtained from EMD Biosciences (San Diego, CA, USA). Chiraldex G-TA (2,6-di-O-pentyl-3-trifluoroacetyl-*γ*-cyclodextrin), G-PN (2,6-di-O-pentyl-3-propionyl-*γ*-cyclodextrin), B-DM (di-O-methyl-*β*-cyclodextrin), B-TA (2,6-di-O-pentyl-3-trifluoroacetyl-*β*-cyclodextrin) GC columns were obtained from Advanced Separation

Technologies (Whippany, NJ, USA). All columns used are 20 m long, with inner i.d. of 250 lm and stationary phase film thickness of 0.25 μm.

3.3.2 Apparatus and methods

The GC equipment used was Agilent Technologies (Santa Clara, CA, USA) model 6850 network gas chromatograph equipped with a flame ionization detector. All analyses were performed with a helium carrier gas flow rate of 1 mL/min and a split ratio of 100/1. The injector and detector temperature was set at 250 and 280 ºC, respectively.

The GC–MS instrument from Agilent Technologies was equipped with a 6890N network GC system, a 5975 inert mass selective detector, a 7683B series autosampler injector and a G1701DA GC/MSD ChemStation data collection software. The MS detector was used in the electron impact ionization mode with an ionization voltage of 70 eV. All GC–MS measurements were performed with the flow rate of 1.0 mL/min and split ratio of 100:1. The injector temperature and the MS transfer line temperature were set at 250 and 280 ºC, respectively. All enantiomeric separations were confirmed by GC–MS fragment comparisons.

3.4 Results and Discussion

3.4.1 Performance and influence of stationary phases on chiral recognition

Four GC chiral stationary phases were used for the separation of all racemic *β*-lactam compounds. They are the derivatized *γ*- and *β*- cyclodextrins: Chiraldex G-TA, G-PN, B-DM, and B-TA columns. The retention factor (*k*), selectivity (*α*), resolution (R_s) and separation temperature (T) for each compound is listed in Table 3.1. The first eluted enantiomers are indicated in the parentheses after the retention factors. The cyclodextrin-based columns exhibited good enantiomeric separations of the 19 target compounds. The numbers of overall separations and partial separations achieved by the four CSPs are shown in Figure 3.1. Examples of the best and worst separations obtained are shown in Figure 3.2. The most effective column tested was the Chiraldex G-TA, which produced 18 baseline and 1 partial separations for the 19 compounds examined. Compounds **1** through **8**, with the only exception

of compound **7**, showed resolutions over 4.0. Compound **2** had a resolution of 11.1 with a retention factor (*k*) of 8.88, which implies that even faster separations are possible by simply sacrificing some of the ample resolution by going to higher temperatures (compound **1** eluted with a resolution of 10.5 and a *k* of only 3.82). Clearly these *β*-lactams, even though they are solids, are quite amenable to fast, efficient GC analysis.

While showing comparable resolving power to the Chiraldex G-TA column, the smaller B-TA CSP displayed complementary separations to its *γ*-cyclodextrin analog. All samples except compound **12** and compound **17** were nicely separated on this column. Although some of the enantiomers were as well separated on this stationary phase, the B-TA CSP produced the best separations for compounds **2**, **3**, **4**, **6**, **7, 9**, **10, 14, 15,** and **16**. The resolution of compound **9** showed a substantial increase from 2.6 to 6.7 from the G-TA to the B-TA column. Also, this column produced a baseline separation for compound **7**, which only eluted with a resolution of 1.4 on the G-TA column. The *β*-cyclodextrin CSP seems to favor the resolution of bicyclic and aromatic tricyclic lactams as compared to the *γ*-cyclodextrin CSP. The detailed enantiomeric separation mechanism remains unclear, but it is undoubtedly analogous to that found in previous studies on cyclodextrin-based CSPs.[182]

The propionyl derivatized *γ*-cyclodextrin CSP showed 15 baseline separations and four partial separations. Almost all the compounds eluted with retention times similar to those on the G-TA column, but with significantly lower resolution. However the resolution of compound **11** increased from 2.6 to 4.6 when the G-PN column was used. An increase in resolution from 1.5 to 2.0 was also observed for compound **13** with the G-PN CSP. Furthermore, while most other columns encountered problems separating compound **12**, the G-PN CSP produced a resolution of 2.5 for this particular *β*-lactam under the same experimental conditions. Therefore, the G-PN CSP showed it has special ability for the separation of aliphatic tricyclic *β*-lactam derivatives.

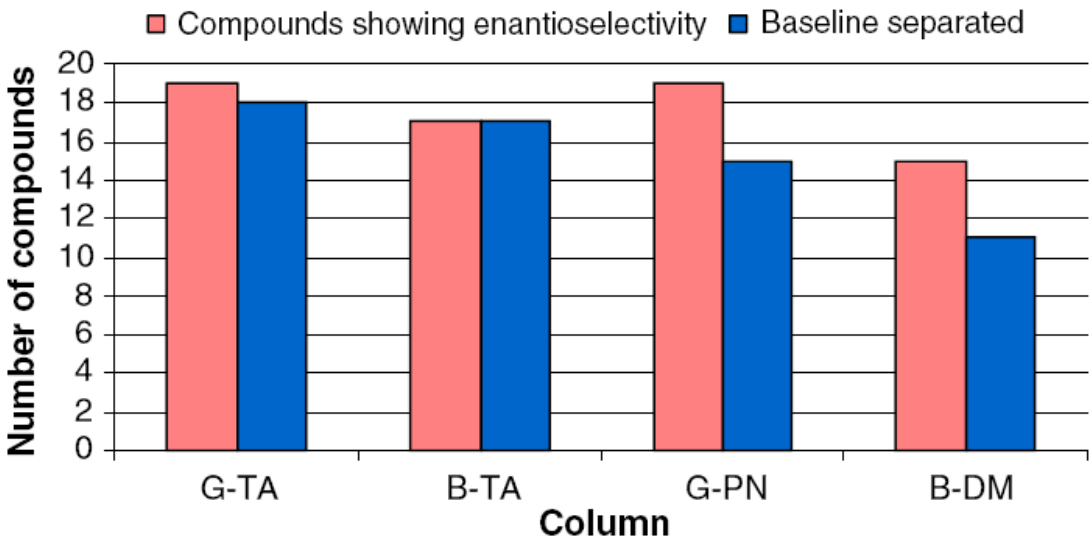

Figure 3.1 Summary of the total number of enantiomeric separations (Rs≥ 0.3) and the number of baseline separations (Rs≥ 1.5) achieved on different GC CSPs.

Table 3.1 Enatiomeric separation of 19 *β*-Lactams with GC CSPs.

Compd Nr.	Structure	CSP	*T* (°C)	k_1[a]	α[b]	R_s[c]
1	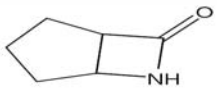	G-TA	150	3.82 (1S,5R)	1.53	10.5
		B-TA	150	4.26 (1R,5S)	1.46	6.2
		G-PN	150	4.02 (1R,5S)	1.20	5.6
		B-DM	150	2.42 (1R,5S)	1.08	1.8
2	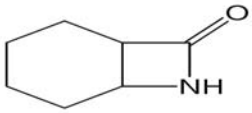	G-TA	150	8.88 (1S,6R)	1.30	11.1
		B-TA	150	7.19 (1R,6S)	1.39	12.4
		G-PN	150	8.30 (1R,6S)	1.20	9.8
		B-DM	150	5.24 (1R,6S)	1.10	3.3
3	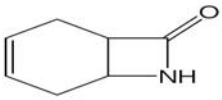	G-TA	150	10.22 (1S,6R)	1.25	7.1
		B-TA	150	7.89 (1R,6S)	1.34	12.7
		G-PN	150	9.92 (1R,6S)	1.14	5.7
		B-DM	150	5.67 (1R,6S)	1.14	3.4
4	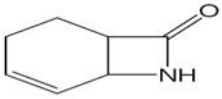	G-TA	150	6.70 (1S,6R)	1.15	6.4
		B-TA	150	5.45 (1R,6S)	1.20	9.3
		G-PN	150	6.46 (1R,6S)	1.09	4.5
		B-DM	150	4.57 (1R,6S)	1.14	4.5
5	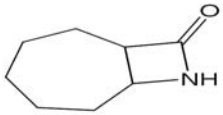	G-TA	150	13.68 (1S,7R)	1.20	8.2
		B-TA	150	10.82 (1R,7S)	1.15	7.0
		G-PN	150	13.37 (1R,7S)	1.15	6.7
		B-DM	150	8.46 (1R,7S)	1.10	3.4
6	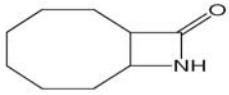	G-TA	170	8.22 (1S,8R)	1.08	4.6
		B-TA	170	6.63 (1S,8R)	1.13	6.0
		G-PN	170	8.41 (1S,8R)	1.05	2.5
		B-DM	N.A.	N.A.	N.A.	N.A.
7	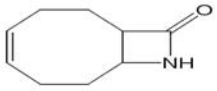	G-TA	160	14.23 (1S,8R)	1.02	1.4
		B-TA	160	11.80 (1S,8R)	1.06	2.1
		G-PN	140	45.49 (1S,8R)	1.02	0.5
		B-DM	N.A.	N.A.	N.A.	N.A.
8	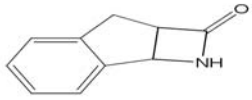	G-TA	180	7.62 (1S,5S)	1.08	4.1
		B-TA	180	6.91(1R,5R)	1.06	2.2
		G-PN	190	5.95 (1R,5R)	1.05	2.4
		B-DM	190	4.00 (1R,5R)	1.05	1.5
9	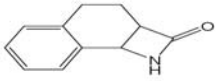	G-TA	180	11.11 (1S,6S)	1.05	2.6
		B-TA	180	10.15 (1R,6R)	1.13	6.7
		G-PN	190	8.58 (1R,6R)	1.03	1.5
		B-DM	200	4.22 (1R,6R)	1.14	5.3
10	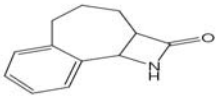	G-TA	180	20.71	1.04	2.4
		B-TA	180	16.35	1.08	4.4
		G-PN	180	27.00	1.05	2.9
		B-DM	180	16.43	1.02	0.9
11	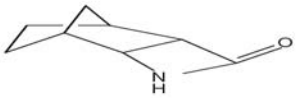	G-TA	150	14.43 (1S,2R,5S,6R)	1.05	2.6
		B-TA	150	10.83 (1S,2R,5S,6R)	1.05	2.7
		G-PN	150	14.00 (1R,2S,5R,6S)	1.10	4.6
		B-DM	150	9.01 (1R,2S,5R,6S)	1.04	1.7
12	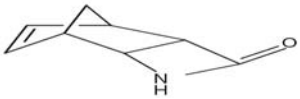	G-TA	170	3.82 (1R,2R,5S,6S)	1.03	1.5
		B-TA	N.A.	N.A.	N.A.	N.A.
		G-PN	150	9.95 (1S,2S,5R,6R)	1.05	2.5
		B-DM	N.A	N.A	N.A	N.A

Table 3.1 – *Continued*

Compd Nr.	Structure	CSP	T (°C)	k_1[a]	α[b]	R_s[c]
13	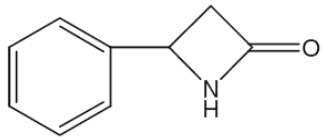	G-TA	160	13.96 (R)	1.02	1.5
		B-TA	160	13.01 (R)	1.06	2.4
		G-PN	160	13.62 (R)	1.05	2.0
		B-DM	160	9.65 (R)	1.13	4.2
14	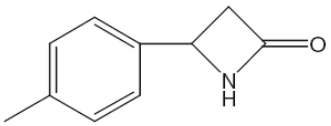	G-TA	160	21.99 (R)	1.03	1.6
		B-TA	160	22.50 (R)	1.05	3.1
		G-PN	160	20.73 (R)	1.02	0.7
		B-DM	160	N.A	N.A	N.A
15	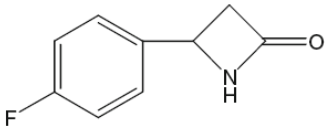	G-TA	160	17.06 (R)	1.02	1.5
		B-TA	160	19.93 (R)	1.05	2.4
		G-PN	160	20.06 (R)	1.03	1.5
		B-DM	160	19.78 (R)	1.02	0.5
16	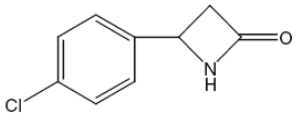	G-TA	160	47.92 (R)	1.03	1.8
		B-TA	160	60.49 (R)	1.05	2.0
		G-PN	160	58.73 (R)	1.02	0.7
		B-DM	160	31.48 (R)	1.03	0.8
17	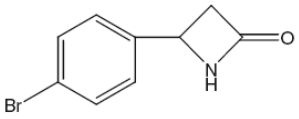	G-TA	160	80.89 (R)	1.03	2.0
		B-TA	160	N.A	N.A	N.A
		G-PN	160	99.15 (R)	1.02	0.4
		B-DM	160	51.08 (R)	1.04	0.9
18	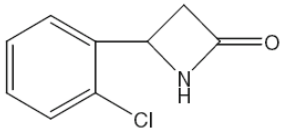	G-TA	160	31.15 (R)	1.05	1.5
		B-TA	160	26.95 (R)	1.05	1.5
		G-PN	160	35.41 (R)	1.04	2.4
		B-DM	160	20.34 (R)	1.13	3.6
19	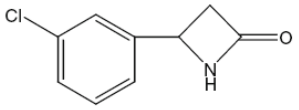	G-TA	160	44.04 (R)	1.04	2.4
		B-TA	160	41.91 (R)	1.07	2.0
		G-PN	160	52.43 (R)	1.03	1.6
		B-DM	160	26.31 (R)	1.12	1.9

a: $k'=(t_R-t_0)/t_0$, whereas t_R is the retention time of the analyte, and t_0 is the dead time of the column.
b: $\alpha= k_2'/k_1'$, whereas k_2' and k_1' is the retention factor of the second and first eluted enantiomer respectively.
c: $Rs=2(t_2-t_1)/(W_1+W_2)$, t_1 and t_2 is the retention time for the first and second eluted peak, whereas W_1 and W_2 is the baseline peak width of the first and second eluted peak.

The Chiraldex B-DM column separated 11 analytes with baseline resolution. Compounds **10** and **15-17** were partially separated on this column under the same conditions used with other columns. Nevertheless, baseline separation of these compounds can be achieved when the separation are done at lower temperatures, with however, a substantial increase in retention. No separation was observed for compounds **6**, **7**, **12,** and **14**. Although the enantiomeric separation accomplished on this stationary phase is generally not as good as on other columns, several analytes exhibited the best separations on the dimethylated *β*-cyclodextrin stationary phase. The resolution of compound **13** increased from 2.4 to 4.2 when using the B-DM column rather than the trifluoroacetylated stationary phase analog. Also, compound **18** showed the highest resolution of 2.4 on the B-DM column compared to the other CSPs employed in this study. While the Chiraldex B-DM column produces lower resolutions for most of the sample investigated, it also produced significantly shorter retention time for all compounds under analogous conditions. Therefore, the B-DM column may be the best choice for rapid enantiomeric separations.

3.4.2 Influence of compound structure on chiral recognition

It was observed that the aryl-substituted *β*-lactams (compounds **13-19**) generally have longer retention times than most of the bicyclic and tricyclic *β*-lactams, except for the aromatic tricyclic structures (compounds **8-10**). Although all seven aryl-substituted compounds investigated showed baseline separation on the trifluoroacetylated *γ*-cyclodextrin chiral stationary phase, their retention factors are all greater than 13. To obtain a decent separation of compound **17** with a 2.0 resolution, a retention factor of 81 was needed. These aryl-substituted analytes required higher temperatures for elution due to their lower volatility. Since the Chiraldex G-TA column exhibited the most comprehensive selectivities towards all *β*-lactams tested, the data from this stationary phase are chosen for this study. The first 12 compounds (bicyclic and tricyclic structures) were tested at 150°C to study the influence of their structures

on chiral recognition (Table 3.2). Due to the lower volatilities of the aryl-substituted *β*-lactams, compounds **13-19** were tested at 160°C (Table 3.1).

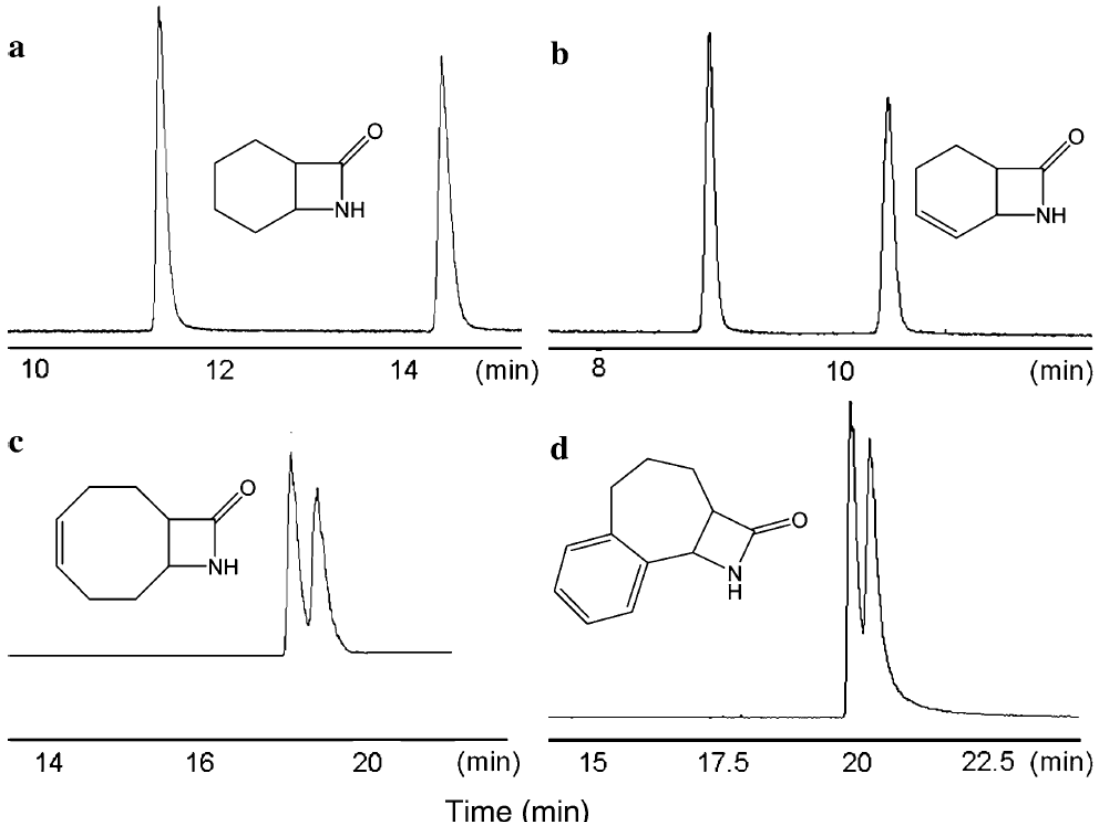

Figure 3.2 Examples of the best (A and B) and worst (C and D) enantiomeric separations for *β*-lactams obtained by GC CSPs. (analytes in chromatogram C and D are baseline separated using other CSPs, see Table 3.1).
A. Chiraldex G-TA column, 150 °C, helium carrier gas, FID
B. Chiraldex B-TA column, 150 °C, helium carrier gas, FID
C. Chiraldex G-TA column, 150 °C, helium carrier gas, FID
D. Chiraldex B-DM column, 180 °C, helium carrier gas, FID

For compounds **1-12**, as the bicyclic ring size increases from a 5-membered ring, to 6, 7, and 8-membered ring, that is from compound **1**, to compounds **2**, **5** and **6**, the retention factor of the compounds increased sequentially from 3.82, to 8.88, 13.68, and 22.66. The selectivity (*α*), however, decreased from 1.53 for compound **1**, to 1.12 for compound **6**. This trend is indicated

in Figure 3.3. Compound **2** with a 6-membered ring appeared to possess the best enantioresolution in this case. For the aromatic tricyclic *β*-lactams, the increase of retention time and decrease of enantioselectivity was also found when the ring size goes from a 5 to a 6 to a 7-membered ring. Therefore, on Chiraldex G-TA column, a smaller ring size accentuates the stereospecific interactions of *β*-lactams with this chiral stationary phase despite the shorter retention times.

The addition of an aromatic moiety to compound **1** produced a considerably larger retention factor (*k*), a significantly smaller selectivity (*α*), and a notably smaller enantioresolution (R_s) of 8.1 for compound **8**. The same trend was found when comparing compound **2** with compound **9**, and compound **5** with compound **10**. Therefore, the aromatic functionality seems to have an adverse effect on the enantiomeric selectivity.

The influence of analytes' degree of saturation on the enantiomeric separation can be seen by comparing the separation of compound **2** with compound **3**, and compound **6** with compound **7**. At 150°C, the retention factor increased from 8.88 (compound **2)** to 10.22 (compound **3)**, and from 22.66 (compound **6)** to 23.74 (compound **7)**. The selectivity, on the other hand, decreased from 1.30 (compound **2)** to 1.25 (compound **3)**, and from 1.12 (compound **6)** to 1.03 (compound **7)**. The resolution factors of racemic *β*-lactams decreased as the degree of saturation decreased. Therefore the addition of double bonds favors retention of bicyclic compounds on the stationary phase but somewhat impairs their selectivities. The position of double bond also appears to have an impact on the enantioseparation (see compound **3** and compound **4**). The chromatographic behavior is different for rigid tricyclic *β*-lactams. Although the presence of a double bond increased solute retention, see compound **11** and compound **12**, the enantiomeric selectivity increased for the unsaturated rigid tricyclic structure of compound **12**.

Table 3.2. Enatiomeric separation of 12 *β*-lactams with G-TA CSP under the same chromatographic conditions.

Compd Nr.	Structure	CSP	T (°C)	k_1	α	R_s
1	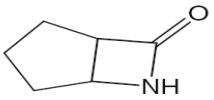	G-TA	150	3.82	1.53	10.5
2	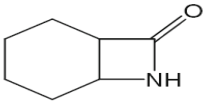	G-TA	150	8.88	1.30	11.1
3	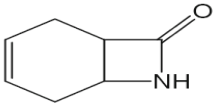	G-TA	150	10.22	1.25	7.1
4	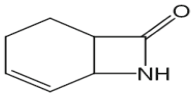	G-TA	150	6.70	1.15	6.4
5	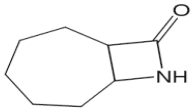	G-TA	150	13.68	1.20	8.2
6	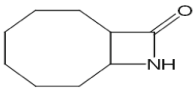	G-TA	150	22.66	1.12	4.6
7	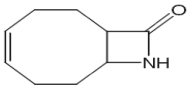	G-TA	150	23.74	1.03	1.3
8	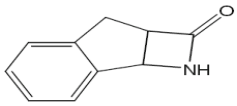	G-TA	150	34.79	1.17	8.1
9	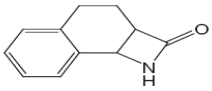	G-TA	150	50.97	1.10	4.8
10	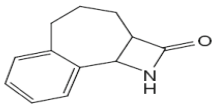	G-TA	150	105.95	1.07	3.2
11	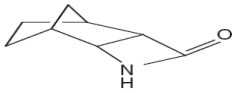	G-TA	150	9.01	1.04	1.7
12	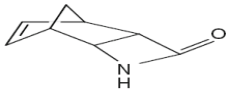	G-TA	150	9.92	1.06	2.6

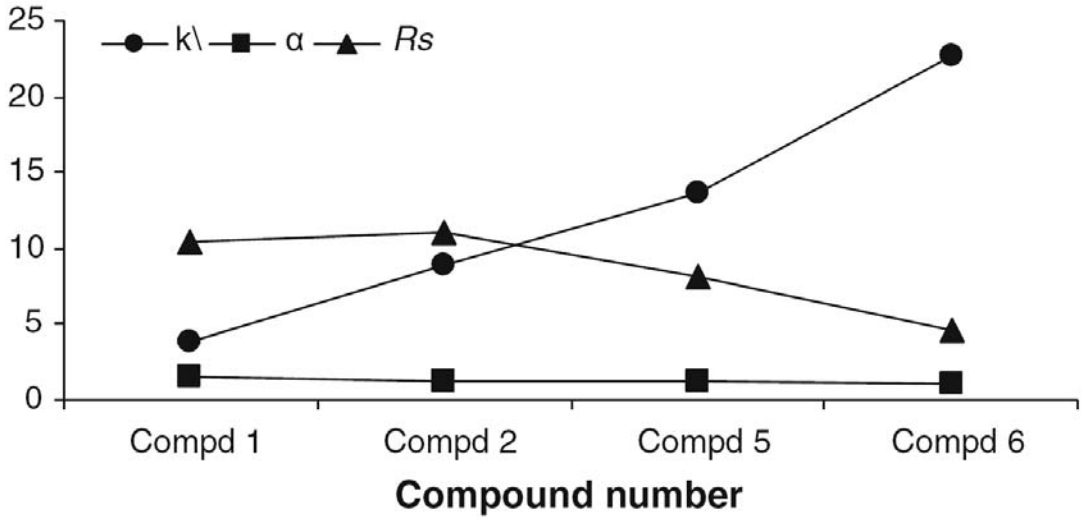

Figure 3.3 The influence of substituent ring size of *β*-lactams on the retention factor (k'), selectivity (*α*), and resolution (Rs) of the enantioseparation.

For the aryl-substituted *β*-lactams, compound **13** had the shortest retention at 160°C. The addition of a single methyl group at the 4-position increased compound retention factor from 13.96 (compound **13)** to 21.99 (compound **14)**. The introduction of halogen atoms onto the aryl moiety resulted in even longer retention times and higher resolution factors for compounds **15** to **19**. This experimental outcome is not unexpected since the G-TA stationary phase is known to have high selectivity for halogenated chiral compounds.[183] It was noted that the analytes with larger halogen substituents were more strongly retained. The data in Table 3.1 (compound **15**-**17**) indicates that the halogen substituents make an important contribution to solute retention, but their effect on compound stereoselectivity is highly variable depending on the cyclodextrin stationary phases.

When the chromatographic behavior of compound **16** is compared with that of compound **18** and compound **19**, it is apparent that the position of substitution also has an impact on the

enantioresolution of the analytes. As is indicated by the data, the para-substituted analytes have the longest retention while ortho-substitution produces the highest selectivity.

3.4.3 Reversal of the enantiomeric elution order

The Chiraldex G-TA column produced the most distinct selectivity in this study in that it retained the (R,S) enantiomers longer for all bicyclic *β*-lactams (compounds **1**-**7**). Conversely, the (R,S) enantiomers are the first eluted peaks on the other three stationary phases. Also, G-TA showed greater retentions for (R,R) enantiomers of the aromatic tricyclic compounds (compounds **8** and **9**) while all the other stationary phases showed stronger interactions with the (S,S) enantiomers. The reversal of enantiomer elution orders from compound **5** to compound **6** suggests a size effect of the target compounds on their chromatographic retentions. The different enantioselectivity exhibited by the G-TA stationary phase and B-TA stationary phase for compound **1**-**9** (except compound **6**) suggests possible compound inclusion complexation in the cyclodextrin cavity. Therefore, both the nature of the derivatization and the size of cyclodextrin can affect the enantiomeric elution order. Indeed this effect has been noted previously for other compounds.[20]

3.5 Conclusions

Greater than baseline separations were achieved for all the *β*-lactams under study. Most of the target molecules were easily separated on all of the tested derivatized cyclodextrin based GC CSPs. The overall best results were obtained using the Chiraldex G-TA stationary phase while for a few analytes better or complementary enantiomeric resolutions were achieved on the Chiraldex B-TA stationary phase. The dimethylated Chiraldex B-DM stationary phase produced the fastest separations for most of the sample compounds investigated albeit with lower resolutions. Compound structures have a great influence on chiral recognition. It was found that for both bicyclic and aromatic tricyclic *β*-lactams, an increase in the substituent ring size increases the retention of the samples, but significantly lowers their enantiomeric selectivity and resolution. The addition of an aromatic substituent also increases the retention of the sample

molecules while compromising the enantiomer resolutions. The presence and position of unsaturated C-C bond have an effect on the enantiomeric separation of both bicyclic and tricyclic enantiomers. The aryl-substituted *β*-lactams exhibited longer retention and lower resolution on all GC stationary phases. The presence and position of halogen substitution on these tested *β*-lactams have profound impact on their enantiomeric separations. The elution order study indicated the importance of cyclodextrin size and functionalization on the chiral recognition ability of the stationary phase. The Chiraldex G-TA column showed the most distinct enantioselectivities in that it produced the opposite retention order (compared to the other CSPs) for many of the analytes in this study.

Although the tested lactams are solids, they are sufficiently volatile that GC can be used to separate their enantiomers and often their performance exceeds that of HPLC and CE.[175-176] The extraordinary high efficiency, selectivity and resolving power of GC, along with its ease of operation and optimization, makes it a useful analytical method for fast and efficient enantiomeric separation of these *β*-lactams.

CHAPTER 4

GC/MS ANALYSIS OF CROCETANE, PHYTANE AND SOME OF THEIR STEREOISOMERS USING CYCLODEXTRIN-BASED STATIONARY PHASES

4.1 Abstract

The detection and complete separation of crocetane (2,6,11,15-tetramethylhexadecane) and phytane (2,6,10,14-tetramethylhexadecane), two widely investigated hydrocarbon biomarkers for archaea in geological environments, are reported. The essential components of the analysis are a series of derivatized cyclodextrin capillary GC stationary phases. In addition, the further separation of stereoisomers of both compounds was observed on the highly selective permethyl-2-hydroxypropyl-b-cyclodextrin stationary phase. In Nature, as in the laboratory, the synthesis (diagenesis) of these biomarkers determines their structures and stereochemistry. Hence, methods that allow their characterization and quantitation provide useful geochemical information.

4.2 Intoduction

Acyclic isoprenoids have been known as biomarkers of geochemical importance for decades.[184] The separation of stereoisomers of acyclic isoprenoid hydrocarbons has been reported since the early 1970s.[185-187] Crocetane (2,6,11,15-tetramethylhexadecane, Figure 4.1), an irregular tail-to-tail linked isoprenoid hydrocarbon, is considered to be diagnostic of, and solely related to, the anaerobic oxidation of methane by archaea in anoxic geological environments.[188-190] The high isotopic depletion of 13C in naturally occurring crocetane is most likely the result of selective carbon uptake from the reduced biogenic sources available to these archaeal organisms in anoxic environments.[191] Phytane (2,6,10,14-tetramethylhexadecane, Figure 4.1), a regular head-to-tail linked isomer of crocetane, is produced via diagenesis of

chlorophyll and from ether-bound membrane lipids in archaea.[192] Also, it is one of the important biomarkers for hypersaline depositional environments.[193] Over the past two decades, crocetane and phytane have been detected in a wide range of crude oils, microbial colonies and sediments containing archaea.[194-203] There has been increasing interest in these two C20 isomers as geochemical biomarkers. It has been suggested that crocetane could be a possible tracer for ancient sulfate-methane transition zones. Recently, it has been proposed as a new signature diagenetic product for aromatic carotenoids from green/brown sulfur bacteria.

It has always been problematic to detect and quantify crocetane and phytane in the complex hydrocarbon distributions isolated from crude oil and sediment samples. It is analytically challenging to achieve complete separation of these two structural isomers because of their lack of functionality and high structural similarity. Previously, both polar (*β*-Cydex) and apolar (polysiloxane and squalane) capillary gas chromatography (GC) columns had been investigated and these showed partial separations of the two compounds.[194, 204-205] However, no complete separation has been reported. The best separation corresponds to a resolution factor (Rs) of 0.8 (with an Rs factor of 1.5 being a baseline separation) achieved on a cyclodextrin-based GC stationary phase.[205]

Indeed, previous work has shown that functionalized cyclodextrins are the most effective class of GC stationary phases for separating compounds with alkane backbones. In 1991 and 1998, the enantiomeric separations of several stereoisomeric hydrocarbons of geochemical importance were reported.[206-207] Enantiomeric separations of some bicyclic monoterpenes were achieved sequentially with high performance liquid chromatography (HPLC), GC and capillary electrophoresis (CE), all by using cyclodextrin-based chiral selectors.[208-210] It was noted that different derivatives of the cyclodextrin (i.e. the chiral separating agent) had vastly different selectivity for isoprenoid stereoisomers. Indeed, previous work suggested that the chiral environment provided by cyclodextrin is not only good for chiral recognition of enantiomers but is also advantageous for the separation of other stereoisomers.[207] The power of cyclodextrins

for the assay of isoprenoids compounds makes them an obvious choice for the separation of crocetane and phytane. In this work, a series of derivatized cyclodextrin- based capillary GC columns was investigated for their ability to perform complete separation of crocetane from phytane, and to see if the stereoisomers of the compounds could also be resolved. If successful, this would provide a more facile means of analyzing geochemically important samples and would also provide access to additional structural data for complex samples.

4.3 Experimental

4.3.1 Materials

Crocetane (99+%) was obtained from ChemSamp Co. Inc. (Dallas, TX, USA). Phytane (1000 µg/ml) was obtained from Sigma–Aldrich (St. Louis, MO, USA). High purity OmniSolv dichloromethane (DCM) was obtained from EMD Biosciences (San Diego, CA, USA). The Canning Basin crude oil samples were obtained from Geoscience Australia (Canberra, Australia). Silica gel was from Sorbent Technologies (Twinsburg, OH, USA). The Appalachian Basin, Louisiana and Nigeria samples were retrieved from ONTA (Toronto, Ontario, Canada). The pretreatment and fractionation of oil samples was performed according to the procedure of Greenwood and Summons (2003). Briefly, the sample was first washed through an activated silica gel column and the saturated hydrocarbon fractions were collected with an appropriate volume of pentane. After solvent removal, the sample was redissolved in cyclohexane and treated with 5 Å molecular sieve to yield branched/cyclic fractions which were then subjected to GC analysis. GC columns coated with Chiraldex G-TA (2,6-di-O-pentyl-3-trifluoroacetyl-*γ*-cyclodextrin), G-PN (2,6-di-O-pentyl-3-propionyl-*γ*-cyclodextrin), G-DM (2,3-di-O-methyl-6-t-butylsilyl-*γ*-cyclodextrin), G-BP (2,6-di-O-pentyl-3- butyryl-*γ*-cyclodextrin), B-DM (2,3-di-O-methyl-6-t-butylsilyl-*β*-cyclodextrin), B-TA(2,6-di-O-pentyl-3-trifluoroacetyl-b-cyclodextrin), B-PH (S-2-hydroxylpropyl-*β*-cyclodextrin) and B-DA (2,6-di- O-pentyl-3-methoxyl-*β*-cyclodextrin) stationary phases and the 5 Å 0 molecular sieve were obtained from Supelco (Bellefonte, PA,

USA). All columns were 20 m or 30 m long, with i.d. 250 μm and stationary phase film thickness of 0.12 μm.

4.3.2Apparatus and methods

The GC-MS instrument from Agilent Technologies (Santa Clara, CA) was equipped with a 6890N network GC system, a 5975 inert mass selective detector, a 7683B series autosampler injector and the G1701DA GC/MSD ChemStation data collection software. The MS detector was used in the electron impact ionization mode with an ionization voltage of 70 eV. All GC-MS measurements were performed with the flow rate of 1.0 mL/min and split ratio of 100:1. The injector temperature and the MS transfer line temperature were set at 250°C and 280°C, respectively. All enantiomeric separations were confirmed by GC-MS fragment comparisons with the NIST library.

Eight cyclodextrin columns were used in this study. The retention factor (*k'*), selectivity (*α*), resolution (Rs) and separation temperature (T) for all samples on each column are listed in Table 4.1. The first eluted isomer is indicated with an asterisk. The best separations for these C_{20} isomers are shown in Figure 4.2.

4.1 Results and Discussion

The method of synthesis of the test analytes determines their isomeric compositions. Phytane was produced from the catalytic hydrogenolysis of phytol [(2E,7R,11R)-3,7,11,15-tetramethyl-2-hexadecen-1-ol, Figure 4.1]. This generates two configurations at C-14, so the product consists of two epimers. Crocetane was synthesized by hydrogenation of 2,6,11,15-tetramethyl-2,6,8-hexadecatriene. The resulting compound contains two chiral centers (C-6 and C-11) and consists of three stereoisomers (a pair of enantiomers and a meso compound).

Eight different derivatized cyclodextrin GC stationary phases were evaluated. Three of the columns produced baseline separation of crocetane and phytane. Six showed stereoisomeric selectivity toward one or both of the tetramethyl hexadecanes. Chiraldex B-PH proved to be the most effective stationary phase as it produced baseline separation of the two phytane epimers

at 100°C and a partial separation of crocetane stereoisomers at 90°C (Figure 4.2). Baseline separation of crocetane and phytane was achieved with resolution >1.5 at 140°C with this column, with a small retention factor of 4.90 for the first eluted phytane stereoisomer peak (Figure 4.2). Note that, since the crocetane peaks are of the same area, it is likely that this is a separation of the meso-crocetane (6S,11R or 6R,11S) configuration from the enantiomers (6R,11R and 6S,11S). However, the full identification of each peak requires further investigation. The results support previous findings that the permethyl 2-hydroxypropyl derivatized cyclodextrin GC stationary phase provides best separation for hydrocarbon biomarkers of geochemical importance,[206] probably because of the steric interaction between the cyclodextrin pendant hydroxypropyl groups and the included hydrocarbon analytes.[21]

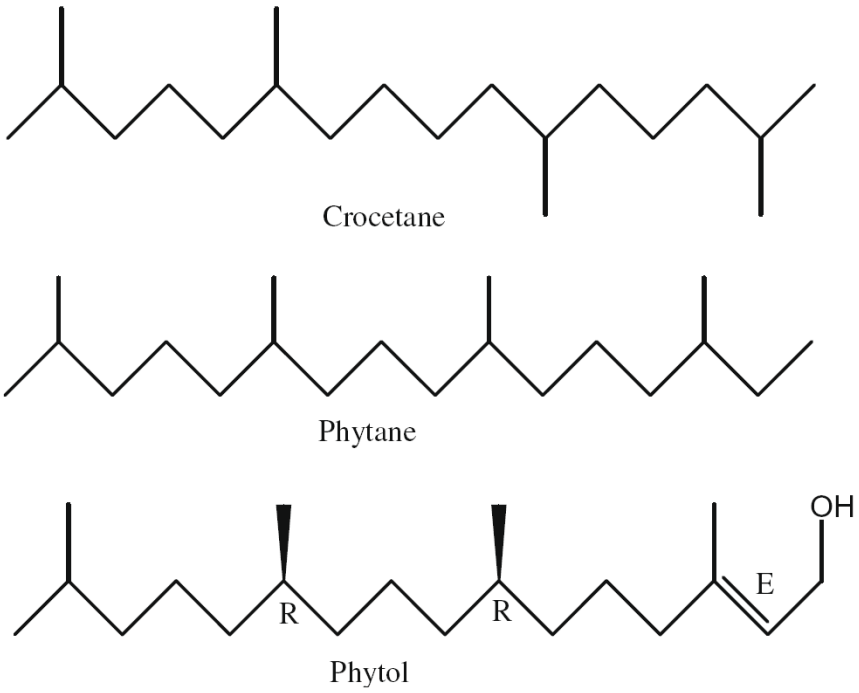

Figure 4.1 Molecular structures of crocetane, phytane, and phytol.

The Chiraldex B-DM and B-TA columns were the second and third most selective stationary phases, both showing baseline separation for crocetane and phytane. The two phytane epimers were also well separated with the B-DM phase. G-DM and G-TA did not, however, exhibit comparable selectivity for these isomeric hydrocarbons. Chiraldex G-PN and G-BP showed no selectivity for any isomer mixture tested. Therefore, *β*-cyclodextrin demonstrated better separating power than the larger *γ*-cyclodextrin analogs. Clearly, the size of the cyclodextrin cavity plays an important role in the isomeric recognition of these compounds as well.

It was also noted that phytane stereoisomers are more easily separated than those of crocetane. Six of the eight columns showed selectivity for the two phytane epimers. However, the best separation for the crocetane stereoisomers corresponded to Rs 0.9 with the Chiraldex B-PH (Figure 4.1). No selectivity for crocetane isomers was observed on any of the other stationary phases, except for a slight shoulder with the Chiraldex G-DM. The separation of crocetane enantiomers remains a subject of interest as they could provide even more information on the diagenesis of archaeal lipids.

Given the superior performance of the Chiraldex B-PH stationary phase with the phytane and crocetane standards, this column was used for the analysis of selected crude oil samples. These included an Appalachian Basin oil, a Louisiana oil and a Nigerian oil, as well as Devonian age Canning Basin oils from Australia (Blina-1 and Blina-2). The latter were chosen on the basis of their high crocetane/phytane values.[192] However, according to previous findings,[192] large discrepancies were found for the different fragment ion measurements with the selected ion monitoring (SIM) of crocetane and phytane. It was hypothesized that coelution of unidentified hydrocarbons complicated the complete quantitation of the two C20 isoprenoid hydrocarbons. In our work, baseline separation of crocetane and phytane was achieved with the Blina-1 and Blina-2 samples within 15 min. (Table 4.2). The peak area investigation shows that the ratio of the two isomers was ca. 0.08 for both samples. These data could be used to facilitate the full

Table 4.1 Optimized separation achieved for crocetane, phytane and their stereoisomers.

Stationary phase (Chiraldex)	Analyte[a]	Temperature (°C)	k_1'[b]	α[c]	Rs[d]
B-PH	Mixture	140	4.90	1.05	1.6
	Crocetane	90	82.29	1.01	0.9
	*Phytane	100	41.31	1.02	1.5
B-DM	Mixture	135	26.49	1.04	1.5
	Crocetane	N.A.[e]	N.A.	N.A.	N.A.
	*Phytane	110	90.82	1.02	1.4
G-DM	Mixture	N.A.	N.A.	N.A.	N.A.
	Crocetane	110	66.67	1.01	0.4
	Phytane	110	65.97	1.01	0.8
B-DA	Mixture	120	28.79	1.01	0.4
	*Crocetane	N.A.	N.A.	N.A.	N.A.
	Phytane	120	28.94	1.01	0.7
G-TA	Mixture	N.A.	N.A.	N.A.	N.A.
	*Crocetane	N.A.	N.A.	N.A.	N.A.
	Phytane	110	72.72	1.01	0.8
B-TA	Mixture	140	15.12	1.05	1.5
	Crocetane	N.A.	N.A.	N.A.	N.A.
	*Phytane	140	15.12	1.01	0.4
G-PN	Mixture	N.A.	N.A.	N.A.	N.A.
	Crocetane	N.A.	N.A.	N.A.	N.A.
	Phytane	N.A.	N.A.	N.A.	N.A.
G-BP	Mixture	N.A.	N.A.	N.A.	N.A.
	Crocetane	N.A.	N.A.	N.A.	N.A.
	Phytane	N.A.	N.A.	N.A.	N.A.

a: The first eluted peaks are indicated with the sign *

b: $k' = (t_R - t_0)/t_0$, whereas t_R is the retention time of the analyte, and t_0 is the dead time of the column.

c: $\alpha = k_2'/k_1'$, whereas k_2' and k_1' is the retention factor of the second and first eluted enantiomer respectively.

d: $Rs = 2(t_2 - t_1)/(W_1 + W_2)$, t_1 and t_2 is the retention time for the first and second eluted peak, whereas W_1 and W_2 is the baseline peak width of the first and second eluted peak.

e: N.A.= not applicable

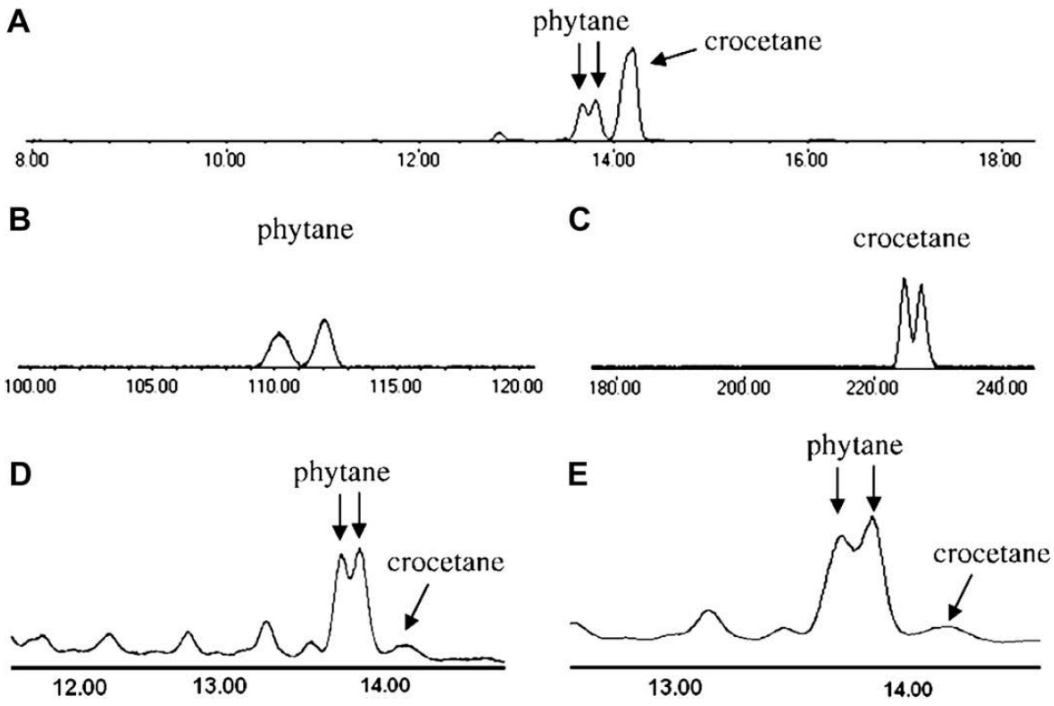

Figure 4.2 The best separation obtained for phytane and crocetane, and their stereoisomers. (A) Separation of phytane isomers from crocetane, Chiraldex B-PH column, 140°C. (B) Separation of phytane epimers, Chiraldex B-PH column, 100°C. (C) Separation of crocetane stereoisomers, Chiraldex B-PH column, 90°C. (D) Separation of phytane isomers from crocetane in the branched/cyclic fraction of Blina-2 Canning Basin oil, Chiraldex B-PH column, 140°C. (E) Separation of phytane isomers from crocetane in the branched/cyclic fraction of Blina-1 Canning Basin oil, Chiraldex B-PH column, 140°C.

quantitation of the two C20 isomers. Further investigation of the oils at 90°C produced information on the individual stereoisomers of phytane and crocetane. Conversely, the Appalachian Basin, Louisiana and Nigeria oils showed no discernable (i.e. below limit of detection) amounts of crocetane in the branched/cyclic hydrocarbon fractions. However, the two phytane isomers were well separated (Table 4.2, Figure 4.2). Note that there are equivalent concentrations of these two epimers in all the crude oils. Furthermore, the identical areas of the crocetane peaks also shed light on the stereoisomeric composition of this compound in the samples.

Table 4.2 Crocetane and phytane composition of branched/cyclic hydrocarbon fractions of Australian, North American and West African crude oils.

Sample	Crocetane/ phytane	Phytane peak 1/ peak 2	Crocetane peak 1/ peak2
Blina-1	0.08	~1	~1
Blina-2	0.08	~1	~1
Appalachian Basin	N.A.[a]	~1	N.A.
Louisiana oil	N.A.	~1	N.A.
Nigeria oil	N.A.	~1	N.A.

The fact that differently derivatized cyclodextrin stationary phases displayed largely distinct separating ability for the two tetramethylhexadecane isomers illustrates the importance of proper functionalization of cyclodextrin hydroxyl groups in the isomeric separation process. It is noteworthy that a reversal of elution order is observed using the B-DA and G-TA stationary phases compared with the other derivatized cyclodextrin columns. Indeed, there have been studies as early as 1990 showing the influence of stationary phase derivatization (polarity) on enantiomeric selectivity.[20]

4.1 Conclusions

The first fast and effective baseline separation of crocetane from phytane, as well as chromatographic resolution of some of their stereoisomers, was achieved using derivatized cyclodextrin GC stationary phases. Different stationary phase derivatives can reverse the elution order of the sample components. Both cyclodextrin cavity size and the nature of pendant moiety at the mouth of the cyclodextrin cavity act as fundamental points of interaction for the separation of crocetane and phytane isomers. The baseline separation of crocetane and phytane enabled the facile detection and analysis of these two compounds in crude oil samples. Crocetane was not detected in the American and Nigerian oil samples but it was detected in the Australian oils. In Blina-1 and Blina-2 oils the crocetane to phytane values are ca. 0.08. The

stereoisomeric ratios for phytane and crocetane in the oil samples were ca. 1. The Chiraldex B-PH cyclodextrin stationary phase has proved to be the most powerful for the isomeric separations of this type, which suggests their potential for more extensive assays and studies of complex geological samples.

PART TWO IONIC LIQUIDS AS GC STATIONARY PHASES

CHAPTER 5

OVERVIEW OF IONIC LIQUIDS IN ANALYTICAL CHEMISTRY

Ionic liquids (ILs) are liquid salts with melting point below 100°C. Room temperature ionic liquids (RTILs) are a subclass of ionic liquids that are liquids at ambient temperatures. Typically ILs consist of bulky organic cations of low structural symmetry plus organic or inorganic anions with weak coordinating abilities. Due to their ionic nature, ILs possess a wide range of unique physicochemical properties, including electrolytic conductivities, negligible vapor pressures, high thermal stabilities, wide liquid ranges, etc. Their structures can be easily engineered to "fine tune" their properties, such as hydrophobicities, viscosities, polarities and solvation properties. Thus it is not surprising that ionic liquids have been playing important roles in many different fields of scientific research. They have been employed as solvent medium for organic syntheses, liquid-liquid extractions, electrolytes for electrochemical studies, enzyme-catalyzed reactions, matrix material for matrix-assisted laser desorption ionization (MALDI), stationary phase material for GC, run buffer additive for capillary electrophoresis (CE), lubricant material development, sensor development and spectroscopy. This manuscript will only deal with the application of ionic liquids as stationary phases in gas chromatography.

Historically, the report of the first IL is a little ambiguous. Although ethanolammonium nitrate (m.p. 52-55°C) was reported in 1888,[211] the first discovered true room temperature ionic liquid was ethylammonium nitrate (m.p. 12°C) reported in 1914 by Paul Walden.[212] 1,3-Dialkylimidazoliumn halogenaluminate was developed later by Wilkes, et al and was used for electrochemical interests.[213] However it is unstable towards air and moisture, and reactive to various organic compounds. The more inert ionic liquids with hexafluorophosphate (PF_6^-) and tetrafluoroborate (BF_4^-) anions were reported by Wilkes and Zawarotko in 1992.[214] These ionic

liquids not only are more air and water stable, but also exhibit wider liquid ranges.[214] Since then, ionic liquids started to be used in broad areas of scientific studies.

Extensive research has been conducted on ionic liquid with various cations and anions. Different IL properties have been obtained by varying the cationic and anionic structures. One of the important directions in the evolution of ionic liquids is the development of liquid salts with higher thermal stabilities and wider liquid ranges. The following chapters will elaborate on the development, characterization and application of some of these novel ionic liquids.

CHAPTER 6

PEG-LINKED GEMINAL DICATIONIC IONIC LIQUIDS AS SELECTIVE, HIGH STABILITY GAS CHROMATOGRAPHIC STATIONARY PHASES

6.1 Abstract

It is known that room temperature ionic liquids (RTILs) have wide applicability in many scientific and technological fields. In this work, a series of three new dicationic room temperature ionic liquids functionalized with polyethylene glycol (PEG) linkages were synthesized and characterized via a linear solvation model. The application of these ILs as new GC stationary phases was studied. The efficient separation of several mixtures containing compounds of different polarities and 24 components of the flavor and fragrance mixture indicated comparable or higher resolving power for the new IL stationary phases compared to the commercial polysiloxane and polyethylene glycol based stationary phases. In addition the selectivities of the IL stationary phases could be quite unique. The separation of homologous alkane and alcohol mixture displayed the “dual nature” of these ionic liquids as GC stationary phases. The thermal stability study showed the column robustness up to 350°C. The high separation power, unique selectivity, high efficiency and high thermal stability of the new dicationic ionic liquids indicate that they may be applicable as a new type of robust GC stationary phase.

6.2 Intoduction

Ionic liquids (ILs) are solvents in which the constituents consist entirely of ions. Room temperature ionic liquids are ionic liquids with melting point below ambient temperature. They are known to have unique physicochemical properties. They possess low melting points, negligible vapor pressures, wide thermal liquid ranges, non-flammability, highly variable thermal

stabilities, variable viscosities, tunable hydrophobicities and the broadest range of solvation interactions of any known solvents. Because of these traits, they enjoy a plethora of applications as the solvent medium for organic synthesis,[215-222] organometallic syntheses,[223-224] liquid-liquid extractions,[225-228] electrolytes for electrochemical studies,[229-233] enzyme-catalyzed reactions,[234-237] matrix material for matrix-assisted laser desorption ionization (MALDI),[238-241] chiral selectors,[27, 242-243] and lubricant materials.[244-245] Since ionic liquids can interact with molecules via a range of physicochemical processes, they can act like polar solvents for polar molecules, and like nonpolar solvents for nonpolar molecules. T[246-250]his "dual nature" of ionic liquids makes them desirable materials for GC stationary phases.[251-254] In particular, the imidazolium based ILs are known to possess wide liquid ranges and good GC column efficiencies.

A number of methods have been developed over the years in order to characterize the solvation behavior of liquids. This includes the use of the empirical solvent polarity scales established to explain the solvation process of ionic liquid mediated organic reactions.[255] Subsequently the solvatochromic dye approach developed by organic chemists was adapted to characterize solvents and solvent mixtures used as mobile phase for liquid chromatography.[256] However these "single parameter polarity approaches" proved to be completely inadequate for ionic liquids since they indicated that all ionic liquids had similar polarities, i. e., close to propanol.[257] The "polarity" approach failed to explain the fact that ILs with apparently identical "polarity parameters" can exhibit completely different solvation behaviors. Clearly, the solvation interactions are more complicated than one average parameter could define. Henceforth, attempts were made with inverse GC measurements to define each individual type of interaction. Initially the Rohrschneider-McReynolds approach was used.[251, 257-258] In this method, 5 judiciously selected probe molecules are used to characterize 5 different types of interactions, respectively. Analogous approaches were developed for liquid chromatography, such as Snyder's P' scale, Hoy and Karger's "solubility parameter", the MOSCED scale of Eckert, the SPACE and the UNIFAC models.[259] The Abraham solvation parameter model was first used to

characterize ILs and used to categorize and quantify the variety of actions and interactions between ILs and dissolved solutes.[253] This represented a fundamental change in our understanding and characterization of ILs. This work resembles the Rohrschneider-McReynolds method in principle but has the advantage of perhaps better defined interaction types and it takes advantage of a larger pool of probe molecules.[260-261] The linear solvation energy relationship can be described by Equation 6.1.

Equation 6.1 $\log k' = c+eE+sS+aA+bB+lL$

The higher case letters are the solute descriptors that can be obtained from the literature.[262] *E* is the extra molar refraction of the solute at 20 °C; *S* is the solute dipolarity/polarizabiltiy; *A* and *B* are the solute hydrogen bond acidity and basicity, respectively; *L* is the solute gas-hexadecane partition coefficient at 25°C. The lower case letters are the interaction parameters that characterize the properties of the solvents (the ILs in this case) under study: *c* is the system constant; *e* is the ability of the solvent to interact with the solute probes through π and n electrons; *s* is the measurement of the dipolarity/polarizability of the solvent; *a* and *b* are the solvent hydrogen bond basicity and acidity, respectively; and *l* is the dispersion forces that the solvent is able to provide. *k'* is the retention factor of the probe molecules which can be measured chromatographically. By subjecting the logarithm of *k'* and the solute descriptors to multiple linear regression, values of all the solvation parameters can be obtained and hence the solvation behavior of the solvent can be described (see Experimental).

Several ionic liquids have been evaluated using this method. Previously, we evaluated the properties of 17 imidazolium, pyridinium, and ammonium based monocationic ionic liquids. The dipolar, hydrogen bonding and dispersion forces were found to be the dominant interaction forces with these ILs and they are largely influenced by the anion.[253] Subsequently, new ionic liquids with bulky substituents on imidazolium rings were synthesized.[246] These ionic liquids showed greater thermal stability, up to 260°C. Most recently, 39 geminal dicationic RTILs with hydrocarbon linkages that

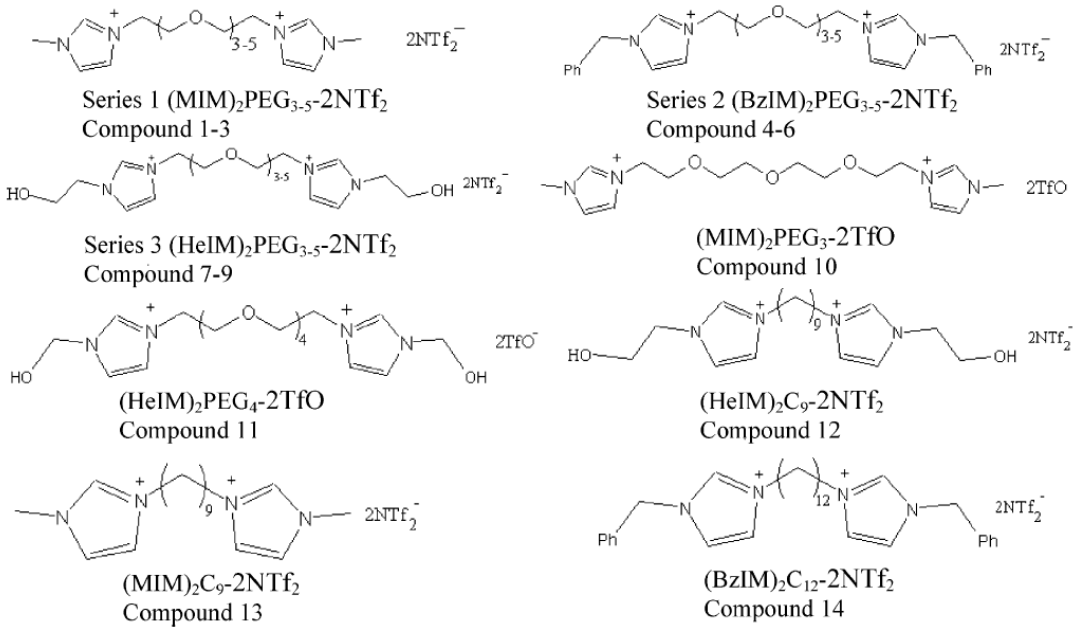

Figure 6.1 Structures of PEG functionalized RTILs.

showed even higher thermal stability were reported.[247] One pyrrolidinium based dicationic liquid displayed thermal stability to over 400°C.[247] Meanwhile the interaction parameters of these dicationic ILs were found to be similar to the corresponding monocationic type ILs, which explained the parallel or slightly better resolving power of these dicationic ILs in gas chromatography as compared to the corresponding monocationic ILs. In an effort to expand the polar solvation properties of the "ultrastable" dicationic ionic liquids, we have synthesized a series of polyethylene glycol linked geminal dicationic ionic liquids (Figure 6.1) and evaluated both their thermal stabilities and their molecular interaction parameters. They are then evaluated as GC stationary phases for the first time. Preliminary indications on analogous compounds indicate that this new class of ILs could have great potential as GC stationary phases.[1, 247]

6.3 Experimental

6.3.1 Materials

The reagents, 1-methylimidazole, 1-benzylimidazole, 1-(2-hydroxyethyl) imidazole, phosphor tribromide, tetraethylene glycol, pentaethylene glycol, hexaethylene glycol , silver trifluoromethanesulfonate, lithium bis(trifluoromethanesulfonyl)imide, ethyl acetate, toluene, alkanes and alcohols homologs and flavor and fragrance mixture kit were obtained from Aldrich. All the probe compounds also were obtained from Aldrich. The GC capillaries were purchased from Supelco (i.d. 250 μm). The polysiloxane column (RTX-5, 5% phenyl methyl polysiloxane) was purchased from Restek (Columbia, MD). The INNOWAX column (polyethylene glycol) was purchased from Agilent Technologies (Santa Clara, CA).

6.3.2 Methods

Around 30 probe molecules carrying specific functional groups were used in this work to meet the statistic requirement that a minimum number of 4 probe molecules are required to meaningfully define each parameter.[259] The probe molecules used are listed in Table 6.2 with their solute descriptors.[262] It is the most recent and widely accepted linear solvation energy relationship (LSER) model in use nowadays. In this inverse GC method, ILs are coated on GC capillaries and used as GC stationary phases. The probe molecules (Table 6.1) are then individually injected and their retention factors are recorded. In this way, the stationary phase solvation behaviors are deconvoluted into five different types of individual interactions using mathematic regression methods.

All the GC columns were made via the static coating method. The ionic liquids were dissolved in dichloromethane to make a coating solution of 0.25% (w/v). The capillary was filled with the coating solution with one end clamped tightly to ensure a complete seal. The column was placed under vacuum from another end while the temperature of the column was maintained at 40°C in water bath. The vacuum was controlled so that the coating rate was maintained at 3-4 loops per hour. The column was then conditioned from 30°C-120°C with the

rate of 3°C/min. The column efficiency was tested at 100 °C with the carrier gas (helium) flow rate of 1 ml/min. The efficiencies of these columns were approximately 2600 plates/m. Each individual probe molecule was injected into the column at 3 different temperatures, 50°C, 70°C and 100°C, respectively.

$(MIM)_2PEG_{3-5}$-NTf_2 and $(BzIM)_2PEG_{3-5}$-NTf_2 were synthesized using similar methods to those reported in the literature.[1] $(HeIM)_2PEG_{3-5}$-NTf_2 were synthesized by reacting polyethylene dibromide with 2 equimolar of 1-hydroxylimidazole with toluene reflux overnight. The product was dissolved in methanol and mixed with $LiNTf_2$. The mixture was stirred at room temperature for 2 hours. The product was extracted with ethylene chloride then washed with water and ether. The final product was dried in vacuum oven with P_2O_5 before usage. All ionic liquids were characterized using ^1H NMR and electrospray ionization (ESI). All ^1H NMR (400MHz) tests were taken in deuterated DMSO. The purities of the final products were between 96%-99%.

Multiple linear regression was performed using Analyse-it. The linearity (R^2) for all evaluations was ≥ 0.96.

6.3.3 Equipments

The GC equipment used was an Agilent (Columbia, MD) model 6892N (G 1540N) gas chromatograph equipped with a flame ionization detector and Agilent ChemStation data acquisition software. All analyses were performed with a helium carrier gas flow rate of 1 ml/min and a split ratio of 100/1. The injector and detector temperature was set at 250 ºC and 300ºC, respectively.

Table 6.1 Probe molecules employed in the RTILs characterizations, and their solute descriptors. (see Fig. 1 for the IL structures and abbreviations)

Probe molecules	R_2	$\Pi_2{}^{H}$	$\alpha_2{}^{H}$	$\beta_2{}^{H}$	log L^{16}
Acetic acid	0.265	0.65	0.61	0.44	1.75
Acetophenone	0.818	1.01	0	0.49	4.501
Aniline	0.955	0.96	0.26	0.53	3.993
Benzaldehyde	0.82	1	0	0.39	4.008
Benzonitrile	0.742	1.11	0	0.33	4.039
1-Butanol	0.224	0.42	0.37	0.48	2.601
2-Chloroaniline	1.033	0.92	0.25	0.31	4.674
1-Chlorohexane	0.201	0.4	0	0.1	3.777
p-Cresol	0.82	0.87	0.57	0.31	4.312
Cyclohexanol	0.46	0.54	0.32	0.57	3.758
Cyclohexanone	0.403	0.86	0	0.56	3.792
1,2-Dichlorobenzene	0.872	0.78	0	0.04	4.518
N,*N*-Dimethylformamide	0.367	1.31	0	0.74	3.173
Naphthalene	1.34	0.92	0	0.2	5.161
Nitrobenzene	0.871	1.11	0	0.28	4.511
1-Nitropropane	0.242	0.95	0	0.31	2.894
1-Octanol	0.199	0.42	0.37	0.48	4.619
Octyl aldehyde	0.16	0.65	0	0.45	4.36
2-Pentanone	0.143	0.68	0	0.51	2.755
Phenetole	0.68	0.7	0	0.32	4.242
Phenol	0.805	0.89	0.6	0.31	3.766
Propionitrile	0.162	0.9	0.02	0.36	2.082
Pyridine	0.794	0.87	0	0.62	3.003
Pyrrole	0.613	0.73	0.41	0.29	2.865
Toluene	0.601	0.52	0	0.14	3.925
m-Xylene	0.623	0.52	0	0.16	3.839
o-Xylene	0.663	0.56	0	0.16	3.939
p-Xylene	0.613	0.52	0	0.16	3.839
Valeraldehyde	0.163	0.65	0	0.45	2.851

6.4 Results and Discussion

6.4.1 Thermal stability test

The ionic liquids under study are polyethylene glycol (PEG) coupled imidazolium based salts with bis[(trifluoromethyl)sulfonyl]imide (NTf_2) or trifluoromethanesulfonate (triflate, TfO) anions. Three series of RTILs were synthesized and evaluated. Their structures are shown in Figure 6.1. The imidazolium cations possess methyl (Series 1, compounds **1-3**), benzyl (Series 2, compounds **4-6**) and 2-hydroxylethyl (Series 3, compounds **7-9**) groups on the 3 position of the imidazolium rings, respectively. All dicationic liquids were coated on short (5 m) fused silica capillaries (see Experimental) and subjected to increasing temperature regions in order to evaluate their thermal stabilities. Typical results are shown in Figure 6.2. The most thermally stable monocationic IL was reported to be 1-(4-methoxylphenyl)imidazolium triflate (MPMIM-TfO) with a bleeding temperature of 260°C.[246] Generally dicationic ILs possess higher bleeding temperatures than their monocationic analogues due to their higher charge, higher molecular weight and greater intermolecular interactions.[247] Imidazolium based $(BzIM)_2C_{12}$-$2NTf_2$ and $(MIM)_2C_9$-$2NTf_2$ (compound **14** and **13**, Figure 6.1) also showed thermal stabilities exceeding 350°C.[247] Almost the same thermal stability was found for the PEG linked dicationic RTILs (Figure 6.2). The column efficiency was retested at 100°C after conditioning the column to 320°C and it was found unchanged prior and after the conditioning. The bis(methylimidazolium)PEG series ILs exhibited highest bleeding temperature of all RTILs tested and the linkage length apparently has only a minor influence on the thermal stability of the compounds. It was also observed that the triflate anion containing ILs were as stable as the NTf_2 anion containing ILs. The extraordinary heat enduring ability of the PEG linked RTIL stationary phases suggests a potential of their development as high temperature GC stationary phases.

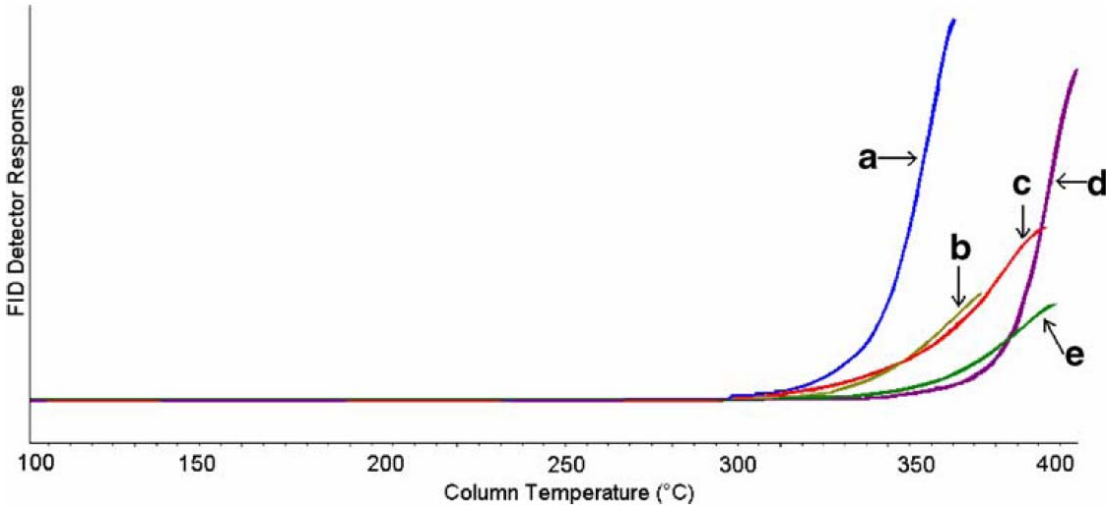

Figure 6.2 Thermal stability of PEG-functionalized dicationic RTILs:
A, $(BzIM)_2PEG_4$-$2NTf_2$; B, $(MIM)_2PEG_4$-$2NTf_2$; C, $(HeIM)_2PEG_4$-$2NTf_2$;
D, $(MIM)_2PEG_4$-2TfO; E, $(MIM)_2PEG_3$-$2NTf_2$.

6.4.2. Solvation parameter coefficient measurements

6.4.2.1 cation effects

Dominant forces and cation structure influence

Each ionic liquid was evaluated for their specific solvation interaction capabilities at 3 different temperatures, 50°C, 70°C and 100°C (see Experimental for details). The results are listed in Table 6.2. The temperature affects the magnitude of each parameter. As temperature increases, the solvation parameter coefficients of the ionic liquids decrease. This is because higher temperature allows higher energy and less orderly orientation of gas molecules hence weaker interactions between the probes and the liquid stationary phases.[253, 259] This is reflected by smaller *Ks* (partition coefficients) and *k'*s (retention factors) of probe molecules at elevated temperatures. On the other hand, lower temperature favors the liquid-stationary phase interactions which are reflected by longer retentions of the probes. Therefore the characterization of ionic liquids at lower temperatures is thought to produce more pronounced and accurate interaction parameters.

As is indicated by the data in Table 2, the dominant interactions for Series 1 and 2 dicationic ionic liquids are dipole-dipole interactions (*s*), hydrogen bond basicity (*a*), followed by dispersion forces (*l*). Due to the lack of hydrogen bond donating moieties, these solvents show weak hydrogen bond acidity (*b*). The *π*-*π* and n-*π* electron interactions are also small relative to the other effects. These findings are in accord with previous studies where it was found that hydrocarbon linked dicationic ILs, together with most of the tested monocationic ionic liquids, have strong dipole-dipole interactions and hydrogen bond basicities.[246-247, 253] However, the

Table 6.2 Regression parameter coefficients of Series 1, Series 2 and Series 3 PEG linked RTILs. (see Fig. 6.1 for the IL structures and abbreviations)

Temperature (°C)	*c*	*e*	*s*	*a*	*b*	*l*	*n*	R^2
$(MIM)_2PEG_3$-$2NTf_2$								
50 (std. err.)	−2.99 (0.12)	0.09 (0.10)	1.91 (0.11)	2.18 (0.10)	0.11 (0.14)	0.56 (0.03)	29	0.99
70 (std. err.)	−3.07 (0.11)	0.12 (0.09)	1.80 (0.10)	1.94 (0.09)	0.07 (0.13)	0.50 (0.03)	29	0.98
100 (std. err.)	−3.21 (0.11)	0.12 (0.08)	1.68 (0.09)	1.65 (0.08)	0.03 (0.12)	0.44 (0.02)	29	0.99
$(MIM)_2PEG_4$-$2NTf_2$								
50 (std. err.)	−3.13 (0.11)	0.16 (0.09)	2.04 (0.10)	2.34 (0.09)	0.19 (0.13)	0.54 (0.03)	29	0.98
70 (std. err.)	−3.20 (0.10)	0.16 (0.08)	1.94 (0.09)	2.11 (0.08)	0.14 (0.12)	0.48 (0.03)	29	0.99
100 (std. err.)	−3.27 (0.09)	0.18 (0.07)	1.77 (0.08)	1.79 (0.07)	0.14 (0.10)	0.41 (0.02)	29	0.99
$(MIM)_2PEG_5$-$2NTf_2$								
50 (std. err.)	−2.99 (0.12)	0.31 (0.10)	1.80 (0.11)	2.16 (0.10)	0.34 (0.14)	0.54 (0.03)	29	0.99
70 (std. err.)	−3.02 (0.11)	0.26 (0.09)	1.71 (0.10)	1.93 (0.08)	0.24 (0.13)	0.48 (0.03)	29	0.99
100 (std. err.)	−3.10 (0.09)	0.23 (0.07)	1.58 (0.08)	1.64 (0.07)	0.19 (0.11)	0.41 (0.02)	29	0.99
$(BzIM)_2PEG_3$-$2NTf_2$								
50 (std. err.)	−3.06 (0.10)	0.06 (0.08)	1.86 (0.09)	2.01 (0.08)	0.21 (0.11)	0.60 (0.03)	29	0.99
70 (std. err.)	−3.09 (0.09)	0.06 (0.07)	1.76 (0.08)	1.80 (0.07)	0.15 (0.11)	0.54 (0.02)	29	0.99
100 (std. err.)	−3.19 (0.08)	0.07 (0.07)	1.62 (0.08)	1.52 (0.07)	0.10 (0.10)	0.47 (0.02)	29	0.99
$(BzIM)_2PEG_4$-$2NTf_2$								
50 (std. err.)	−2.98 (0.12)	0.08 (0.10)	1.79 (0.11)	2.04 (0.10)	0.21 (0.14)	0.59 (0.03)	29	0.99
70 (std. err.)	−3.02 (0.11)	0.07 (0.09)	1.69 (0.10)	1.81 (0.09)	0.13 (0.12)	0.54 (0.03)	29	0.99
100 (std. err.)	−3.08 (0.10)	0.09 (0.08)	1.55 (0.09)	1.54 (0.08)	0.03 (0.11)	0.46 (0.02)	29	0.99
$(BzIM)_2PEG_5$-$2NTf_2$								
50 (std. err.)	−3.03 (0.10)	0.14 (0.08)	1.80 (0.09)	2.05 (0.08)	0.29 (0.11)	0.58 (0.02)	29	0.99
70 (std. err.)	−3.09 (0.09)	0.13 (0.07)	1.71 (0.08)	1.82 (0.07)	0.21 (0.10)	0.53 (0.02)	29	0.99
100 (std. err.)	−3.18 (0.08)	0.14 (0.06)	1.56 (0.07)	1.54 (0.06)	0.17 (0.09)	0.46 (0.02)	29	0.99
$(HieM)_2PEG_3$-$2NTf_2$								
50 (std. err.)	−2.71 (0.20)	0.51 (0.15)	1.35 (0.19)	1.81 (0.15)	1.24 (0.22)	0.43 (0.05)	28	0.96
70 (std. err.)	−2.85 (0.18)	0.46 (0.14)	1.32 (0.16)	1.60 (0.13)	1.07 (0.20)	0.39 (0.04)	28	0.97
100 (std. err.)	−3.04 (0.15)	0.37 (0.12)	1.27 (0.14)	1.38 (0.11)	0.83 (0.17)	0.35 (0.04)	28	0.97
$(HeIM)_2PEG_4$-$2NTf_2$								
50 (std. err.)	−2.73 (0.17)	0.43 (0.13)	1.48 (0.16)	1.94 (0.13)	1.01 (0.19)	0.46 (0.04)	28	0.98
70 (std. err.)	−2.80 (0.14)	0.37 (0.11)	1.42 (0.13)	1.73 (0.10)	0.82 (0.15)	0.42 (0.03)	28	0.98
100 (std. err.)	−2.86 (0.15)	0.17 (0.11)	1.40 (0.14)	1.44 (0.11)	0.49 (0.16)	0.37 (0.04)	27	0.97
$(HeIM)_2PEG_5$-$2NTf_2$								
50 (std. err.)	−2.95 (0.11)	0.31 (0.09)	1.71 (0.11)	2.15 (0.09)	0.78 (0.13)	0.49 (0.03)	28	0.99
70 (std. err.)	−3.03 (0.10)	0.30 (0.08)	1.62 (0.09)	1.91 (0.08)	0.68 (0.11)	0.44 (0.02)	28	0.99
100 (std. err.)	−3.12 (0.09)	0.25 (0.07)	1.53 (0.09)	1.63 (0.07)	0.50 (0.10)	0.38 (0.02)	28	0.99

Series 3 ionic liquids (which have hydroxyethyl groups attached to the imidazolium moiety) show some deviations from this trend (compound **7-9,** Table 6.2). While dipole-dipole interactions (*s*), hydrogen bond basicity (*a*) and dispersion forces (*l*) remain major solvation parameters, the significantly larger hydrogen bond acidity (*b*) also plays an important role in the probe molecule solvation processes. The increase of the *b*-term and *e*-term compared to the methylated and benzylated ILs implies a significant influence of cation structure on the hydrogen bond acidity and the π-π and n-π electron interactions of these ILs. Chromatographically, the hydroxyl groups of series 3 act as powerful hydrogen bond donors that notably increase the retention of basic probe molecules. For example, at 50°C, the retention factor (*k'*) of pyridine increased from 2.45 on the $(MIM)_2PEG_3$-$2NTf_2$ column to 22.31 on the $(HeIM)_2PEG_3$-$2NTf_2$ column. However, the similarities in the interaction parameters for Series 1 and Series 2 ILs suggest a much less pronounced influence of the methyl versus the benzyl substitutions on the IL solvation behaviors (Table 2). Since most of the commercial GC stationary phases available have essentially negligible hydrogen bond acidities (*b*-term),[263-264] the development of these new ILs, especially the Series 3 ILs, has a great potential to fill a huge gap of selectivities of available GC stationary phases.

Influence of "linker" chain length

As is shown in Table 6.2, varying the linkage from PEG3 to PEG5 does not significantly alter the solvation coefficients for the Series 1 and Series 2 RTILs. For the Series 3 RTILs, a small but steady increase in the *s*-terms and *a*-terms was discovered as the length of the linkage chain increases. This is probably due to the additional oxygen atoms on the linkage chain that make these ionic liquids better hydrogen bond acceptors and slightly more polar molecules. The progressive decrease in hydrogen bond acidities (*b*) with increasing linkage chain length may be due to the formation of internal hydrogen bonds which makes these ILs weaker hydrogen bond donors for probe molecules. Chromatographically, this is reflected by a steady decrease in the retention of basic compounds. For example, pyridine had a *k'* of 22.31

on IL 7 at 50°C. This value sequentially decreased to 16.62 and 7.79 on IL 8 and IL 9, respectively. The detailed mechanism for this hydrogen bond acidity decrease requires further investigation on the structures and interactions of these ionic liquids as coated GC stationary phases. However, these findings indicate a moderate influence of the linkage chain length on the solvation parameters of this specific type of ionic liquids.

Influence of linkage type

A comparison of the interaction parameters of PEG linked and hydrocarbon linked geminal dicationic ionic liquids with similar linkage lengths was undertaken in order to study the role of linkage types on the solvation properties of these ionic liquids (Table 6.3). The solvation parameter coefficients for $(MIM)_2C_9$-$2NTf_2$ and $(BzIM)_2C_{12}$-$2NTf_2$ RTILs were obtained from previous work [41]. As is suggested by the coefficients, the hydrocarbon linked stationary phases and the PEG linked stationary phases share similar solvation behavior patterns. The dipole-dipole (*s*) and hydrogen bonding interactions (*a*) are the dominant forces with dispersion interactions (*l*) being the third strongest force. However, the PEG linked RTILs show slightly higher dipolarity/polarizability and hydrogen bond basicity terms due to the additional oxygens within the PEG linkers. They provide good dipole-dipole interaction sites and hydrogen bond accepting sites. Again the Series 3 (2-hydroxylethyl-containing) ILs differ from the others by having significantly larger "*e*" and "*b*" terms. Indeed these terms appear to be somewhat larger for the hydrocarbon-linked dicationic ionic liquid as compared to the PEG linked one.

influence of the anion on the solvation parameter coefficients (Table 6.4).

By comparison of the bis(methylimidazolium)PEG3 NTf_2 (compound **1**) and bis(2-hydroxylethylimidazolium)PEG4 NTf_2 (compound **8**) stationary phases with their triflate analogs (compounds **10** and **11**), a significant difference is noted with the *s* (dipolar) and *a* (hydrogen bond basicity) terms. At 50ºC the *s* term increased from 1.91 to 2.18 from compound **1** to compound **10**, and from 1.48 to 2.11 for compound **8** to compound **11**. The *a* term increased from 2.18 to 3.39 for compound **1** to compound **10**, and from 1.94 to 3.19 for compound **8** to

compound **11**. However, while the *e*-term and the *b*-term were slightly increased by replacing the NTf_2 anion with triflate anion for the bis(methylimidazolium)PEG3 IL, the change in the anion did not maintain the high *e*-term and *b*-term of bis(2-hydroxylethylimidazolium)PEG4 NTf_2 IL. Despite the fact the bis(2-hydroxylethylimidazolium)PEG4 NTf_2 possesses a high *e*-term and *b*-term, and the fact bis(methylimidazolium)PEG3 triflate possesses a high *s*-term and *a*-term, bis(2-hydroxyethylimidazolium)PEG4 triflate did not produce an ionic liquid with both high hydrogen bond acidity (*b*) and hydrogen bond basicity (*a*) as expected. Therefore, the solvation properties of a ionic liquid are not just simple additive effects of its individual components. The microscopic structure of a specific type of IL also has great influence on the IL properties. These results indicate that the anions play a major role on the solvation behaviors of these ionic liquids through their dominant control of the *s* and *a* properties. This same trend has been reported previously for other ionic liquids.[246, 253]

Table 6.3 A comparison of the interaction parameters for analogous RTILs linked by PEG. versus hydrocarbons (see Figure 6.1 for the IL structures and abbreviations)

Temperature (°C)	*c*	*e*	*s*	*a*	*b*	*l*	*n*	R^2
$(MIM)_2PEG_3$-$2NTf_2$								
70 (std. err.)	−3.07 (0.11)	0.12 (0.09)	1.80 (0.10)	1.94 (0.09)	0.07 (0.13)	0.50 (0.03)	29	0.98
100 (std. err.)	−3.21 (0.11)	0.12 (0.08)	1.68 (0.09)	1.65 (0.08)	0.03 (0.12)	0.44 (0.02)	29	0.99
$(MIM)_2C_9$-$2NTf_2$								
70 (std. err.)	−2.95 (0.09)	0.11 (0.07)	1.76 (0.08)	1.75 (0.07)	0.20 (0.10)	0.51 (0.02)	33	0.99
100 (std. err.)	−3.06 (0.08)	0.11 (0.06)	1.64 (0.07)	1.50 (0.06)	0.15 (0.09)	0.43 (0.02)	32	0.99
$(BzIM)_2PEG_4$-$2NTf_2$								
70 (std. err.)	−3.02 (0.11)	0.07 (0.09)	1.69 (0.10)	1.81 (0.09)	0.13 (0.12)	0.54 (0.03)	29	0.99
100 (std. err.)	−3.08 (0.10)	0.09 (0.08)	1.55 (0.09)	1.54 (0.08)	0.03 (0.11)	0.46 (0.02)	29	0.99
$(BzIM)_2C_{12}$-$2NTf_2$								
70 (std. err.)	−3.07 (0.08)	0.07 (0.05)	1.62 (0.08)	1.75 (0.06)	0.57 (0.09)	0.56 (0.02)	30	0.99
100 (std. err.)	−3.12 (0.09)	0 (0.04)	1.47 (0.09)	1.44 (0.06)	0.52 (0.10)	0.46 (0.02)	30	0.99
$(HeIM)_2PEG_3$-$2NTf_2$								
70 (std. err.)	−2.85 (0.18)	0.46 (0.14)	1.32 (0.16)	1.60 (0.13)	1.07 (0.20)	0.39 (0.04)	28	0.97
100 (std. err.)	−3.04 (0.15)	0.37 (0.12)	1.27 (0.14)	1.38 (0.11)	0.83 (0.17)	0.35 (0.04)	28	0.97
$(HeIM)_2C_9$-$2NTf_2$								
70 (std. err.)	−3.04 (0.13)	0.35 (0.10)	1.49 (0.11)	1.58 (0.10)	1.03 (0.14)	0.47 (0.03)	29	0.98
100 (std. err.)	−3.08 (0.11)	0.29 (0.09)	1.44 (0.10)	1.34 (0.09)	0.76 (0.12)	0.40 (0.03)	29	0.99

Table 6.4 A comparison of the interaction parameters of PEG-linked RTILs with NTf_2 versus triflate anions. (see Figure 6.1 for the IL structures and abbreviations).

Temperature (°C)	*c*	*e*	*s*	*a*	*b*	*l*	*n*	R^2
$(MIM)_2PEG_3$-$2NTf_2$								
50 (std. err.)	−2.99 (0.12)	0.09 (0.10)	1.91 (0.11)	2.18 (0.10)	0.11 (0.14)	0.56 (0.03)	29	0.99
70 (std. err.)	−3.07 (0.11)	0.12 (0.09)	1.80 (0.10)	1.94 (0.09)	0.07 (0.13)	0.50 (0.03)	29	0.98
100 (std. err.)	−3.21 (0.11)	0.12 (0.08)	1.68 (0.09)	1.65 (0.08)	0.03 (0.12)	0.44 (0.02)	29	0.99
$(MIM)_2PEG_3$-2TfO								
50 (std. err.)	−3.38 (0.15)	0.51 (0.12)	2.18 (0.13)	3.39 (0.12)	0.32 (0.17)	0.44 (0.04)	29	0.99
70 (std. err.)	−3.38 (0.15)	0.55 (0.12)	2.02 (0.13)	3.03 (0.12)	0.34 (0.17)	0.37 (0.04)	29	0.99
100 (std. err.)	−3.49 (0.11)	0.45 (0.09)	1.95 (0.98)	2.72 (0.09)	0.22 (0.13)	0.31 (0.03)	26	0.99
$(HeIM)_2PEG_4$-$2NTf_2$								
50 (std. err.)	−2.73 (0.17)	0.43 (0.13)	1.48 (0.16)	1.94 (0.13)	1.01 (0.19)	0.46 (0.04)	28	0.98
70 (std. err.)	−2.80 (0.14)	0.37 (0.11)	1.42 (0.13)	1.73 (0.10)	0.82 (0.15)	0.42 (0.03)	28	0.98
100 (std. err.)	−2.86 (0.15)	0.17 (0.11)	1.40 (0.14)	1.44 (0.11)	0.49 (0.16)	0.37 (0.04)	27	0.97
$(HeIM)_2PEG_4$-2TfO								
50 (std. err.)	−3.43 (0.13)	0.30 (0.10)	2.04 (0.11)	3.12 (0.10)	0.27 (0.15)	0.50 (0.03)	29	0.99
70 (std. err.)	−3.25 (0.12)	0.30 (0.09)	1.89 (0.11)	2.83 (0.09)	0.18 (0.13)	0.44 (0.03)	29	0.99
100 (std. err.)	−3.28 (0.11)	0.27 (0.08)	1.76 (0.09)	2.42 (0.08)	0.14 (0.12)	0.36 (0.03)	28	0.99

6.4 3. GC application study

The PEG functionalized dicationic RTIL stationary phases were tested for their separation abilities. Two standard mixtures were prepared. Each mixture was run on a $(MIM)_2PEG_3$-$2NTf_2$ coated column, a $(MIM)_2PEG_3$-2TfO coated column, a polar commercial INNOWAX column and a nonpolar commercial Rtx-5 (Crossbond® 5% diphenyl - 95% dimethyl polysiloxane) column. Figure 6.3 shows the separation of a homologous series of alkanes and alcohols on the four columns. The highly polar INNOWAX column shows good retention for alcohols but poor selectivity for the alkanes. On the contrary, the low polarity Rtx-5 column tends to hold alkane strongly however many alcohols were eluted quickly. The $(MIM)_2PEG_3$-$2NTf_2$ and the $(MIM)_2PEG_3$-2TfO column has their selectivity lying in between the 2 commercial columns. For example, 1-hexanol is retained for obviously longer on the INNOWAX column than on the Rtx-5

column, whereas on the $(MIM)_2PEG_3$-$2NTf_2$ column it eluted with moderate retention. Also, octane eluted with a retention factor in between those of the Rtx-5 and the INNOWAX column.

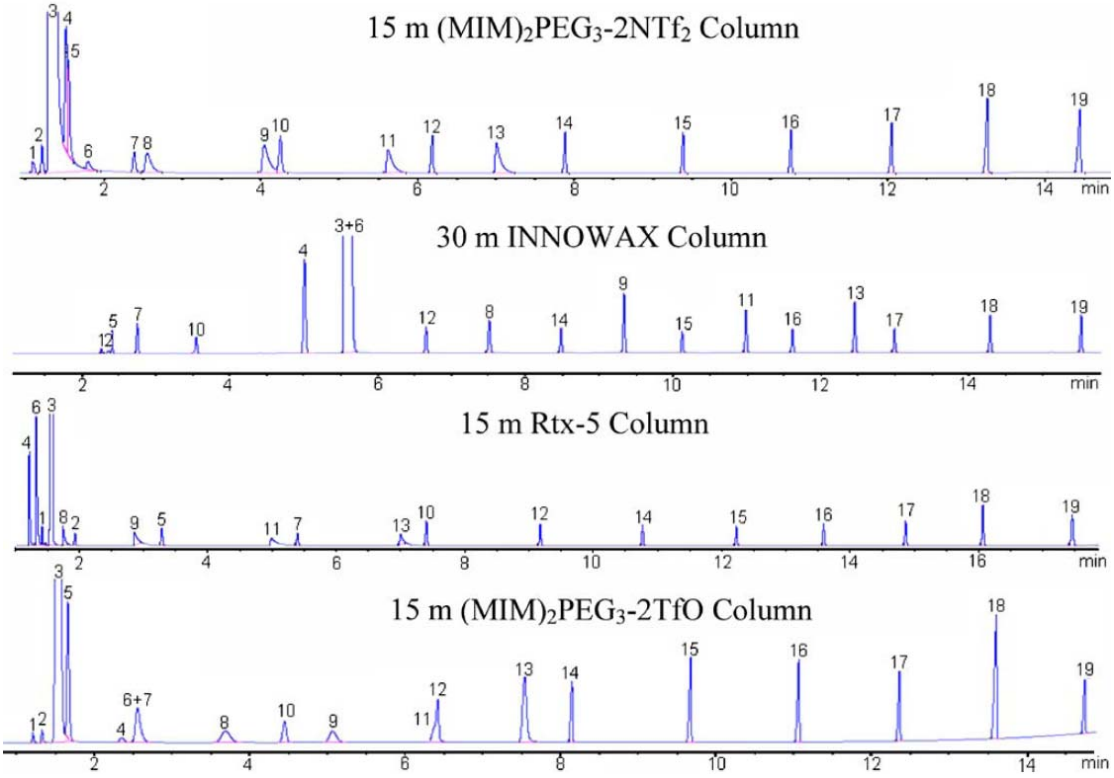

Figure 6.3 Separation of homologous alkane and alcohol mixture, 1, pentane; 2, hexane; 3, dichloromethane; 4, methanol; 5, heptane; 6, ethanol; 7, octane; 8, 1-propanol; 9, 1-butanol; 10, nonane; 11, 1-pentanol; 12, decane; 13, 1-hexanol; 14, undecane; 15, dodecane; 16, tridecane; 17, tetradecan; 18, pentadecane; 19, hexadecane.
Conditions: 30°C for 3 min, 10°C/min to 160°C.

It is apparent that this new stationary phase has reasonable retention for both polar alcohols and nonpolar alkanes. This is another demonstration of the “dual nature” of ionic liquids based GC stationary phases. That is they can retain polar compounds as if they were polar stationary

phases, and retain nonpolar compounds as if they were nonpolar stationary phases. The disadvantage of the $(MIM)_2PEG_3$-$2NTf_2$ column is the tailing peaks for alcohols. Earlier studies suggested that the NTf_2 columns suffer from worse mass transfer of hydrogen bond acidic molecules probably because these molecules can more conveniently interact with the delocalized negative charge on the S-N-S moiety of the NTf_2 ILs.[257] However, the $(MIM)_2PEG_3$-2TfO column shows comparable separation power to the NTf_2 column but symmetric peaks for all sample components. It seems to be a more useful GC stationary phase for the separation of hydrogen-bond acidic compound mixtures.

Figure 6.4 shows the separation of a mixture of 24 flavor and fragrance compounds, which are primarily homologous esters. All 24 peaks were baseline separated on the $(MIM)_2PEG_3$-$2NTf_2$ column while there was coelution of isopropyl tiglate and ethyl hexanoate on the INNOWAX column and a partial separation of propyl butyrate and ethyl valerate on the Rtx-5 column. For this mixture, the selectivity of the $(MIM)_2PEG_3$-$2NTf_2$ column and the $(MIM)_2PEG_3$-2TfO column lean more towards the polar INNOWAX column with only a few compound elution order switches. Their extraordinary resolving power for intermediate to high polarity homologous molecules seems to be a point of virtue to be further explored.

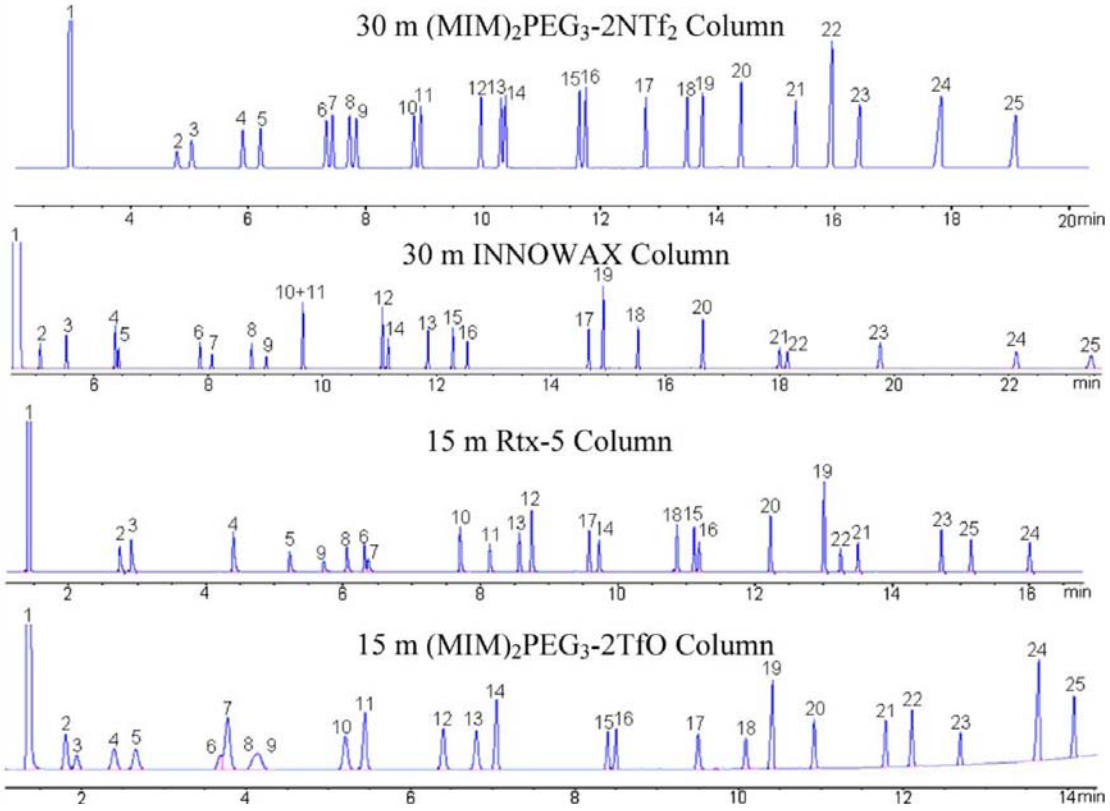

Figure 6.4 Separation of flavor and fragrance mixture, 1, dichloromethane; 2, ethyl propionate; 3, methyl butyrate; 4, ethyl butyrate; 5, isopropyl butyrate; 6, propyl butyrate; 7, ethyl valerate; 8, allyl butyrate; 9, methyl tiglate; 10, isopropyl tiglate; 11, ethyl hexanoate; 12, propyl tiglate; 13, allyl tiglate; 14, ethyl heptanoate; 15, hexyl butyrate; 16, ethyl octanoate; 17, furfuryl propionate; 18, fyrfuryl butyrate; 19, hexyl tiglate; 20, furfuryl pentanoate; 21, furfuryl hexanoate; 22, benzyl butyrate; 23, furfuryl heptanoate; 24, furfuryl octanoate; 25, benzo-trans-2-methyl-2-butanoate.
Conditions: 40°C for 3 min, 10°C/min to 150°C.

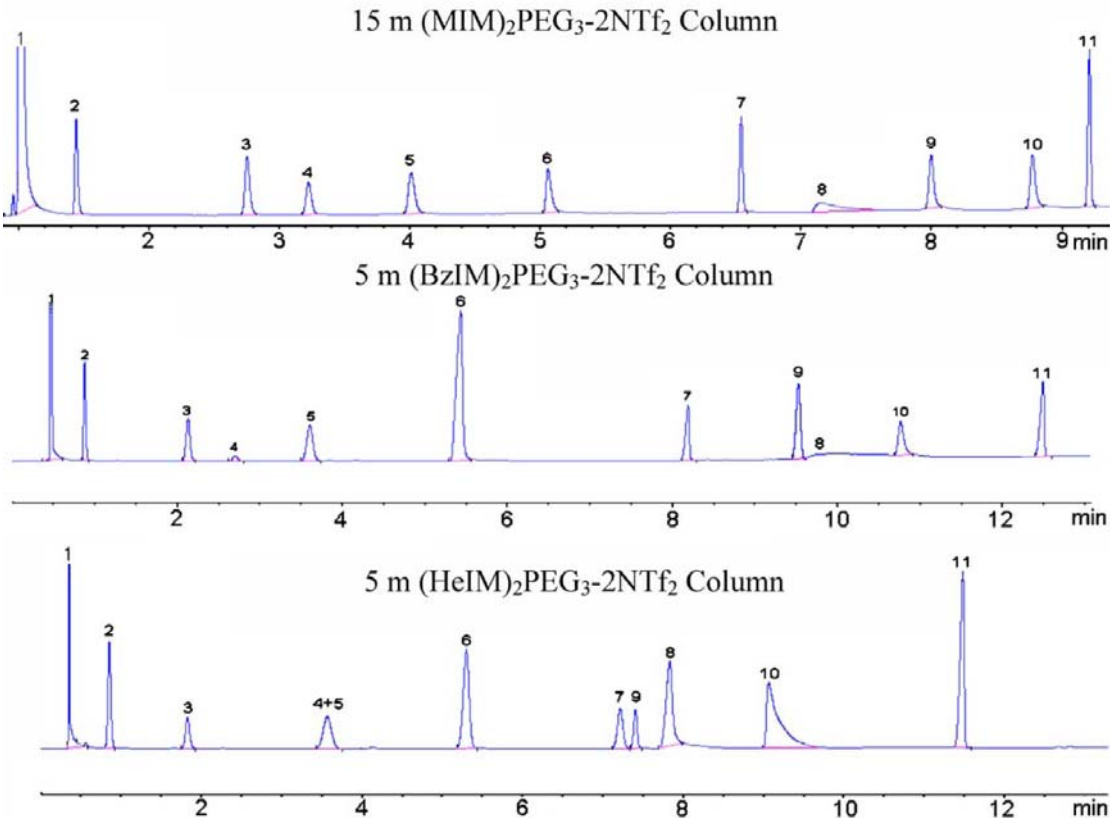

Figure 6.5 Separation of polar and nonpolar compound mixture, 1, dichloromethane; 2, 1-butanol; 3. ethyl hexanoate; 4, octyl aldehydes; 5, cyclohexanone; 6, 1-octanol; 7. tridecane; 8, hexanoic acid; 9, naphthalene; 10, aniline; 11, pentadecane. Conditions for $(MIM)_2PEG_3$-$2NTf_2$ Column: 70°C for 3 min, 10°C/min to 150°C. Conditions for $(BzIM)_2PEG_3$-$2NTf_2$ and $(HeIM)_2PEG_3$-$2NTf_2$ Column: 50°C for 3 min, 6°C/mim to 140°C.

In order to study the relationship between the solvation parameters of the ILs and their corresponding chromatographic behaviors, a mixture of compounds from low polarity to high polarity was injected on the $(MIM)_2PEG_3$-$2NTf_2$ column, the $(BzIM)_2PEG_3$-$2NTf_2$ column, and the $(HeIM)_2PEG_3$-$2NTf_2$ column, respectively (Figure 6.5). As indicated by their solvation parameters, all three stationary phases produced similar retention behaviors and elution orders of the component compounds. However, hexanoic acid showed severely tailing peaks on the $(MIM)_2PEG_3$-$2NTf_2$ column and the $(BzIM)_2PEG_3$-$2NTf_2$ column. In contrast, the $(HeIM)_2PEG_3$-

$2NTf_2$ column showed a perfectly symmetric peak for hexanoic acid, while producing a slightly tailing peak for aniline. This distinct behavior is probably caused by the high hydrogen bond acidity (*b*-term) and correspondingly low hydrogen bond basicity (*a*-term) of the Series 3 type ILs. Thus, aside from anions, the cations can also be engineered to custom make ILs in order to change or improve peak symmetries.

6.5 Conclusions

The solvation parameter evaluation of PEG functionalized dicationic RTILs shows that the dominant interactions for this type of ILs are the dipolar interactions (*s*), hydrogen bond basicity (*a*), followed by dispersion forces (*l*). The nature of the anion affects both the *s*-terms (dipolar interactions) and the *a*-terms (hydrogen bond basicity) of the ILs. The bis(2-hydroxylethylimidazolium)PEG stationary phases have higher hydrogen bond acidities than bis(methylimidazolium)PEG and bis(benzylimidazolium)PEG stationary phases. The cation structure affects both the *b*-terms and *e*-terms of these ILs. The linkage type shows slight influence on the *s* and *a* terms while the linkage length only has an effect on the Series 3 ILs. However the microscopic structure of individual type of ILs may cause some deviations of these solvation behavior patterns. Compared to commercial INNOWAX and Rtx-5 columns, the PEG functionalized dicationic RTILs possess somewhat better separation powers and distinct selectivities of complex samples. With their dual nature and high thermal stability, they show great potential of making a novel class of potent and robust GC stationary phases.

CHAPTER 7

THE APPLICATION OF DICATIONIC ROOM TEMPERATURE DICATIONIC IONIC LIQUIDS IN THE GAS CHROMATOGRAPHIC ANALYSIS OF VOLATILE HERBAL ESSENCES

7.1 Abstract

Room temperature ionic liquids with polyethylene glycol linkages are studied as neat GC stationary phases for the separation of a range of herbal essence samples. Their performances are evaluated against literature results. The results obtained on the neat stationary phases are comparable to those obtained on the best column reported previously, which is a polymerized mixture stationary phase with dicationic IL, monocationic IL and polysiloxane components.

7.2 Introduction

Ionic liquids (IL) have attracted considerable attention over the last a few years in the scientific world. They have been used for a wide range of applications, such as the solvent medium and/or catalyst for organic synthesis[215, 217, 219, 221, 265-267], liquid-liquid extraction,[225-226, 228, 268] additives for HPLC mobile phases,[229-232] and CE run buffers,[269-271] matrix material for matrix-assisted laser desorption ionization (MALDI),[238-239, 272] chiral selectors for enantiomeric resolution,[27, 242] GC stationary phases,[246-247, 251, 253-254, 273-274] etc. In 2005, Armstrong et al. developed hydrocarbon coupled dicationic ionic liquids which greatly increased the thermal stability of RTILs to around 350°C.[247] Later in the same year, totally and partially polymerized dicationic 1,9-Di(3-vinylimidazolium)nonane bis[(trifluoromethyl)sulfonyl]imidate. ($(VIM)_2C_9$-$2NTf_2$) stationary phases were shown to be even more thermally stable and had potential to make exceptional high temperature GC stationary phases.[254] Recently, polymerized and unpolymerized dicationic ionic liquid stationary phases were tested for their chromatographic properties using complex essential oil natural products for the first time.[275] In comparison with

the results obtained on the unpolymerized $(VIM)_2C_9$-$2NTf_2$ column, the commercial polysiloxane (HP-5 MS) column, and the commercial polyethylene glycol column (HP-INNOWAX), The best compound selectivity and resolution was achieved with a stationary phase that was mixed with 1,9-Di(3-vinylimidazolium)nonane bis[(trifluoromethyl)sulfonyl]imidate ((VIM)2C9-2NTf2), 1-Vinyl-3-nonylimidazolium bis[(trifluoromethyl)sulfonyl]imidate (VIMC9-NTf2), and polysiloxane with 1:1:1 ratio.

More recently, a series of polyethylene glycol (PEG) coupled dicationic room temperature ionic liquids were studied for their solvation properties using the linear solvation energy model.[276] The oxygen containing linkage and the triflate anion both contributed to the higher dipolarity and hydrogen bond basicity of these ILs. Also these ILs possess considerable hydrogen bond acidity, which has been found to be negligible for most of the commercial columns available nowadays.[1, 263-264] Superior separations of alkane and alcohol mixtures and flavor and fragrance mixtures were found for the new IL columns. In this work, three herbal essence samples and the Grob test mixture were separated on these new PEG coupled dicationic IL stationary phases so their performance can be evaluated against the results obtained from a previous study.[275]

7.3 Experimental

7.3.1 Materials

Three ionic liquids, 1,11-di(3-methylimidazolium)-3,6,9-trioxaundecane bis(trifluoromethane)sulfonimide ((MIM)2PEG3-2NTf2), 1,14-di(3-(2-hydroxylethyl)limidazolium)-3,6,9,12-tetraoxaundecane bis(trifluoromethane)sulfonimide ((HeIM)2PEG4-2NTf2)), and 1,11-di(3-methylimidazolium)-3,6,9-trioxaundecane trifluoromethanesulfontate ((MIM)2PEG3-2TfO) were synthesized as reported previously.[1, 276] Dichloromethane (purity of 99.9% or greater) was purchased from Aldrich (Milwaukee, WI, USA). Helium carrier gas was purchased from American Air Liquide (Houston, TX, USA). Three samples of essential oils were purchased from Aromaland (Santa Fe, NM. USA). The Grob test mixture was also obtained from Aldrich

(Milwaukee, WI, USA). The HP-5 MS and HP-INNOWAX column was purchased from Agilent Technologies (Santa Clara, CA). The bare GC capillaries were purchased from Supelco (Bellefonte, PA, USA).

7.3.2 Methods

A 30 m (MIM)2PEG3-2NTf2, 15 m (MIM)2PEG3-2TfO column, and a 30 m (HeIM)2PEG4-2NTf2 column are coated via the static coating method. The structures of these ILs are shown in Figure 7.1. The ionic liquids were dissolved in dichloromethane to make a coating solution of 0.25% (w/v). The capillary is filled with the coating solution with one end clamped tightly to ensure a complete seal. High vacuum is applied on the other end while the temperature of the column is maintained at 40°C in a water bath. The vacuum is controlled so that the coating rate is maintained at 3-4 loops per hour. After coating, the column is conditioned from 30°C-120°C with the rate of 3°C/min. The column efficiency was tested at 100°C with a carrier gas (helium) flow rate of 1 ml/min. The efficiency of these columns is between 2200 and 3000 plates/m. The test conditions for each sample are listed in Table 8.1

7.3.3 Equipment

A GC-MS instrument from Agilent Technologies (Santa Clara, CA, USA) was equipped with a 6890N network GC system, a 5975 inert mass selective detector, a 7683B series autosampler injector and aG1701DA GC/MSD ChemStation data collection software. All measurements were taken with a flow rate of 1.0 mL/min, an injector temperature of 250°C, a split ratio of 100:1 and a MS transfer line temperature of 280°C. Identification of the compounds was based on comparison of their mass spectra with those of the NIST Library.

7.4 Results and Discussion

7.4.1. Separation of essential oils

Two IL GC columns are studied for the separation of essential oils, the 30 m (MIM)2PEG3-2NTf2 column A and the 15 m (MIM)2PEG3-2TfO column B (see Figure 7.1). The separation of the three samples are shown in Figure 7.2 (fennel), 7.3 (cinnamon) and 7.4 (nutmeg),

respectively. The separation conditions for each sample are listed in Table 7.1. The results are compared with the mixture stationary phase C ((VIM)2C9-2NTf2, VIMC9-NTf2, and polysiloxane 1:1:1 mixture), the neat (VIM)2C9-2NTf2 stationary phase D, the neat polysiloxane stationary phase E and the neat polyethylene glycol stationary phase F. The data for column C through F are obtained from Reference.[275] According to previous studies, the mixture column shows the best separation for these samples in terms of selectivity and resolution power.[227]

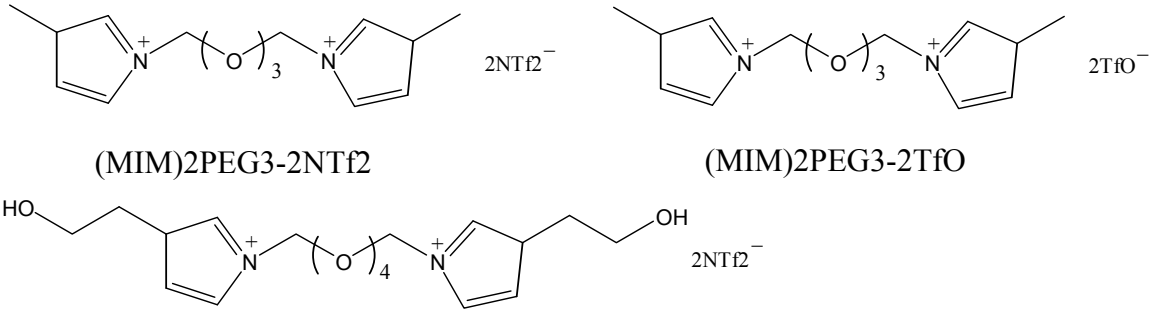

(MIM)2PEG3-2NTf2 (MIM)2PEG3-2TfO

(HIM)2PEG4-2NTf2

Figure 7.1 Structures of PEG functionalized RTILs used.

Table 7.1 Temperature programs for the separation of essential oils.

Column	Fennel	Cinnamon	Nutmeg
A	60°C(10min), 8°C/min, 180°C (10min)	60°C(5min), 8°C/min, 180°C (10min)	60°C(10min), 8°C/min, 180°C (5min)
B	60°C(10min), 8°C/min, 200°C	60°C(5min), 8°C/min, 200°C (5min)	60°C(10min), 8°C/min, 200°C
C	60°C(5min), 8°C/min, 180°C (10min)	60°C(5min), 10°C/min, 200°C(5min),	60°C(10min), 10°C/min, 200°C(6min)
D	60°C(10min), 8°C/min, 200°C (5min)	60°C(5min), 8°C/min, 180°C(10min),	60°C(10min), 8°C/min, 200°C(10min)
E	60°C(5min), 8°C/min, 200°C (10min)	60°C(5min), 8°C/min, 190°C(10min),	60°C, 2°C/min, 100°C, 8°C/min, 180°C/(5min)
F	60°C(5min), 8°C/min, 190°C (10min)	60°C(5min), 10°C/min, 220°C(15min),	60°C(5min), 10°C/min, 220°C(10min)

Column A: (MIM)2PEG3-2NTf2
Column B: (MIM)2PEG3-2TfO
Column C: (VIM)2C9-2NTf2, VIMC9-NTf2, and polysiloxane 1:1:1 mixture, polymerized
Column D: (VIM)2C9-2NTf2
Column E: HP-5MS
Column F: HP-INNOWAX

For the separation of fennel oil (Figure 7.2), column C was reported to show better separation of the sample components than columns D and E. Also because of its polysiloxane composition, it showed better resolution for nonpolar hydrocarbons compared to the polyethylene glycol based column F. In this work, All 11 target compounds were baseline separated on column A and B. The same elution order was found on these two columns, as that on columns C and F. The hydrocarbons also were separated as well. Also, the selectivity between fenchone (peak 7) and estragole (peak 8) is greater on column A and B. In fact, on column B, all oxygenated polar species from compound 8 to compound 11 are better separated from the nonpolar hydrocarbon clusters of compounds 1 to 7. This illustrates the greater selectivity of triflate-based stationary phases to retain and separate polar molecules through dipole-dipole and hydrogen bonding interactions.[275] Also, the separations on the new neat stationary phases appeared to be better than on any other neat stationary phase (column B, C and D).

Analogous results were found for the separation of cinnamon oil (Figure 7.3). All 13 peaks are well separated with identical elution order on column A and column C. Although peak 9 (2-methoxy-3-(2-propenyl)phenol) and peak 10 ((E)-cinnamaldehyde) are not baseline separated on column A, they eluted with great resolution on column B, which indicates the structural influence of these ILs upon their chromatographic behaviors. There is a switch of elution order of peak 7 (isosafrole) and 8 (*α*-caryophyllene) on column B. The retention increase for peak 7 is probably due to a stronger stationary phase-solute molecule interactions induced by the higher polarity of the triflate stationary phase. This also explains why compound 9 is also retained longer on this column. Furthermore, the high hydrogen bond basicity of triflate stationary phase generated much longer retention for acidic species, such as compounds 5 and 9. As an overall effect, the cinnamon components are chromatographically much more dispersed on column B.

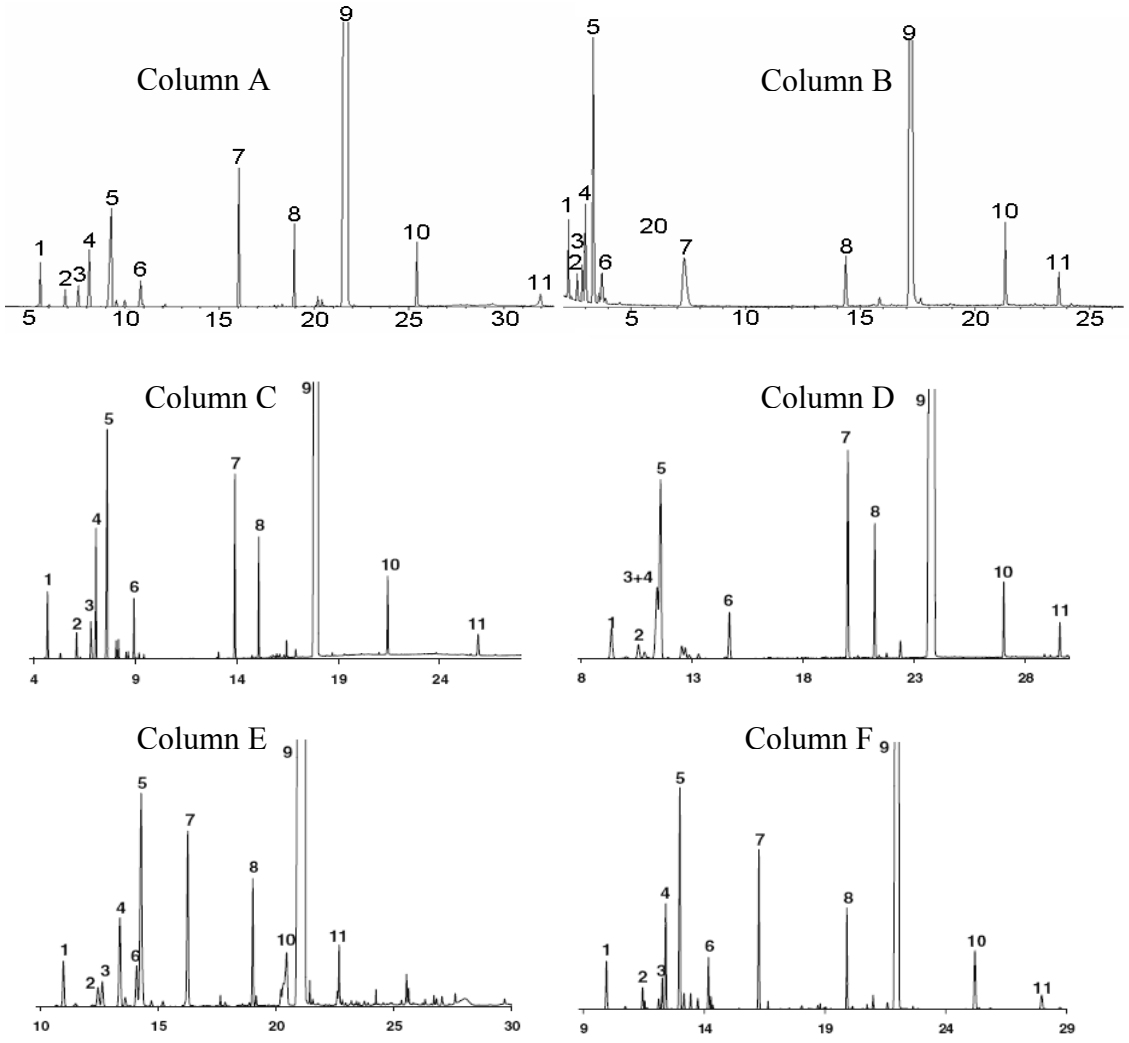

Figure 7.2 Separation for fennel. 1. *α*-pinene 2. *β*-pinene 3. *β*-myrcene 4. *α*-phellandrene 5. D-limonene 6. *p*-cymene 7. fenchone 8. estragole 9. trans-anethole 10. 4-methoxybenzaldehyde 11. *p*-acetonylarisole.
See Table 7.1 for column composition.

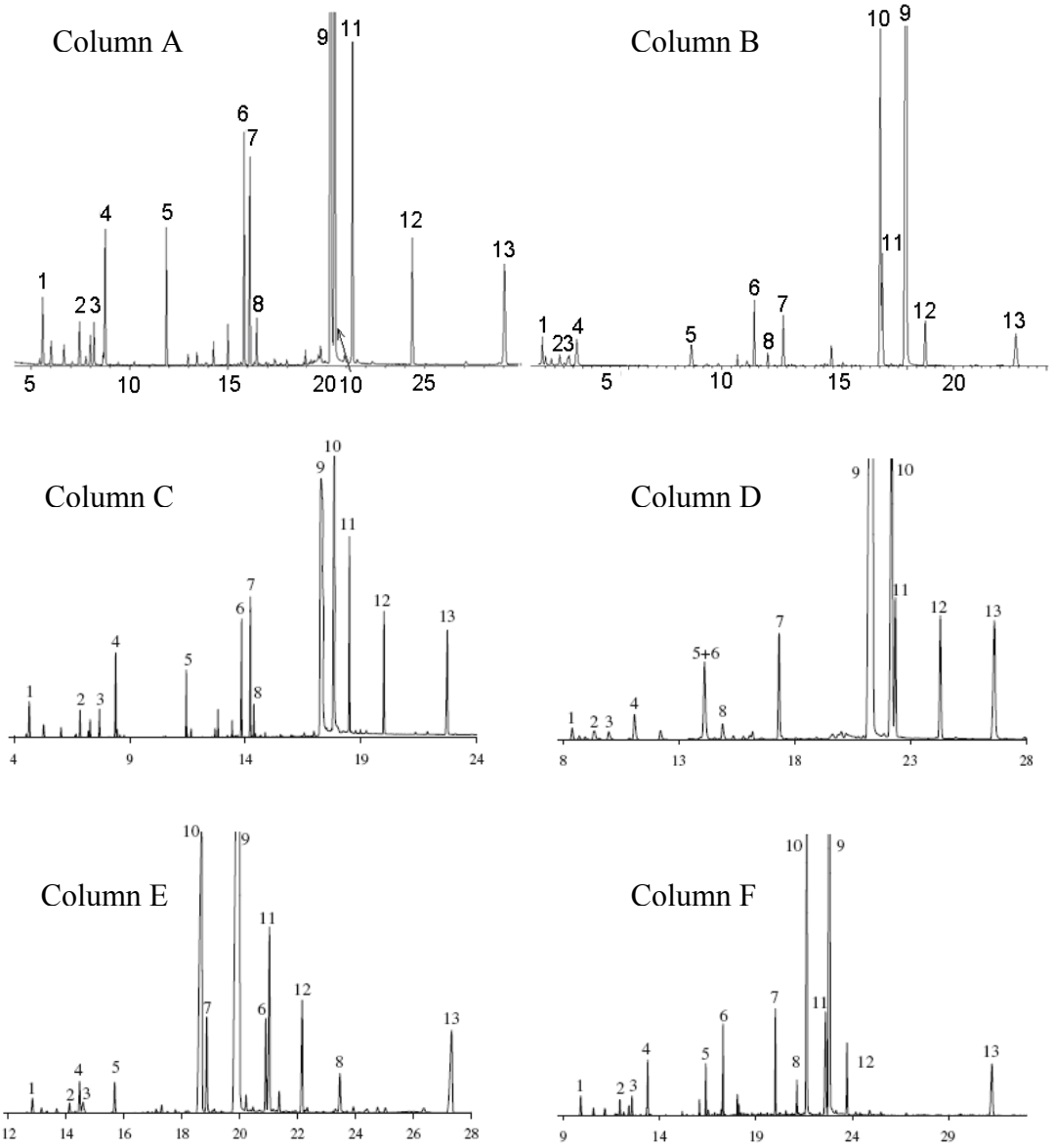

Figure 7.3 Separation for cinnamon. 1. *α*-pinene 2. *α*-phellandrene 3. *β*-phellandrene 4. 1-methyl-2-(1-methylethyl)benzene 5. 3, 7-dimethyl-1, 6-octadien-3-ol 6. *β*-caryophyllene 7.isosafrole 8. *α*-caryophyllene 9. 2-methoxy-3-(2-propenyl)phenol 10. (E)-cinnamaldehyde 11. (E)-cinnamyl acetate 12. 2-methoxy-4-(2-propenyl)phenol acetate 13. benzyl benzoate.

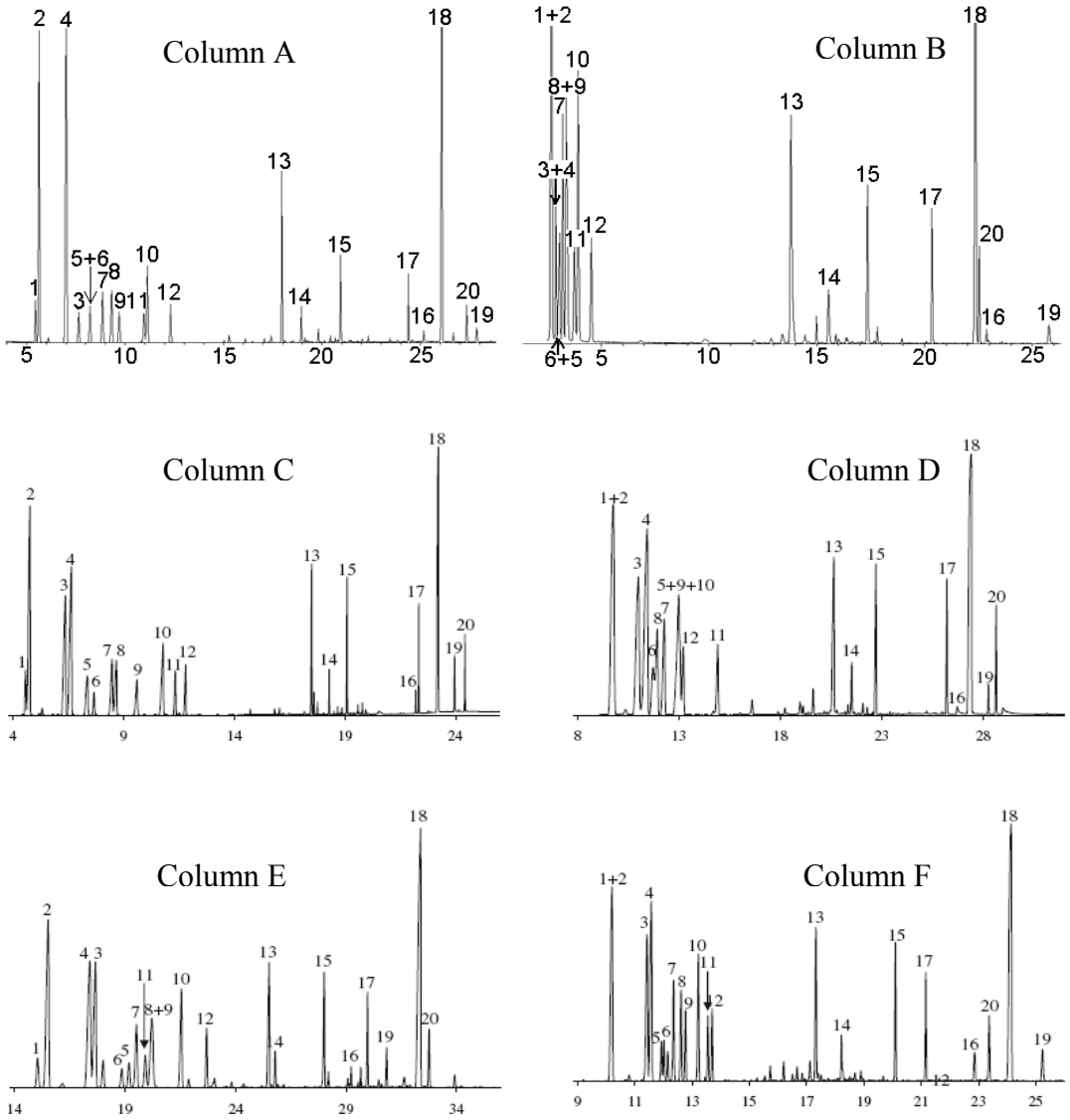

Figure 7.4 Separation for nutmeg. 1. 2-methyl-5-(1-methylethyl)-bicyclo[3, 1, 0]hex-2-ene 2. *α*-pinene 3. *β*-pinene 4. 4-methylene-1-(1-methylethyl)bicyclo[3, 1, 0]hexane 5. 3-carene 6. *α*-phellandrene 7. 4-carene 8. D-limonene 9. *β*-phellandrene 10. 1-methyl-4-(1-methylethyl)-1, 4-cyclohexadiene 11. 1-methyl-2-(1-methylethyl)benzene 12. 1-methyl-4-(1-methylethylidene)cyclohexene 13. 4-methyl-1-(1-methylethyl)-3-cyclohexen-1-ol 14. terpineol 15. isosafrole 16. eugenol 17. methyl isoeugenol 18. myristicin 19. isoeugenol 20. elemicin.

The stationary phase E produced significantly less retention for polar molecules, such as compounds 4, 7, and 10, while showing considerably stronger interaction with nonpolar compounds 6 and 8. Thus, for this sample, the triflate column B most resembles the high

polarity stationary phase F. In contrast, column A behaves almost identical with stationary phase C.

Figure 7.4 shows the separation of nutmeg essential oil. While most compounds showed the same elution order on columns A and C, peak 3 (*β*-pinene) and 4 (4-methylene-1-(1-methylethyl)bicyclo[3, 1, 0]hexane), 10 (1-methyl-4-(1-methylethyl)-1, 4-cyclohexadiene) and 11 (1-methyl-2-(1-methylethyl)benzene), 16 (eugenol) and 17 (methyl isoeugenol), 19 (isoeugenol) and 20 (elemicin) have their elution order switched. Again, the triflate stationary phase B successfully separated the cluster of polar compounds from the cluster of nonpolar compounds.

8.4.2. Separation of Grob test mixture

The lack of compound diversity within the essential oil samples failed to adequately reveal the broader separation capability of these new IL stationary phases. The essential oils are mainly composed of monoterpenes, sesquiterpenes, oxygenated and/or aromatic compounds (ethers, ketones, aldehydes, alcohols, esters, etc.). The Grob test mixture including compounds of low polarity (decane and undecane) to high polarity (dicyclohexylamine and 2-ethylhexanoic acid) was examined on a $(MIM)_2PEG_3$-2NTf2 (A), a $(MIM)_2PEG_3$-2TfO (B) and a $(HeIM)_2PEG_3$-2NTf2 (G) column. The same test mixture also was separated on stationary phase C and the two commercial columns (E and F). The separation results are shown in Figure 7.5. All 12 components were baseline separated on the (MIM)2PEG3-2TfO stationary phase (B) as well as on the INNOWAX stationary phase (F). Coelution of methyl undecanoate and dicyclohexylamine was observed on the HP-5 MS column and a partial separation of methyl undecanoate and 2, 6-dimethylphenol was observed on the (MIM)2PEG3-2NTf2 column (A). No separation of methyl decanoate and 2, 6-dimethylphenol was observed on column C.

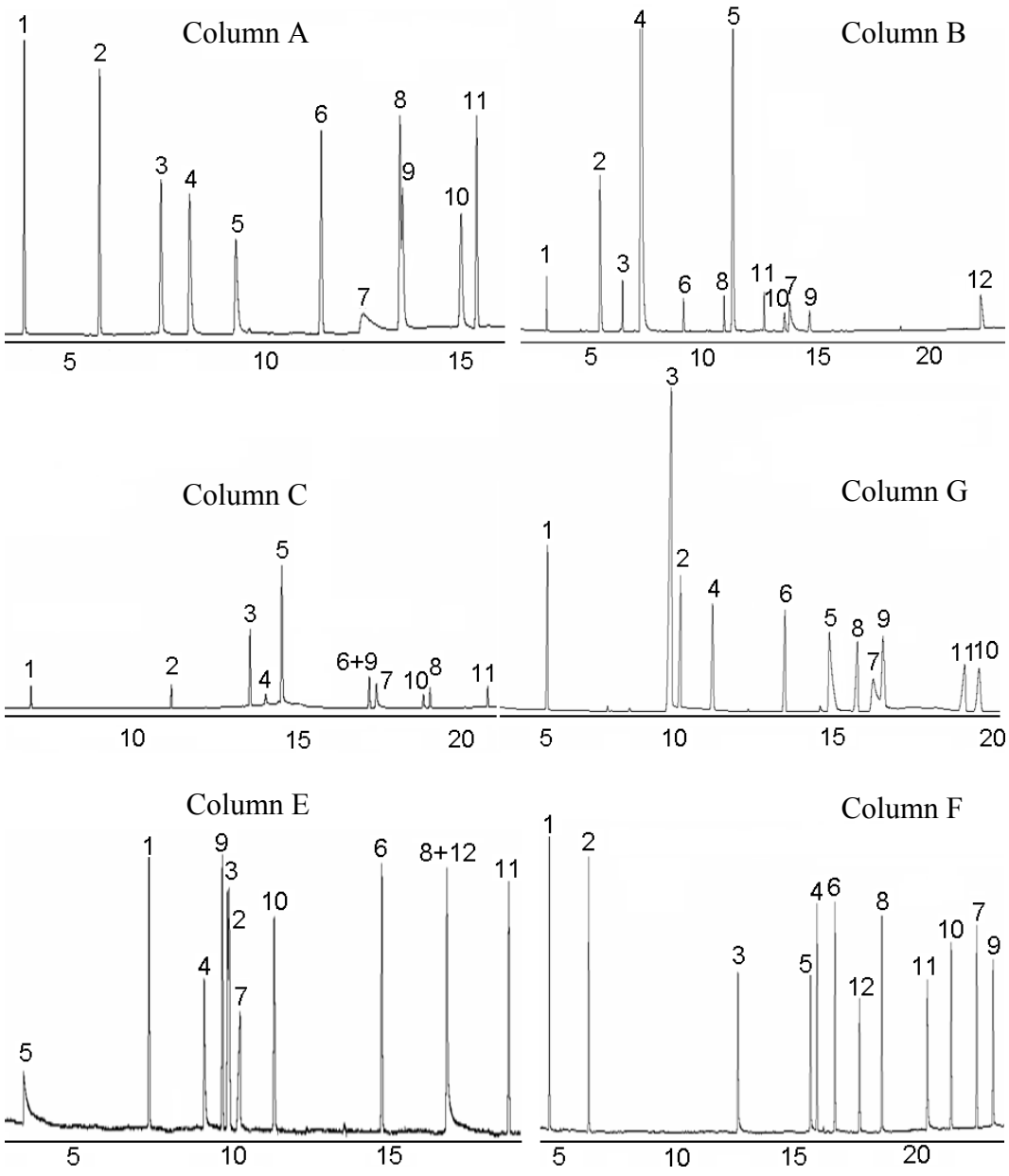

Figure 7.5 Separation for Grob test mixture. 1. n-decane 2. n-undecane 3. 1-nonanal 4. 1-octanol 5. 2, 3-butanediol 6. methyl decanoate 7. 2-ethylhexanoic acid 8. methyl undecanoate 9. 2, 6-dimethylphenol 10. 2, 6-dimethylaniline 11. methyl dodecanoate 12. dicyclohexylamine.
See Table 8.1 for composition of column A-F, column G: (HIM)2PEG4-2NTf2.

It is obvious that polar compounds, such as 2,6-dimethylaniline and 2-ethylhexanoic acids, were retained longer on the high polarity INNOWAX column than on the low polarity Rtx-5 column, while the nonpolar compounds had greater retention on the Rtx-5 than on the INNOWAX stationary phase. In terms of relative retention of polar molecules, it is clear that the IL columns exhibited similar polarity to the polyethylene glycol stationary phase. However, the elution order for the intermediate to high polarity molecules was different on the IL columns and was indicative of the unique selectivity of these stationary phases. The polarity of the mixture column lies in between the nonpolar HP-5 MS column and the (MIM)2PEG-2NTf2 column due to its polysiloxane composition.

Furthermore, the individual IL columns also produced different selectivities corresponding to their different structures. While the IL column produced the same elution order for alkanes and straight chain alcohols, their retention behavior for acidic and basic species varied considerably. The higher hydrogen bond basicity of triflate stationary phase generated the greatest retention for 3-butanediol, 2-ethylhexanoic acid and 2, 6-dimethylphenol. It appears that these new PEG functionalized IL stationary phases have good separating power for complex compound mixtures and their selectivity can be tuned via use of different cations and anions.

7.5 Conclusions

The neat PEG functionalized dicationic ILs showed better separating power and different selectivities for the components of complex essential oil samples compared to the neat (VIM)2C9-2NTf2 column, polysiloxane column and a polyethylene glycol column. The results achieved on the (MIM)2PEG3-2NTf2 column was analogous to that found on the mixture column. The selectivity observed with the (MIM)2PEG3-2TfO column were distinct when compared to all other columns.

The ether moieties within the PEG linkage allowed polar compounds to be retained longer on the (MIM)2PEG3-2NTf2 column than on the mixture column. The (MIM)2PEG3-2TfO

stationary phase had apparent polarity and hydrogen bonding basicity approaching that of the PEG stationary phase. Furthermore, it is capable of better separation between the polar and nonpolar compound clusters. The (HeIM)2PEG4-2NTf2 stationary phase showed good retention for compounds capable of hydrogen bonding because of its hydroxyl moieties. The (MIM)2PEG3-2TfO IL has stronger interaction with acidic compound species due to its high hydrogen-bond basicity. The PEG–linked IL stationary phases permit separations that previously were only obtained on mixed stationary phases. It appears that they will be a useful addition to the current “pool” of commercial stationary phases.

PART THREE DEVELOPMENT OF NEW CHIRAL STATIONARY PHASES

FOR GC AND HPLC

CHAPTER 8

IONIC CYCLODEXTRINS IN IONIC LIQUID MATRICES AS CHIRAL STATIOANRY PHASES FOR GAS CHROMATOGRAPHY

8.1 Abstract

Ionic liquids (ILs) are used to dissolve ionic cyclodextrin (CD) derivatives to produce a new type of gas chromatographic chiral stationary phase. Compared to the previous studies with neutral cyclodextrin chiral selectors, the new ionic liquid-based stationary phase exhibits broader enantioselectivities, up to 7 times higher efficiencies, and greater thermal stabilities. When compared to the analogous commercial column with polysiloxane matrix, it exhibits different selectivities, more symmetric peak shapes and often complementary separations. The most profound separation enhancements are usually found for more polar analytes.

8.2 Introduction

Cyclodextrins (CDs) have been used successfully in different chromatographic techniques for enantiomeric separations.[20, 167, 176, 206, 277-280] Modified cyclodextrins constitute the dominant type of chiral selectors for gas chromatography. They can be coated either as neat chiral stationary phases (CSPs) if they are viscous liquids at ambient temperatures, or as cyclodextrin-polysiloxane mixtures if they possess high melting points. Extensive studies have been performed on the use of different polysiloxanes as cyclodextrin solvent matrices.[281-282] However, no comparable applicability has been obtained with any solvent matrices other than polysiloxanes.

Room temperature Ionic liquids (RTILs) possess unique physicochemical properties including low melting points, negligible vapor pressures, wide liquid ranges, non-flammability, high thermal stabilities, tunable viscosities and variable polarities. They have been developed

as a very important and new class of GC stationary phase materials over the last a few years.[246-247, 276, 283-284]

A single report has appeared on the use of achiral ionic liquids as stationary phase solvents for derivatized cyclodextrins in 2001.[252] In this work, methylated *β*-cyclodextrins were dissolved in 1-butyl-3-methylimidazolium chloride (BMIM-Cl) and the column performance was evaluated against that of analogous polysiloxane-based commercial columns. It was found that the IL-based column efficiencies were up to ten times higher than the commercial columns. However, it separated only about a third of the racemic analytes that could be separated on the commercial columns. A reason for the narrower range of enantioselectivity was proposed by the authors and confirmed in later reports.[285-286] It was that the small BMIM-Cl ion pair can be included in the cyclodextrin cavity and consequently reduced the inclusion complexation interaction between the chiral selector and analyte molecules, which can be crucial for chiral recognition of some molecules. Conversely, molecules that separated by an external adsorption process were unaffected and showed excellent resolutions (because of the higher efficiencies).[22] Since this report, neat chiral ionic liquids have been used as GC chiral stationary phases,[27] but there have been no further developments involving functionalized cyclodextrins dissolved in ionic liquids. The question arises, can a system be developed that combines the higher efficiency of the IL matrix based chiral stationary phases as well as the superb selectivity of the polysiloxane based chiral stationary phases. Such a stationary phase could greatly enhance the GC separation of enantiomers.

In this work, two strategies are proposed to reduce the accessibility of IL matrices to the cyclodextrin cavity while maintaining the higher efficiencies observed in the 2001 study,[252] they are: 1. use of bulkier ILs to make the IL molecule less able to fit inside the cyclodextrin cavity; and 2. attachment of pendent charged groups to the cyclodextrin structure, thereby providing an electrostatic barrier to other cations. In addition, we expect that by introducing ionic moieties to the cyclodextrin molecule, stronger solute-solvent interactions will occur, thereby enhancing the

limited solubility of cyclodextrins in many ionic liquids. Also these bulky charged moieties could offer different selectivities.

Charged cyclodextrin derivatives have been widely employed as chiral selectors in capillary electrophoresis (CE) for years.[176, 280, 287-289] However, the use of charged cyclodextrins as chiral selectors has not been reported in GC. In this study, permethylated mono-6-(butylimidazolium)-cyclodextrin (BIM-BPM) and mono-6-(tripropylphosphonium)-cyclodextrin (TPP-BPM) were synthesized and dissolved in various dicationic and tricationic ionic liquids and examined as GC chiral stationary phases. The performance of these columns was compared to that of their neutral cyclodextrin containing IL-based predecessors. The new IL column was also evaluated against the commercial polysiloxane-based CSPs with analogous chiral selectors.

8.3 Experimental

8.3.1 Materials

The reagents, imidazole, 1-methylimidazole, 1-butylimidazole, 1-(2-hydroxyethyl) imidazole, 1-tosylimidazole, tripropylphosphine, tris(2-aminoethyl)amine, pentaethylene, glycol, 1,12-dibromododecane silver trifluoromethanesulfonate (TfO), lithium bis(trifluoromethanesulfonyl)imide (NTf2), *p*-toluenesulfonyl chloride, *β*-cyclodextrin, methyl iodide, sodium hydroxide, sodium hydride, ammonium chloride (NH4Cl), trifluoroacetic anhydride and silicone OV-101 were purchased from Sigma-Aldrich (Milwaukee, WI). The solvents, anhydrous dimethyl sulfoxide (DMSO), dimethylformamide (DMF), acetone, chloroform were also obtained from Sigma-Aldrich. Dichloromethane, ethyl acetate and toluene were obtained from EMD Chemicals (Gibbstown, NJ). The 70 test compounds were attained from different commercial sources (Sigma-Aldrich, etc.). Chiraldex BPM column (2,3,6-tri-O-methyl-*β*-cyclodextrin, 30 m * 250 *μ*m i.d. *0.12 *μ*m film thickness) was obtained from Supelco (Bellefonte, PA). A 10 m segment of this column was tailored and used for testing.

8.3.2 Methods

6-(butylimidazolium)-*β*-cyclodextrin tosylate was prepared following the literature procedures.[290] First, 6-tosyl-*β*-cyclodextrin was synthesized by reacting 35 g of *β*-cyclodextrin with 8 g of 1-tosylimidazole in 350 mL of deionized water. After the addition of 50 mL of aqueous NaOH (20% w/v), the solids were filtered from the solution and the filtrate was collected and subsequently neutralized by NH4Cl, washed by acetone and vacuum dried overnight. Subsequently, 13 g of the synthesized 6-tosyl-*β*-cyclodextrin was weighed out and reacted with 3 g of 1-butyllimidazole in 25 ml DMF at 100℃ for two days. Acetone was then added to induce precipitation at ambient temperature. The reaction workup involved filtration of the product followed by acetone washing and vacuum drying to afford the dry white powder of 6-(butylimidazolium)-*β*-cyclodextrin. The ^{1}H NMR spectrum indicates the 6-position substitutions on the cyclodextrin primary rim. Subsequently, this material was permethylated using the method described in a 1984 publication.[291] Resultantly, Permethyl 6-(butylimidazolium)-*β*-cyclodextrin iodide (BIM-BPM-I) was obtained as the final product, which can be exchanged to trifluoromethanesulfonimide ($NTf2^-$) and trifluoromethanesulfonate (TfO) salt if needed. 6-(tripropylphosphonium)-*β*-cyclodextrin tosylate is prepared and permethylated in the same fashion. The structure of the two charge bearing cyclodextrins are illustrated in Figure 8.1. Dicationic and tricationic ionic liquids were synthesized according to the literature guidelines [247, 276, 283-284] and their structures are depicted in Figure 8.2.

For comparison purposes, all GC columns were prepared following the literature recipe.[252] The derivatized cyclodextrins were dissolved in ionic liquids to make solution of 25% (w/w) concentration. The mixture was then dissolved in dichloromethane to give a coating solution of 0.45% (w/v) concentration. The static coating method was used in this work. In a water bath maintained at 40^{o}C, the coating solution was injected to completely fill a segment of the salt pretreated capillary. The capillary is then sealed at one end and the solvent is evaporated at a steady speed from the other end under vacuum. Coated columns were flushed with dry helium

gas overnight and conditioned at 120^{o}C for two hours prior to use. Column efficiency was measured using naphthalene at 100^{o}C. Columns prepared in this study are made of a uniform length of 10 meters. They are all determined to possess efficiencies of 4000~5000 plates/m and film thickness of 0.25 μm.

The samples assayed by thermogravimetric analysis (TGA) were made by dissolving target cyclodextrins in ionic liquids (25%, w/w). These solutions were analyzed in 20 mg aliquot and they were heated in a platinum pan from 100°C to 500°C at 10°C/min in a dynamic nitrogen atmosphere. The decomposition profile for each sample is recorded and the 5% weight loss temperatures are marked to determine the stationary phase thermal stabilities.

8.3.2 Equipment

The GC equipment used was an Agilent (Columbia, MD) model 6892N (G 1540N) gas chromatograph equipped with a flame ionization detector and Agilent ChemStation data acquisition software. All analyses were performed isocratically with a helium carrier gas flow rate of 1 mL/min and a split ratio of 100/1. The injector and detector temperature was set at 250ºC and 300ºC, respectively. TGA measurements were performed using a TGA 2050 (TA Instruments Inc., New Castle, DE, USA).

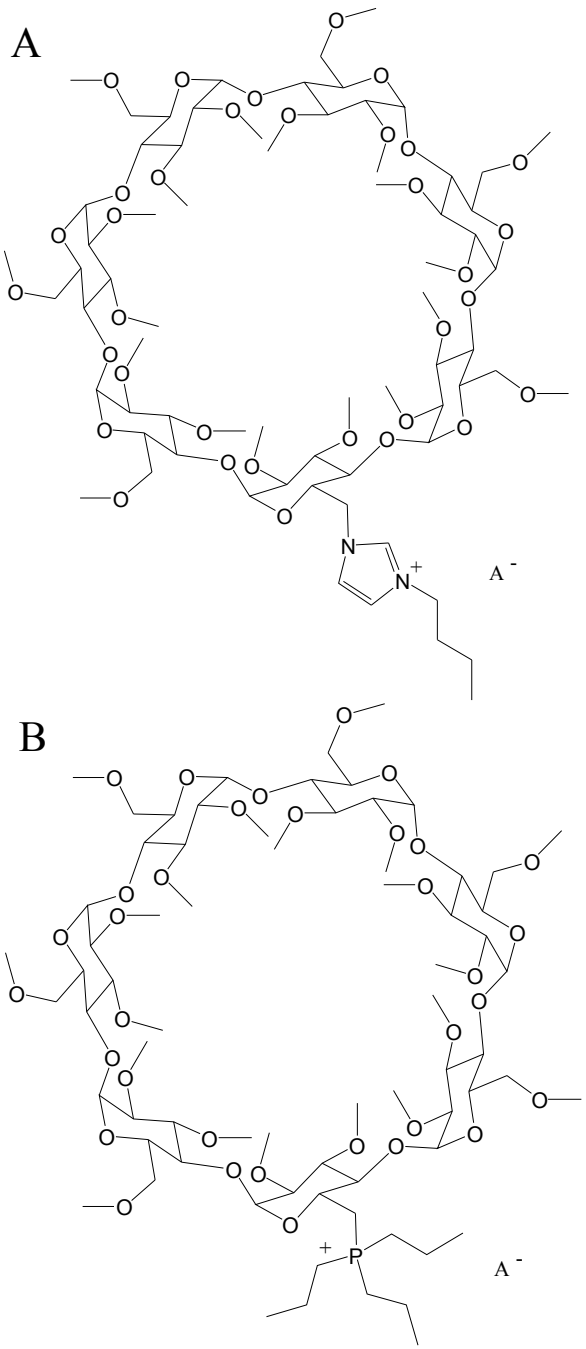

Figure 8.1 Structures of ionic permethyl *β*-cyclodextrins used in this study. A. BIM-BPM-A, B. TPP-BPM-A

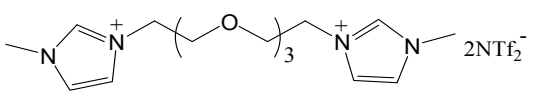

MIM2PEG3-2NTf2

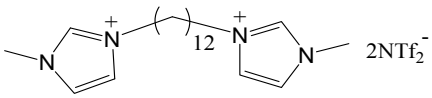

MIM2C12-2NTf2

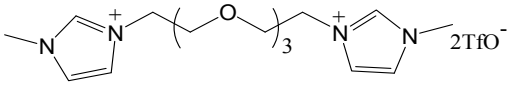

MIM2PEG3-TfO

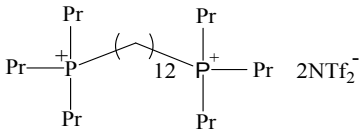

TPP2C12-2NTf2

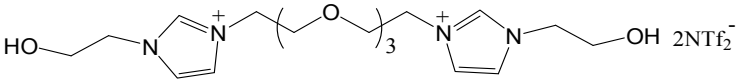

HeIM2PEG3-2NTf2

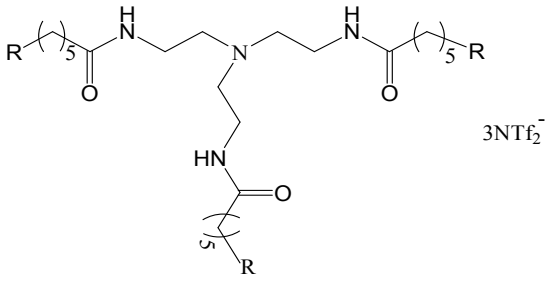

D5

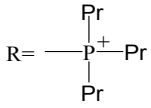

Figure 8.2. Structures of the ionic liquid matrices used for the dissolution of chiral selectors

8.4 Results and Discussion

The structures of the modified cyclodextrins used in this study are shown in Fig 1. They are permethyl 6-(alkylimidazolium)-*β*-cyclodextrin (BIM-BPM) and permethyl 6-(tripropylphosphonium)-*β*-cyclodextrin (TPP-BPM) paired with iodide, NTf2, and triflate anions.

Different cyclodextrin and ionic liquid combinations were evaluated for optimization of the stationary phase composition.

8.4.1 Optimization of Phase A

8.4.1.1 Optimization of the chiral selector

The two cyclodextrin derivatives investigated as chiral selectors were permethyl-6-(alkylimidazolium)-*β*-cyclodextrin iodide (BIM-BPM-I) and permethyl-6-(tripropylphosphonium)-*β*-cyclodextrin iodide (TPP-BPM-I). They were dissolved in MIM2PEG3-2NTf2 (1,11-di(3-methylimidazolium)-3,6,9-trioxaundecane bis(trifluoromethane)sulfonimide) (see Figure 8.2) and coated as GC stationary phases using the same procedures (see Experimental).

Both columns showed superb efficiencies in the range of 4000~5000 plates/m. However the enantioselectivity of the TPP-BPM-I stationary phase was relatively low. For example, the enantioselectivity of *α*-ionone (α_{ionone}) is only 1.03 on this stationary phase. Even when TPP2C12-2NTf2 (1,12-di(tripropylphosphonium)dodecane bis(trifluoromethane)sulfonimide) was used as the solvent, the enantioselectivity remained low for the TPP-BPM-I chiral selector. On the contrary, the BIM-BPM-I containing IL stationary phase provided not only high efficiencies but also high selectivities (see separation of *α*-ionone in Figure 8.3). Therefore, the BIM-BPM-I matrix appears to be quite advantageous compared to its tripropylphosphonium derivatized counterpart. It appears that while high efficiency columns can be achieved with both these ionic chiral selectors, the nature of the ionic functionality has a significant impact on the enantioselectivity of the stationary phases.

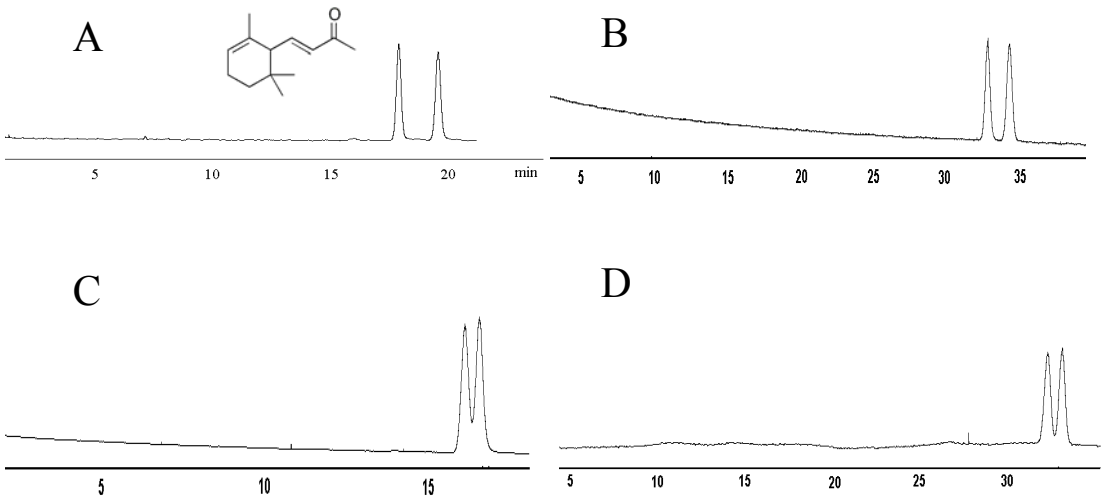

Figure 8.3 Separation of *α*-ionone on: A. BIM-BPM-I plus MIM2PEG3-2NTf2 B.BIM-BPM-I plus TPP2C12-2NTf2 C. TPP-BPM-I plus MIM2PEG3-2NTf2 D. TPP-BPM-I plus TPP2C12-2NTf2.
Helium at 1 mL/min

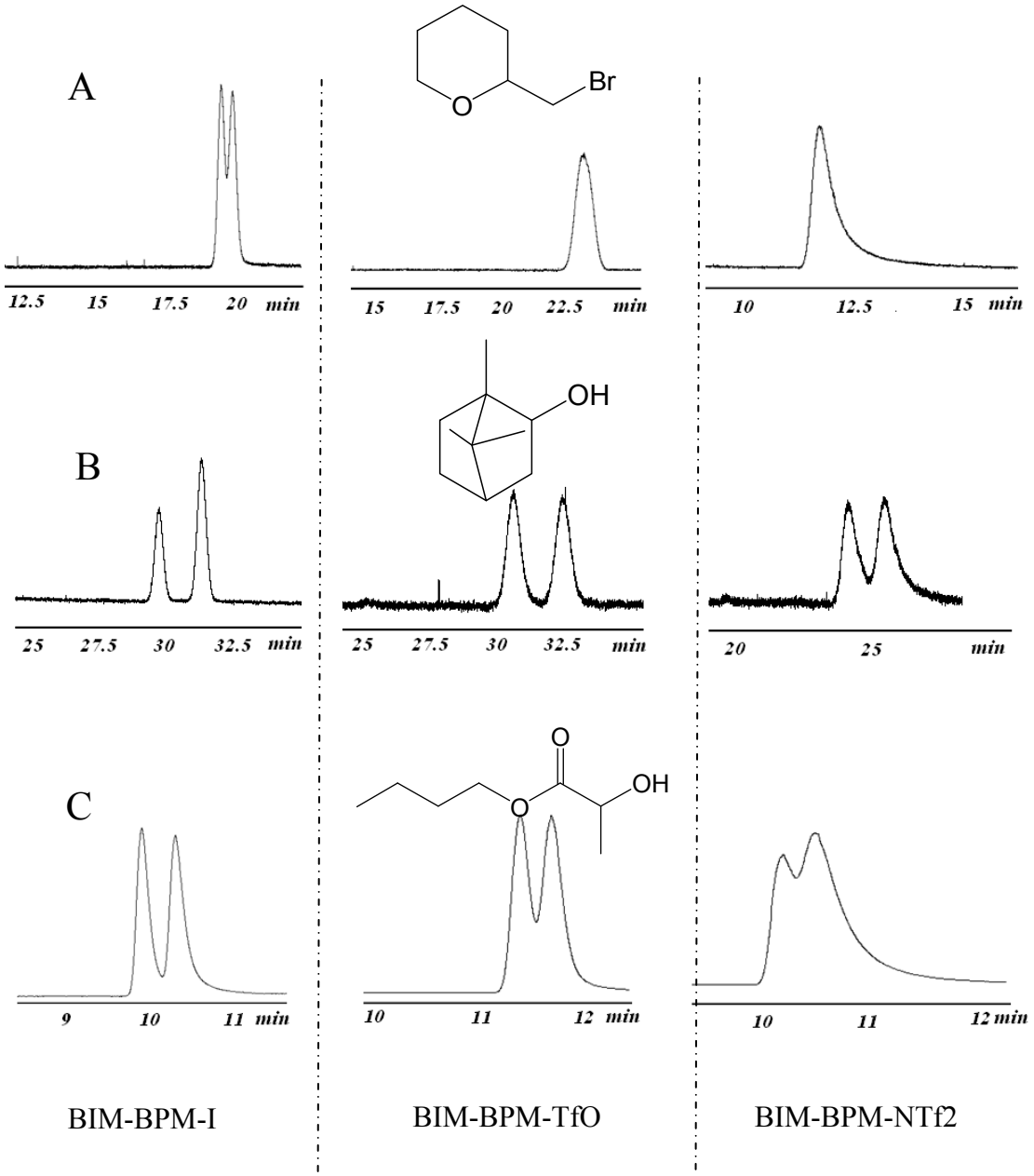

Figure 8.4 Examples of separations achieved on BIM-BPM-I, BIM-BPM-TfO, and BIM-BPM-NTf2 containing columns. Helium at 1 mL/min
A. Separation of 2-(bromomethyl) tetrahydro-2*H*-pyran, 60 °C
B. Separation of borneol, 80 °C
C. Separation of butyl lactate, 80 °C

After BIM-BPM was determined to be the best cationic moiety for the chiral selector, attention was focused on the counter ion that provides the best efficiency, selectivity and thermal stability. For this purpose, BIM-BPM-I, permethyl-6-(alkylimidazolium)-*β*-cyclodextrin bis(trifluoromethane)sulfonimide (BIM-BPM-NTf2), and permethyl-6-(alkylimidazolium)-*β*-cyclodextrin trifluoromethanesulfonate (BIM-BPM-TfO) were prepared for evaluation. To obtain their thermal stabilities, they were individually dissolved in MIM2PEG3-2NTf2 (25%, w/w) and subjected to thermogravimetric analysis (TGA). As is indicated by the TGA readings, when mixed with MIM2PEG3-2NTf2, the three compounds yielded very similar decomposition/volatilization profiles at the temperature range of 100~250°C, all with a weight loss of approximately 5% at 250°C. Thus, at normal chiral GC operating temperatures, the anion identity has little effect on the thermal stability of the chiral selector molecules.

Subsequently, analytes with a range of different functionalities were assayed on the three columns to evaluate the impact of the anions on the stationary phase enantioselectivities. A few examples are given in Figure 8.4. Symmetrical peaks were observed for these analytes on both the BIM-BPM-I and BIM-BPM-TfO columns. However, BIM-BPM-NTf2 induces severe tailings for these analytes. Since BIM-PMBCD-I and BIM-BPM-TfO exhibit similar chromatographic behaviors, the iodide salt form of the chiral selector was used for the rest of the study due to its ease of preparation.

8.4.1.2 Optimization of the matrix

Based on their merits established in previous studies,[247, 276, 283-284] six different ionic liquids were investigated to determination the most appropriate ionic liquid matrix for this work. The ionic liquids tested are shown in Figure 8.2 (referred to as: MIM2PEG3-2NTf2, MIM2C12-2NTf2, MIM2PEG3-2TfO, HeIM2PEG3-2NTf2, D5, and TPP2C12-2NTf2). Silicone OV-101 was also investigated as a solvent for comparison with the selected ionic liquids. The column containing MIM2PEG3-2NTf2 matrix produced the highest efficiency (ca. 5000 plates/m) and the best selectivity (e.g. α_{ionone} = 1.10). Meanwhile the polysiloxane-based stationary phase displayed

extremely low efficiency in the 500-1000 plates/m range. This is probably due to the low polarity of the polysiloxane used which is unfavorable for the dissolution of the ionic substances. Therefore MIM2PEG3-2NTf2 was employed in the following studies.

8.4.2 Improvement over the first ionic liquid containing cyclodextrin-based CSPs

According to the 2001 report,[252] of the 68 pairs of enantiomers separated on a commercial Chiraldex BPM column, only 21 were separated on the neutral permethyl-*β*-cyclodextrin based stationary phase (BPM), albeit with much higher efficiency. Conversely in this study by using an imidazolium salt cyclodextrin derivative, very different results were obtained. A total number of 70 compounds were selected and tested based on their previously proved separation on Chiraldex BPM and/or Chiraldex BDM column.[24] Fifty-one compounds showed enantiomeric separation on the BIM-BPM-I phase. In addition, 6 compounds were that were not separated on the commercial Chiraldex BPM column were separated on the BIM-BPM-I column.

A performance comparison between the BIM-BPM-I stationary phase and the neutral BPM containing IL-based stationary phase was carried out by examination of the separations achieved on the two stationary phases (Table 8.1). When the compounds listed in Table 1 were tested under the same conditions, the BIM-BPM-I column produced up to 7 times more efficient separations than the neutral BPM stationary phase. Generally, the BIM-BPM-I stationary phase produced greater analyte retention than the BPM phase, with two exceptions, i.e. *α*-pinene and *β*-pinene. Moreover, the majority of analytes showed better enantioselectivities on the BIM-BPM-I stationary phase. The biggest improvement of selectivity from 1.04 to 1.10 was achieved for 2-ethoxytetrahydrofuran. With higher selectivities, efficiencies and retentions, the BIM-BPM-I stationary phase afforded up to 6 times greater enantiomeric resolutions than the neutral BPM stationary phase (see tetrahydro-2(2-propynloxy)-*2H*-pyran).

Table 8.1 Performance improvement of the new IL phase gained over its 2001 predecessor.[11]

Compound	T (°C)	BPM in BMIM-Cl, 10 m				BIM-BPM-I in MIM2PEG3-2NTf2, 10 m			
		k'_1[a]	α[b]	Rs[c]	N (plates)	k'_1	α	Rs	N (plates)
camphene	25	10.2	1.11	0.9	1400	11.9	1.05	0.7	1850
α-pinene	25	15.8	1.07	1.2	5000	9.3	1.10	1.0	2100
β-pinene	30	25.8	1.03	1.0	15300	12.1	1.05	1.2	3640
2-ethoxy tetrahydrofuran	30	3.24	1.04	0.8	11200	4.6	1.10	1.5	6820
2-acetyl-5-norbornene	40	55.7	1.05	0.9	6000	105.8	1.04	2.0	43560
Fenchone	40	27.7	1.04	1.0	13600	61.0	1.02	1.0	14570
tetrahydro-2(2-propynloxy) -2*H*-pyran	50	19.1	1.02	0.5	19400	35.8	1.08	2.9	26530
3-chloro-2-norbornanone	60	70.4	1.05	1.1	7500	164.8	1.08	4.0	36560
α-ionone	100	21.2	1.06	1.5	12300	26.8	1.10	4.4	39100
4-methyl-tetralone	100	35.1	1.03	1.2	21500	82.3	1.06	2.7	51650

[a] k'_1 is the retention factor of the first eluted enantiomer. It is calculated as $k'_1 = (t_1-t_0)/t_0$, whereas t_1 is the retention time of the first eluted peak and t_0 is the column dead time.
[b] α is the enantioselectivity exhibited by a pair of enantiomers. It can be obtained from equation $\alpha = k'_2 / k'_1$, whereas k'_1 and k'_2 are the retention factors of the first and second eluted peak, respectively.
[c] *Rs* is the resolution obtained for a pair of enantiomers. It can be retrieved as follows, $Rs = 2*(t_2-t_1)/ (W_1+W_2)$. Note that t_1 and t_2 are the retention times of the first and second eluted enantiomers, while W_1 and W_2 are the baseline peak width of the first and second peaks.

In order to further dissect the contribution from the charged pendent group on the cyclodextrin and the bulkier ionic liquid solvent matrix, an experiment was carried out wherein neutral permethyl *β*-cyclodextrin (BPM) was dissolved in MIM2PEG3-2NTf2 to produce a BPM-MIM2PEG3-2NTf2 stationary phase. This column had poor efficiency (ca. 1700 plate/m), halved retention factors, and limited enantioselectivities. In fact, this column showed little improvement on its previous BMIM-Cl-based version (see Table 8.2). Evidently, the use of bulkier ionic liquid matrix failed to help with the column performance, although it greatly improved the thermal stability of the stationary phase. However, the ionic nature of the cyclodextrin derivative resulted in a CSP that showed enhancements of both column efficiency and selectivity.

Table 8.2 Performance comparison of neutral BPM stationary phases based on the monocationic IL (BMIM-Cl) and a dicationic IL (MIM2PEG3-2NTf2).[252]

Compound	T (°C)	BPM in BMIM-Cl, 10 m				BIM-BPM-I in MIM2PEG3-2NTf2, 10 m			
		k'_1	α	*Rs*	N (plates)	k'_1	α	*Rs*	N (plates)
2-acetyl-5-norbornene	40	55.7	1.05	0.9	6000	48.6	1.0	0	2760
tetrahydro-2(2-propynloxy)-*2H*-pyran	50	19.1	1.02	0.5	19400	4.8	1.0	0.8	7300
3-chloro-2-norbornanone	60	70.4	1.05	1.1	7500	86.9	1.03	0.8	9240
α-ionone	100	21.2	1.06	1.5	12300	18.2	1.04	1.3	15680
4-methyl-tetralone	100	35.1	1.03	1.2	21500	50.0	1.02	0.6	8950

In the previous 2001 work it was also observed that a ring structure was important for enantiomeric separations on the neutral BPM-based CSP. However, compounds without ring structures, e.g. acetoin, 3-butyn-2-ol, linalool, *t*-butyloxy-2-propanol, methyl-2-chloropropionate, methyl-2-bromopropionate, methyl lactate and butyl lactate (see Table 8.3), were easily separated on the new ionic cyclodextrin-based CSP. For example, methyl-2-chloropropionate enantiomers were baseline separated with a retention factor of 4.00 at 55°C. Clearly, structural

rigidity of analytes becomes less of a requirement for enantiomeric separation on the charged CD-based stationary phase.

When the column stability is studied, it is noted that no compounds were tested over 110°C in the previous work.[252] That was because the BMIM-Cl ionic liquid used in this early work was stable only up to around 140°C.[247] Since MIM2PEG3-2NTf2 has a decomposition/volatilization temperature of over 300°C,[276] it clearly is a more robust matrix material for GC stationary phases. The compounds in this study were separated at temperatures up to 175°C (see 2,3-dihydro-7a-methyl-3-phenylpyrrolo[2,1-b]oxazol-5(7aH)-one). Now that the IL column operation temperature has been extended, a broader pool of less volatile compounds can be analyzed.

8.4.3 Comparison of the BIM-PMBCD-I CSP to the corresponding commercial CSP

Given the improved separation power of the charged cyclodextrin containing CSP, it is valid to assume the BIM-BPM-I column may accomplish comparable or possibly better enantiomeric separations than its commercialized analog. The Chiraldex BPM column was selected for comparison as the commercial stationary phase. The stationary phase of this column is composed of permethylated *β*-cyclodextrin (BPM) dissolved in a polysiloxane-based matrix.

In total, 56 compounds achieved enantiomeric resolution on BIM-BPM-I and Chiraldex BPM combined. The retention factors, selectivities, resolutions and theoretical plate numbers of the 56 compounds are shown in Table 8.3. Respectively, 27 and 33 compounds showed baseline separation on the BIM-BPM-I column and the Chiraldex BPM column. In the meantime, 23 compounds showed improved separations on the ionic liquid-based column, while 33 showed comparable or better separation on the commercial column.

The compounds showing better separations on the ionic liquid column were mostly ketones, esters, secondary and tertiary alcohols. Despite the fact there were 5 racemates separated solely on the commercial column, 6 other racemates that displayed no selectivity on Chiraldex BPM were separated on BIM-BPM-I. Figure 8.5 provides examples of the separation of these

compounds on both stationary phases. As is indicated by the structure, 5-norbornene-2-ol is composed of two pairs of enantiomers, one for the endo- conformation and one for the exo conformation. One pair of enantiomers was separated on the BIM-BPM-I column while the other pair was separated on the Chiraldex BPM column. This demonstrates the complementary selectivity of the two stationary phases. When the endo- and exo- isomers of 2-benzoyl-5-norbornene were injected on the commercial column, only one pair of enantiomers was partially separated while the other pair eluted in one single tailing peak. However, both pairs of enantiomers were separated on the IL-based column, with excellent peak shape and one baseline separation. Also on the IL phase, the endo and exo isomer clusters were better separated from each other. Indeed, it has been reported that IL phases show better separations of structural and geometric isomers than conventional GC stationary phases.[292]

Interestingly, for compounds with higher polarities, BIM-BPM-I offered improved peak shapes over the commercial column. The separation of some of these compounds on both stationary phases is shown in Figure 8.6. These analytes were also injected on the neat MIM2PEG3-2NTf2 stationary phase and a neat polysiloxane stationary phase (Rtx-5). Their peak shapes on the two neat stationary phases are shown in Figure 8.7. Slight to moderate peak tailing was observed for these compounds on the polysiloxane stationary phase, however, little tailing was found for the eluted peaks on the MIM2PEG3-2NTf2 stationary phase. Therefore, it is highly possible the distorted peak shapes on Chiraldex BPM are caused by the polysiloxane matrix used for the commercial column.

In this study, it is observed that the separation efficiencies on the two CSPs is also largely dependent on the analytes' polarities. Hydrocarbons, tetrahedro-*2H*-pyrans and ethers are

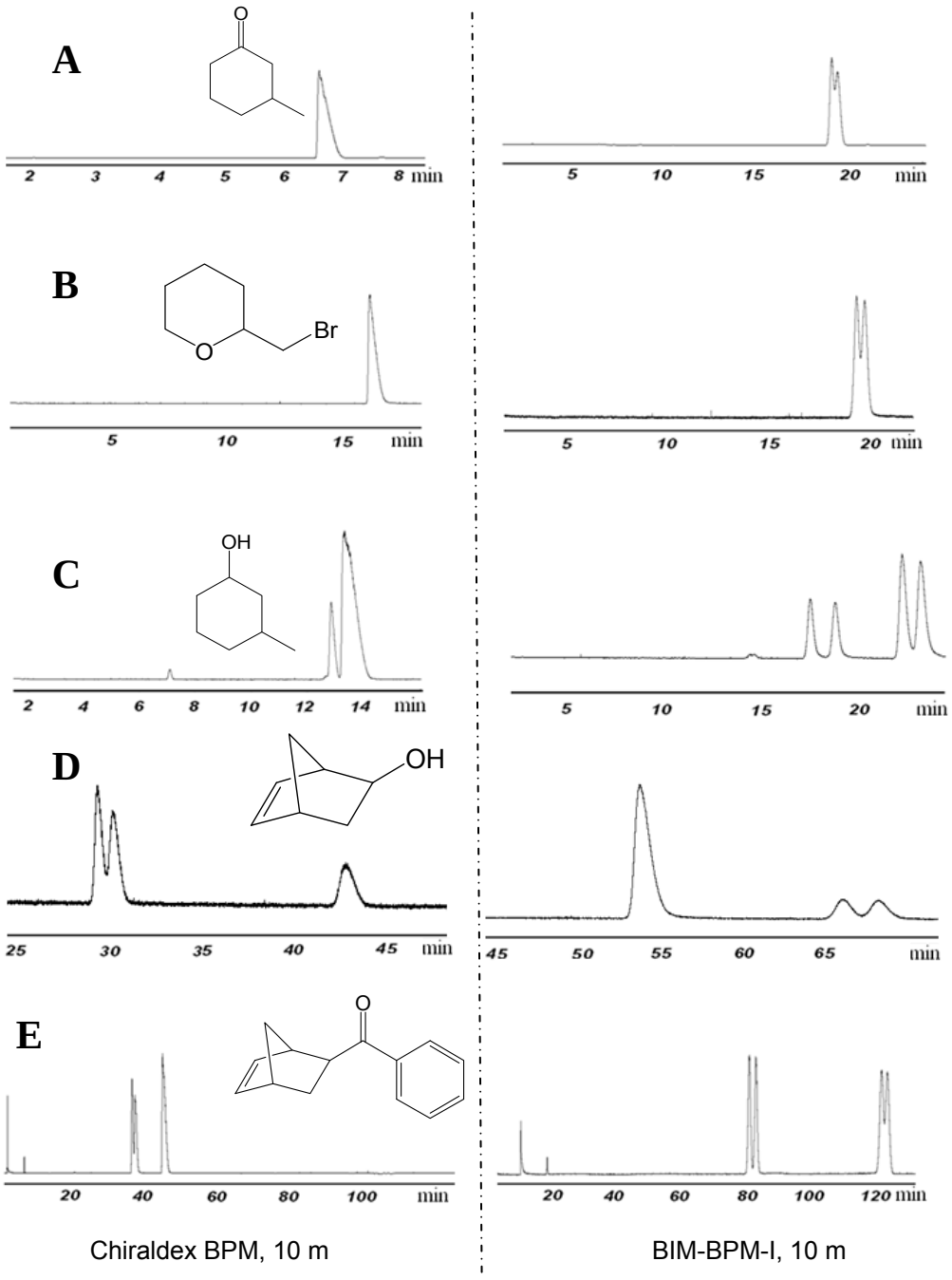

Figure 8.5 Examples of compounds showing improved separation on BIM-BPM-I column compared to on Chiraldex BPM column. Helium at 1 mL/min
A. Separation of 3-methyl-1-cyclohexanone, 60 °C
B. Separation of 2-(bromomethyl) tetrahydro-2*H*-pyran, 60 °C
C. Separation of 3-methylcyclohexanol (cis+trans), 60 °C
D. Separation of 5-norbornene-2-ol (endo+exo), 50 °C
E. Separation of 2-benzoyl-5-norbornene (endo+exo), 110 °C

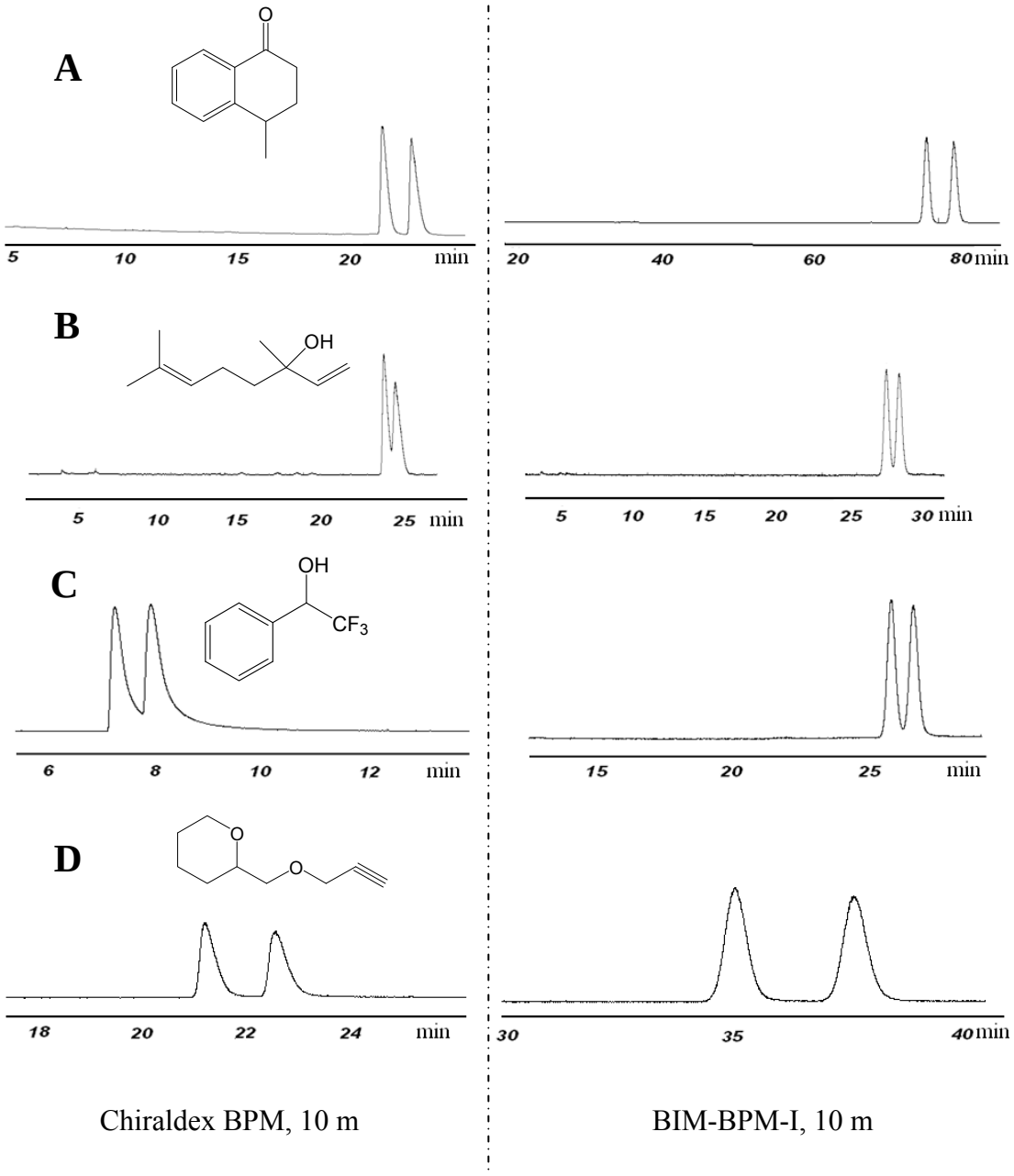

Figure 8.6 Comparison of compound peak shapes obtained on Chiraldex BPM column and the BIM-BPM-I column. Helium at 1 mL/min

A. Separation of 4-methyl-1-tetralone, 100 °C,

B. Separation of linalool, 60 °C

C. Separation of 1-phenyl-2,2,2-trifluoroethano, 100 °C

D. Separation of tetrahydro-2(2-propynloxy)-*2H*-pyran, 50 °C

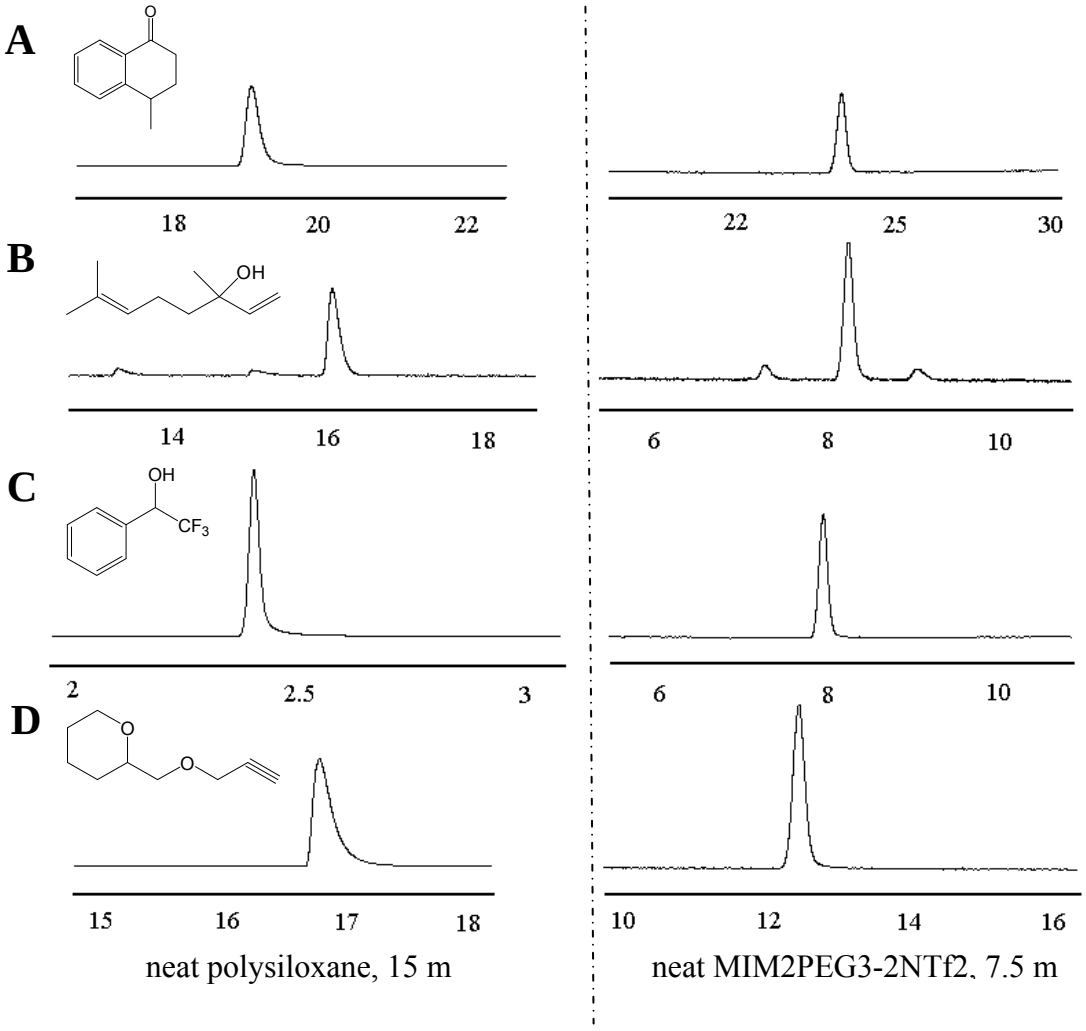

Figure 8.7 Comparison of compound peak shapes obtained on neat polysiloxane column (Rtx-5) and neat MIM2PEG3-2NTf2 column. Helium at 1 mL/min
A. Separation of 4-methyl-1-tetralone, 100°C,
B. Separation of linalool, 60°C
C. Separation of 1-phenyl-2,2,2-trifluoroethano, 100°C
D. Separation of tetrahydro-2(2-propynloxy)-*2H*-pyran, 50°C

compounds of low to moderate polarities. They exhibited worse efficiency on the IL-based column than on the Chiraldex BPM column (see pinenes, 2-methyltetrahydro-*2H*-pyran and 2-ethoxytetrahydrofuran). However, more polar compounds, such as ketones and alcohols, produced plate numbers up to 10 times higher on the BIM-BPM-I CSP than on the Chiraldex BPM CSP (see 3-chloro-2-norbornanone).

8.4 Conclusions

A charged cyclodextrin GC chiral selector was introduced in combination with ionic liquid matrices and successfully applied to the enantiomeric separation of a variety of chiral molecules. While the nature of cationic cyclodextrin chiral selectors makes a crucial contribution to the significantly enhanced column efficiency, the type of ionic functional group on the cyclodextrin has a major impact on the chiral recognition capabilities of the stationary phase. When compared to the most analogous commercial stationary phase, the new IL-based stationary phase not only improved separations for more than one third of the test solutes, but also managed to separate compounds that were not separated on the commercial column. Furthermore, the IL-based column provided better peak shapes and improved peak efficiencies for racemic analytes with higher polarities.

This work demonstrated comparable and complementary performance of IL-based columns to the potent commercial chiral stationary phase. It not only introduced a new concept of using charged cyclodextrins as chiral selectors in GC, but also demonstrated the feasibility of using ionic liquids for high enantioselectivity GC-CSPs. With the large pool of ionic liquids and variety of ionic cyclodextrin structures available nowadays, these types of GC-CSPs offer a new avenue of potentially useful and interesting research and development.

Table 8.3 The separation of 56 compounds on BIM-PMBCD-I and Chiraldex BPM.

Compound[a]	T (°C)	BIM-PMBCD-I in MIM2PEG3-2NTf2				Chiraldex BPM column 2009, 10m			
		k'$_1$	*α*	*Rs*	N (plates)	*k'*$_1$	*α*	*Rs*	N (plates)
Camphene	25	11.9	1.05	0.7	1885	33.0	1.09	2.1	8008
α-pinene	25	9.26	1.10	1.0	2103	25.5	1.15	3.4	8314
2-bromopentane	25	2.08	1.06	0.8	2994	4.96	1.05	1.3	13679
3-butyn-2-ol	25	16.0	1.05	1.2	9116	3.27	1.14	2.7	10050
2-ethoxy-tetrahydrofuran	30	4.62	1.10	1.5	6819	5.75	1.09	2.1	11981
β-pinene	30	12.1	1.05	0.7	3639	30.5	1.06	1.2	6358
2-methyltetrahydro-*2H*-pyran	30	2.06	1.0	0	2067	3.07	1.05	1.0	9110
3,4-dihydro-2-methoxy -*2H*-pyran	30	7.69	1.0	0	3238	8.80	1.06	1.6	13485
2-ethoxy-3,4-dihydro -*2H*-pyran	40	6.54	1.0	0	5496	9.18	1.06	1.7	17789
Fenchone	40	61.0	1.02	1.5	14567	62.2	1.07	1.8	9640
allyl glycidyl ether	40	26.6	1.01	0.5	14502	10.0	1.05	1.9	32163
t-butyl glycidyl ether	40	22.0	1.04	1.3	14425	14.6	1.07	2.4	23408
2-acetyl-5-norbornene,	40	105.8	1.04	2.0	43562	91.3	1.02	0.7	25002
endo and exo*	40	194.5	1.04	1.3	18247	136.2	1.08	1.5	5706
acetoin	50	10.3	1.08	1.6	8158	2.24	1.13	3.7	24230
limonene	50	6.87	1.05	1.3	12776	11.8	1.04	1.5	30659
5-norbornene-2-ol,	50	57.1	1.0	0	18362	37.6	1.03	1.0	25922
endo and exo*	50	70.6	1.03	1.5	39895	55.5	1.0	0	15381
t-butyloxy-2-propanol	50	7.88	1.06	1.4	10706	6.54	1.23	5.2	13024
tetrahydro-2(2-propynloxy)-*2H*-pyran*	50	35.8	1.08	2.9	26526	27.2	1.07	2.4	24179
methyl-2-chloropropionate	55	4.00	1.05	1.6	20634	1.82	1.08	2.4	27545

Table 8.3 *Continued*

2,5-dimethoxy-tetrahydrofuran	60	3.38	1.11	3.7	25734	2.60	1.14	4.0	25173
3-chloro-2-norbornanone*	60	164.8	1.08	4.0	36560	69.0	1.11	1.8	3237
3-methyl-1-cyclohexanone*	60	16.4	1.02	0.7	28797	8.42	1.0	0	7373
2-(bromomethyl)-tetrahydro-2*H*-pyran*	60	21.5	1.02	0.9	25034	22.9	1.0	0	16077
2-(chloromethyl)-tetrahydro-2*H*-pyran*	60	11.3	1.01	0.6	30482	11.3	1.0	0	18679
methyl-2-bromopropionate	60	15.3	1.02	0.8	25097	8.96	1.3	1.0	33036
linalool*	60	30.1	1.03	1.5	31991	32.1	1.6	1.1	28107
3-methyl-cyclohexanol,	60	19.2	1.07	2.4	19751	16.9	1.04	0.9	28107
cis and trans*	60	24.6	1.04	1.5	21643	17.6	1.0	0	27731
4-(chloromethyl)-2,2-dimethyl-1,3-dioxane	70	4.57	1.05	1.7	28762	3.97	1.10	3.0	23203
2-methylpiperidine dr*	70	20.7	1.04	1.6	31324	11.2	1.04	1.5	30048
3-methylpiperidine dr*	70	19.4	1.02	0.8	25601	10.6	1.02	0.7	25380
2-(2-butynyloxy)-tetrahydro-*2H*-pyran	70	19.93	1.0	0	21130	17.48	1.07	2.4	22356
4-methoxymethyl-1,3 -dioxane-2-one	80	68.22	1.0	0	37201	37.75	1.07	3.0	39227
styrene oxide	80	17.6	1.01	0.7	38405	6.22	1.05	2.3	38798
borneol	80	29.4	1.06	2.6	39152	32.3	1.09	3.4	27941
1-phenylethanol	80	48.8	1.04	2.1	40834	15.4	1.14	3.9	16938
N-trifluoroacetyl alanine ethyl ester	80	21.1	1.01	0.7	36699	3.20	1.06	2.9	37246
methyl lactate*	80	3.69	1.07	2.0	20370	0.69	1.08	1.0	1770
butyl lactate*	80	13.0	1.04	1.5	23757	4.93	1.02	0.6	2263
2-(3-chloropropoxy)-tetrahydro-*2H*-pyran	80	21.9	1.01	0.7	35717	24.8	1.02	0.7	11287

Table 8.3 *Continued*

2,5-dihydro-3,6-dimethoxy-2-isopropyl-pyrazine*	90	5.66	1.15	4.9	25214	6.85	1.07	3.1	41296
α-ionone*	100	26.8	1.10	4.4	39098	20.6	1.07	3.4	44336
4-methyl-1-tetralone*	100	82.3	1.06	2.7	51645	34.3	1.06	2.4	28372
4-chloro-*α*-methylbenzyl alcohol	100	58.8	1.03	1.2	34297	23.5	1.16	3.5	10841
1-phenyl-2,2,2-trifluoroethanol*	100	39.0	1.03	1.5	38772	11.0	1.10	1.4	5036
2,3-dihydro-7a-methyl-3-isopropylpyrrolo[2,1,-b]-oxazol-5(7aH)-one	100	41.1	1.04	1.9	34457	13.5	1.08	3.4	40572
3-methyl-1-indanone	110	29.7	1.06	3.2	46574	9.39	1.08	3.7	43872
2-benzoyl-5-norbornene, endo	110	92.9	1.02	1.4	51698	61.4	1.02	1.0	40206
and exo*	110	140.8	1.01	0.8	41551	62.9	1.0	0	11686
di-*t*-butyltartrate dr	110	29.4	1.03	1.5	40201	17.3	1.10	4.7	41520
α-methyl-2-(trifluoromethyl)benzyl alcohol*	120	4.85	1.10	3.6	29770	1.98	1.10	2.7	27092
α-trichloromethyl-benzyl acetate*	125	22.9	1.03	1.5	43794	12.9	1.01	1.0	40381
N-trifluoroacetyl isoleucine methyl ester*	130	2.29	1.07	2.3	31709	0.91	1.04	0.9	32735
2,3-dihydro-7a-methyl-3-phenylpyrrolo[2,1-b]oxazol-5(7aH)-one	175	27.3	1.01	0.7	23785	5.22	1.02	0.8	33227

[a] Compounds that are better separated on Phase A are indicated with the sign *, and compounds that were derivatized prior to assay are noted with dr.

CHAPTER 9

EVALUATION OF DALBAVANCIN AS CHIRAL SELECTOR FOR HPLC AND COMPARISON WITH TEICOPLANIN BASED CIHRAL STATINARY PHASES

9.1 Abstract

Dalbavancin is a new compound of the macrocyclic glycopeptide family. It was covalently linked to 5μm silica particles by using two different binding chemsitries. Approximately two hundred and fifty racemates including (A) heterocyclic compounds; (B) chiral acids; (C) chiral amines; (D) chiral alcohols; (E) chiral sulfoxides and sulfilimines; (F) amino acids and amino acid derivatives; and (G) other chiral compounds were tested on the two new chiral stationary phases (CSP) using three different mobile phases. As dalbavancin is structurally related to teicoplanin, the same set of chiral compounds was screened on two commercially available teicoplanin CSPs for comparison. The dalbavancin CSPs were able to separate some enantiomers that were not separated by the teicoplanin CSPs and also showed improved separations for many racemates. However, there were other compounds only separated or better separated on teicoplanin CSPS. Therefore, the dalbavancin CSPs are complementary to the teicoplanin CSPs.

9.2 Introduction

Macrocyclic antibiotics were first introduced as a new class of chiral selectors for enantioseparations by HPLC and capillary electrophoresis in 1994.[36] The *ANSA* family (rifamycin B and SV)[293-294] and glycopeptides group (vancomycin, ristocetin and teicoplanin[38, 295-298]) were demonstrated to have the most advantageous structures for enantiomeric separations. There are many structurally related oligophenolic glycopeptides belonging to the later group which have proven to be useful. Thus far, vancomycin, ristocetin, teicoplanin,

A82846B,[299] LY307599,[300] avoparcin[301] and A40926[302] of the macrocyclic glycopeptide family, have been evaluated as chiral selectors. These chiral selectors can be further divided into two groups according to the number of fused rings in the aglycone part of their structure. In comparison, vancomycin types have a three ring aglycone, while the teicoplanin-type glycopeptides have one more ring in the aglycone which makes it “semirigid”. They all show great selectivity over a wide rage of chiral molecules including amino acids, carboxylic acids and neutral compounds. Their excellent enantioselective separation capability have been attributed to the richness of different functional groups in their structures such as aromatic rings with and without chloro-substituents, ionizible phenolic moieties, amino groups, amide groups, carboxylates and carbohydrate moieties. Therefore, many kinds of intermolecular interactions, such as π-π and dipole-dipole interactions, hydrophobic interactions and hydrogen bonding, can be involved in the chiral recognition via association with these functional groups.[273]

Although all the macrocyclic glycopeptides are within the same family of compounds, small changes in their structure can result in significant differences in their enantiorecognition abilities. For example, α-amino acids are better separated on the teicoplanin aglycone based CSP, that is produced by cleaving all the carbohydrate moities from teicoplanin.[303] In the case of A40926, there are only a few small structural variations compared to teicoplanin. However, it is found that some compounds can only be separated or better separated on the HPLC chiral stationary phase based on A40926, while the teicoplanin column separates a larger total number of racemates.[302]

Dalbavancin is a new semisynthetic lipoglycopeptide derived from A40926, a naturally occurring glycopeptide produced by actinomycete *Nonomuraea* species.[304] It has enhanced activity against gram-positive bacteria and unique pharmacokinetics compared with existing drugs in its class.[305] In this work, two CSPs were prepared by binding dalbavancin to two different 5-um spherical silica gels respectively as to mirror the synthesis and make up of the Chirobiotic T and T2 columns. They are designated as the D1 and D2. Their enantioseparation

capabilities were evaluated with 250 pairs of enantiomers containing different functional groups. These analytes were also screened on the commercial teicoplanin CSPs (i.e. Chirobiotic T and Chirobiotic T2) for comparison.

9.3 Experimental

9.3.1 Materials

All the racemic analytes tested in this study were purchased from Sigma-Aldirich. All HPLC grade solvents were obtained from VWR (Bridgeport, NJ). HPLC grade Kromasil silica gel (particle size 5 μm, pore size 100 Å, and surface area 310m^2/g) was obtained from Akzo Nobel (EKA Chemicals, Bohus, Sweden). LiChrospher Si(100) silica gel (particle size 5μm, pore size 100 Å, and surface area 400m^2/g) was purchased from (Merck, Darmstadt, Germany). All organosilane compounds were obtained from Silar Laboratories (Wilmington, NC). These include: (3-aminopropyl) dimethylethoxysilane, (3-aminopropyl) triethoxysilane, [2-(carbomethoxy) ethyl] trichlorosilane, [1-(carbomethoxy)ethyl] methyldichlorosilane, (3-isocyanatopropyl) triethoxysilane, and (3-glycidoxypropyl) triethoxysilane. Dalbavancin was the generous gift of Pfizer(Washington, MO).

9.3.2 Methods

Preparation of the D1 CSP. 1g dried Dalbavancin (0.53 mmol) was dissolved by 55 ml anhydrous DMF in a 250 ml 3-neck round flask with mechanical stirring. Then triethylamine (0.72 ml, 5.16 mmol) and 3-(triethoxysilyl)propyl isocyanate (0.865 ml, 3.50 mmol) were added into the solution at room temperature under argon protection. The solution was heated to 95°C for 5 h and cooled to 60°C. The dried Kromasil silica (3.50 g, 5μm, 100 A°) was added into the solution. The mixture was heated to 105°C over night and then cooled to room temperature and filtered. The CSP was washed by methanol, methanol/water (50/50, v/v), pure water, and methanol (50 ml for each solvent), and dried in oven at 100°C overnight. Element analysis showed it has 8.0% carbon loading.

Preparation of the D2 CSP. The D2 stationary phase was prepared as previously described for the teicoplanin CSP. Five gram of Lichrospher silica gel was first dried at 150c under vacuum, and then it is heated in toluene to reflux to remove azaeotropically all residual water. It is followed by adding 2.5mL of (3-aminopropyl triethoxysilane) and the reaction mixture was heated to reflux for 4h. The modified silica gel was filtered and washed with toluene, methanol and dichloromethane and dried at 90°C overnight. Elemental analysis showed the derivatized silica gel has 4.0% carbon loading. A 2.5 mL portion of 1,6-diisocyanatohexane (15 mmol) was added to an ice-bath-cooled slurry of 2.5 g of 3-aminopropyl- Lichrospher in 50 mL of anhydrous toluene. Next, the mixture was heated at 70°C for 2 h. After cooling, the supernatant toluene phase was removed under an argon atmosphere. The excess reactant was removed by dry toluene washing. A suspension of 1 g of Dalbavancin (0.53 mmol) in 100 mL of dry pyridine was added dropwise to the wet activated silica. Next, the mixture was heated at 70°C for 12 h with stirring under an argon atmosphere. After cooling, the Dalbavancin bonded silica was washed with 50mL portions in the sequence pyridine, water, methanol, acetonitrile and dichloromethane. It was dried under vacuum. Element analysis showed it has 11.0% carbon loading (increased by 7.0%).

Chromatographic condition CSPs were slurry packed into 250*4.6mm stainless steel columns at 600 bar. Evaluation of the columns was conducted on HP 1090 HPLC system with a DAD UV detector and autosampler. Detection wavelengths were selected at 220nm, 230nm and 254nm. The injection volumes were 5µl. All sample concentrations were 1mg/ml. Separations w-ere carried out under isocratic conditions at flow rate of 1mL/min at 21°C. The mobile phases were premixed and degassed under vacuum for 10 minutes. The column dead times were tested by injection of solution of 1,3,5-tri-tert-butylbenzene in 100% methanol.

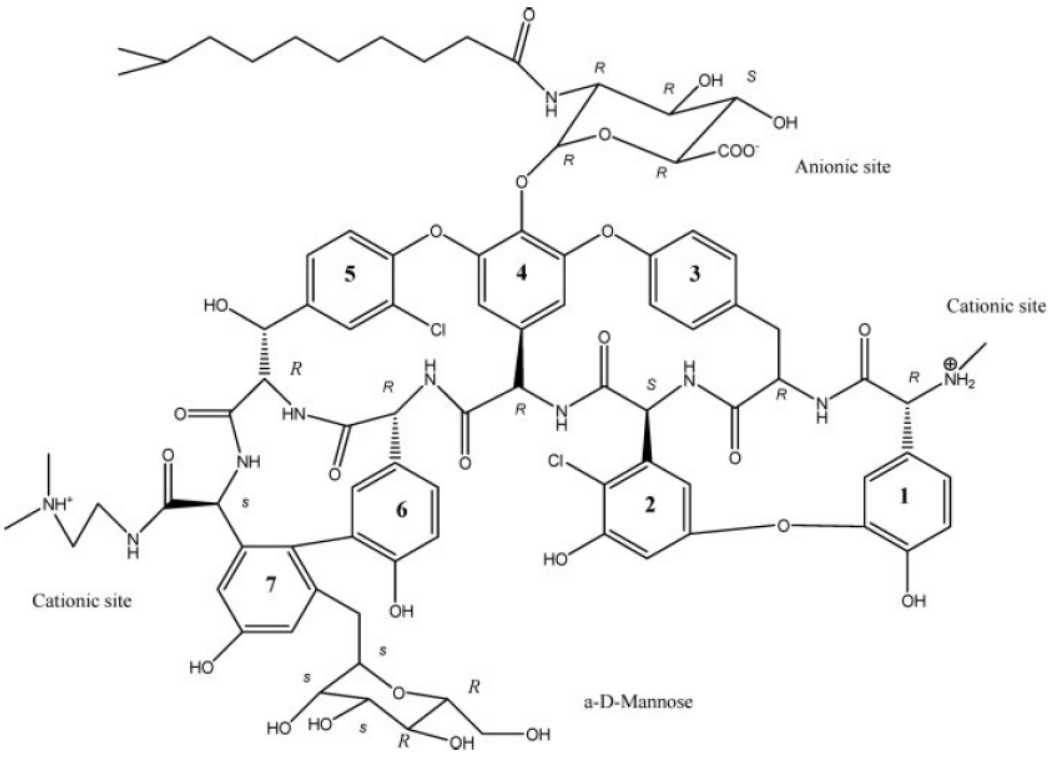

Figure 9.1 The structure of the macrocyclic antibiotic dalbavancin.

9.4 Results and Discussion

The structure of Dalbavancin. Dalbavancin is a second generation glycopeptide antibiotic molecule (see Figure 9.2). The major difference between dalbavancin and teicoplanin are: (a) different phenyl rings are chloro-substituted (see ring 2 and 3, Figs. 1 &2) ; (b) the β-*D*-N-acety-glucosamine unit of teicoplanin (see ring 5, Figures 9.1 and 9.2) is replaced by a simple hydroxyl group; (c) the primary hydroxyl group of N-acyl-glucosamine unit of teicoplanin has been oxidized to a carboxylic acid, which can generate an anion; (d) the primary amine group on the aglycone portion of teicoplanin is a secondary amine substituted by methyl group;(e) the carboxylic group close to phenyl ring 7 is converted to an amide group connected with three methylene groups and it has a dimethylamino group at the end (in dalbavancin); and (f) dalbavancin has 10 carbons in the carbon chain of β-*D*-N-acyl-glucosamine while teicoplanin only has 9. The last difference noted above is the least likely to affect enantioseparation since

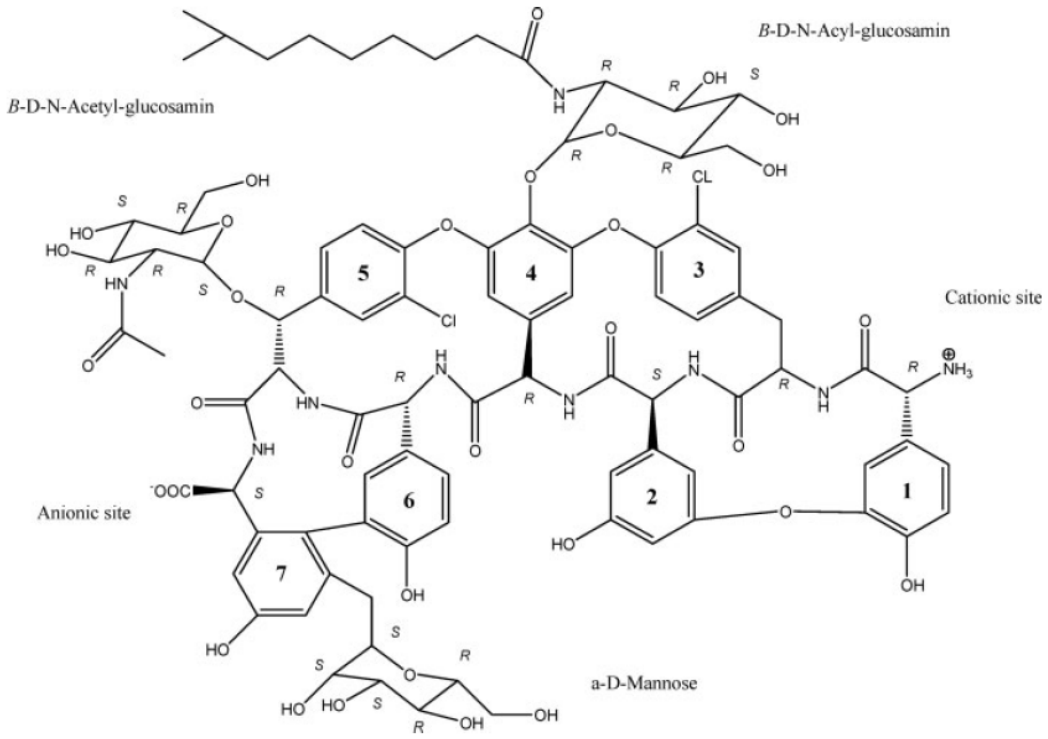

Figure 9.2 The structure of the macrocyclic antibiotic teicoplanin.

one more methylene group does not provide any additional interactions that are beneficial to chiral recognition. Previous studies by our group has shown that the teicoplanin carbohydrate units play an important role in chiral recognition in that it helps in the separation of non-amino acid compounds. However, they also decrease the separation of many α-amino acid enantiomers.[303] Thus, the elimination of the β-*D*-N-acety-glucosamine unit in dalbavancin can substantially affect its the enantioselectivity. The other changes made to carboxylic groups, hydroxyl group and amino groups can also contribute to differences in the enantioselectivity of dalbavancin relative to teicoplanin. Dalbavancin has one tertiary amine and secondary amine respectively, and one carboxylic group on the N-acyl-glucosamine (Figures 9.1 and 9.2). Whereas teicoplanin has only one carboxylic group connected to the aglycone and one primary amino group. As amine and carboxylic acids group are ionizable in aqueous solution and can

interact via electrostatic interactions with charged analytes, these changes could lead to different chiral recognition abilities especially in the reversed phase.

Chromatographic Evaluation. The four columns, D1, D2, T1 and T2 were evaluated in three mobile phase modes: the normal phase, polar organic, and reversed-phase modes. In the normal phase mode, a mixture of 20% ethanol and 80% heptane were used as mobile phase. In the polar organic mode, 100% methanol was evaluated. In the reversed phase mode, methanol and water were mixed at the ratio of 1 to 1, and 0.1% NH4OAc was used as buffer to adjust to pH 4.2. In order to compare the behavior of the different CSPs, results presented were obtained with the same mobile phase compositions for all of the CSPs. However, these conditions are not necessarily optimal for all the enantiomeric separations. Better separations can be obtained in specific cases if the mobile phase compositions and organic modifiers are optimized. The elution order of amino acids is “L” before “D”. Other compounds for which standards are not available can not yet be determined.

Approximately 250 compounds were injected on these columns. These analytes include (A) heterocyclic compounds; (B) chiral acids; (C) chiral amines; (D) chiral alcohols; (E) chiral sulfoxides and sulfilimines; (F) amino acid and amino acid derivatives; and (G) other chiral compounds. To simplify the presentation, Table 9.1, Table 9.2 and Table 9.3 list only the chromatographic results obtained when an enantiomeric separation was achieved.

Comparison of CSPs in the normal phase mode. Table 9.1 lists the separations achieved on the four columns when used in the normal phase mode. The number of successful enantioseparations achieved on D1, D2, T1 and T2 is 16, 17, 17 and 15 respectively. Interestingly, D2 always gives much greater retention for most of the analytes than the other three columns. Conversely, D1 has the least retention for most compounds. In the case of 2-azabicyclo [2.2.1]- hept-5-en-3-one, the retention factor (*k)* on D2 is three times as great as it is on D1. According to elemental analysis results of the CSPs, the carbon loading of D2 is higher than D1 by 3%. This can be caused either by more chiral selector loading or more

unreacted linkages. And both of these factors can contribute to longer retention of analytes. Also, the additional ureic group of the D2 linkage can interact with analytes and increase the retention time. However, longer retention does not necessarily result in better resolution of racemates. Among the racemates that both D1 and D2 can separate, 6 are better separated on D2 and 4 are better separated on D1 according to the separation factors (*α)*. The enantiomeric separations of 2,6-bis(4-isopropyl-2-oxazolin-2-yl)pyridine, DL-3,4-dihydroxyphenyl-alfa-propylacetamide, cis-4,5-diphenyl-2-oxazol-idinone, phenyl vinyl sulfoxide were only achieved on the D1 CSP in the normal phase mode. While methyl trans-3-(4-methoxyphenyl) glycidate and 5-hydroxymethyl-2(5H)-furanone enantiomers were separated on the D2 CSP only. Thus, it is obvious that the binding chemistry not only affects the retention factors, but it also changes the enantioselectivity in some cases. The influences of the nonchiral spacers on chiral separation were first studied for β-cyclodextrin chiral stationary phases.[306] Other studies have been done by several research groups.[38, 307-310] It was found that different types of chiral selectors favor linkages with different nature and length. However, for macrocyclic glycopeptide chiral selectors, each binding methods has its own advantages, and sometimes unique selectivities. Teicoplanin based columns can separate five compounds which the dalbavancin based CSPs did not. 2-Carbethoxy-gamma- phenyl-gamma-butyrolactone was barely separated by T1 and T2. But its separation was greatly improved to baseline on the D2 CSP. Among the total 29 compounds separated by these four columns in the normal phase mode, nineteen compounds are better or only separated by the dalbavancin based CSPs. There are no obvious structural differences between the solutes separated by one CSP versus another CSP. Representative chromatograms of analytes separated on the macrocyclic glycopeptide CSPs are shown in Figure 9.3.

Table 9.1 Chromatographic data for he normal phase resolution of racemic compounds on D1, D2, T1 and T2 columns.

Compound name	Structure	CSPs	80% Heptane/20% ethanol k_1	a	R_s
2,6-Bis(4-isopropyl-2-oxazolin-2-yl)pyridine	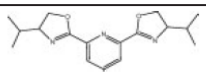	D1	1.04	1.18	1.0
2-Carbethoxy-gamma-phenyl-gamma-butyrolactone	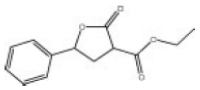	D1 D2 T1 T2	1.34 2.90 1.47 1.15	1.13 1.35 1.03 1.07	0.9 1.5 0.5 0.5
5,5-Dimethyl-4-phenyl-2-oxazolidinone	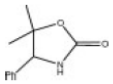	D1 D2 T2	3.93 10.72 4.19	1.38 1.57 1.44	1.4 1.8 1.4
N-(2,3-Epoxypropyl)-phthalimide	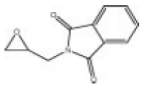	D2 T1	2.28 1.99	1.12 1.07	0.9 1.0
Guaiacol glyceryl ether carbamate	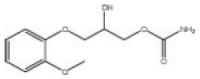	T1	7.72	1.05	0.5
alpha-Methyl-alpha-phenyl-succinimide	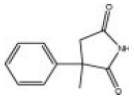	D1 D2 T1 T2	2.02 4.52 2.37 2.40	1.11 1.44 1.23 1.21	0.9 2.2 1.5 1.4
2-Phenylglutaric anhydride	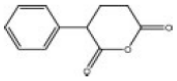	T1	3.27	1.06	0.5
Methyl trans-3-(4-methoxyphenyl)glycidate	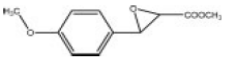	D2	1.07	1.58	1.8
3-(alpha-Acetonyl-4-chlorobenzyl)-4-hydroxycoumarin	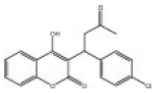	D1 D2 T2	0.88 0.85 0.89	1.39 1.21 1.21	1.4 0.7 1.2
Warfarin	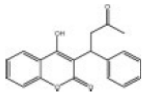	D1 D2 T2	0.83 1.91 0.89	1.44 1.17 1.17	1.5 0.8 1.0

Table 9.1 *Continued*

Compound name	Structure	CSPs	80% Heptane/20% ethanol k_1	a	R_s
2-Azabicyclo[2.2.1]-hept-5-en-3-one	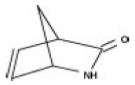	D1 D2 T1	4.26 14.52 7.59	1.29 1.16 1.06	1.5 0.8 0.7
2-(3-Chlorophenoxy)propionamide	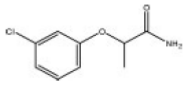	D1 D2 T1 T2	1.49 2.97 2.21 2.18	1.13 1.36 1.09 1.12	1.0 2.2 1.2 1.3
DL-3,4-Dihydroxyphenyl-alfa-propylacetamide		D1	7.43	1.07	0.6
1,5-Dimethyl-2-pyrrolidinone	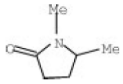	D2 T1	2.62 3.31	1.26 1.03	1.3 1.4
alpha,alpha-Dimethyl-beta-methylsuccinimide	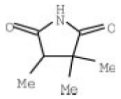	D1 D2 T1 T2	1.05 2.10 1.69 1.55	1.33 1.51 1.10 1.16	1.5 2.5 1.4 1.3
1,5-Dimethyl-4-phenyl-2-imidazolidinone	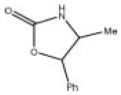	D1 D2 T1 T2	1.57 4.86 3.24 2.78	1.26 1.65 1.70 1.11	1.4 3.6 2.3 1.0
N,N′-Dibenzyl-tartramide	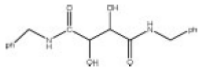	T1	6.41	1.04	0.5
2,2′-Diamino-1,1′-binaphthalene		D2 T2	5.03 3.40	1.05 1.16	0.5 1.3
cis-4,5-Diphenyl-2-oxazolidinone	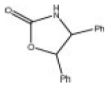	D1	4.52	1.66	2.6
2,3-Dihydro-7a-methyl-3-phenylpyrrolo[2,1-b]-oxazol-5(7aH)-one	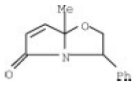	T1 T2	2.29 1.90	1.04 1.05	0.8 0.5

Table 9.1 *Continued*

Compound name	Structure	CSPs	80% Heptane/20% ethanol k_1	a	R_s
Ethyl 11-cyano-9,10-dihydro-endo-9, 10-ethanoanthracene-11-carboxylate	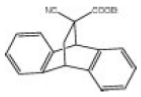	D2 T1	1.03 0.72	1.17 1.05	0.8 0.5
Furoin	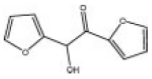	D1 D2 T1 T2	2.61 6.45 3.28 3.88	1.04 1.28 1.22 1.20	1.0 1.3 2.3 1.8
Ftorafur	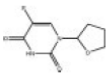	D1 T1	7.58 15.90	1.33 1.17	1.4 0.9
Glycidyl trityl ether	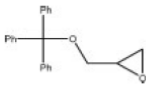	T2	0.24	1.15	0.5
5-Hydroxymethyl-2(5H)-furanone	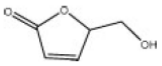	D2	7.77	1.27	1.5
Phenyl vinyl sulfoxide	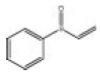	D1	1.41	1.09	0.8
Phensuximide		D2 T1 T2	2.55 2.28 2.13	1.12 1.11 1.22	0.9 1.4 1.6
Ruelene	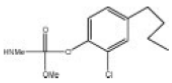	D2 T2	0.79 0.66	1.09 1.71	0.5 1.2
3a,4,5,6-Tetrahydro-succininido[3,4-b]acenaphthen-10-one	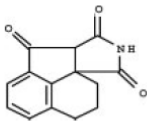	D1 T1 T2	5.93 6.79 0.59	1.44 1.25 1.94	1.8 1.4 0.9

Table 9.2 Chromatographic data for the polar organic phase resolution of racemic compounds on D1, D2, T1 and T2 columns.

Compound name	Structure	CSPs	100% MeOH		
			k_1	a	R_s
Chlorthalidone	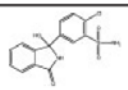	D2	0.44	1.28	0.7
2-Carbethoxy-gamma-phenyl-gamma-butyrolactone	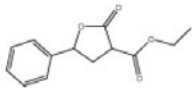	D2	0.13	1.51	0.7
5,5-Dimethyl-4-phenyl-2-oxazolidinone	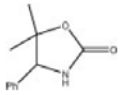	D1 T2	0.22 0.13	1.38 2.03	1.0 1.4
alpha-Methyl-alpha-phenyl-succinimide	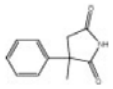	D2	0.23	1.30	0.7
(cis)-(±)−3,3a,8,8a-Tetrahydro-2H-indeno[1,2-d]oxazol-2-one	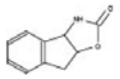	D1 D2 T1 T2	0.84 2.74 1.02 0.70	1.98 1.96 1.23 1.15	3.0 2.7 1.0 0.9
2-(4-Nitrophenyl)propionic acid	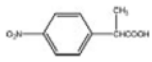	T2	0.17	1.35	0.7
4-Methyl-5-phenyl-2-oxazolidinone	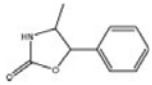	D1 D2 T1	0.26 0.53 0.28	2.36 4.24 2.79	2.5 5.5 4.4
Alprenolol	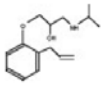	T2	3.46	1.25	2.7
DL-alpha-Aminophenyl-acetic acid	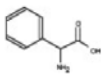	T2	0.30	3.77	1.3
2-Azabicyclo[2.2.1]-hept-5-en-3-one	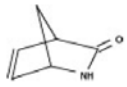	D1 D2	0.24 0.61	1.20 1.19	0.8 0.9

Table 9.2 *Continued*

Compound name	Structure	CSPs	100% MeOH		
			k_1	a	R_s
Bamethane	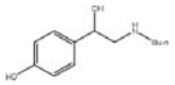	T2	3.88	1.19	1.5
1.1′-Binaphthyl-2,2′-diyl hydrogenphosphate		T1	0.21	1.87	3.2
4-Benzyl-2-oxazolidinone	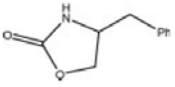	D1	0.61	1.16	0.9
		D2	2.07	1.08	0.5
		T1	0.72	1.29	1.5
		T2	0.39	1.23	0.9
4-Benzyl-5, 5-dimethyl-2-oxazolidinone	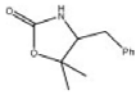	D1	0.29	1.20	0.8
		D2	0.65	1.78	2.3
		T1	0.36	2.73	4.8
		T2	0.15	1.84	1.4
dl-2-(2-Chlorophenoxy)-propionic acid	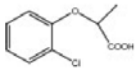	T2	0.04	3.85	1.3
cis-4,5-Diphenyl-2-oxazolidinone	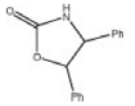	D1	0.22	1.62	1.4
		T1	0.25	1.75	3.2
		T2	0.21	1.71	1.5
4-(Diphenylmethyl)-2-oxazolidinone	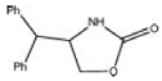	D1	0.38	1.45	1.2
		D2	1.08	1.47	1.5
		T1	0.41	1.55	1.6
2,2′-Diamino-1,1′-binaphthalene	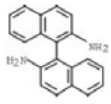	T2	0.24	1.10	0.5
Ftorafur	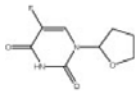	D1	0.29	1.20	0.8
		T1	0.50	1.08	0.6
Glycidyl trityl ether	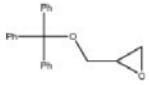	T1	0.09	1.23	0.5

Table 9.2 *Continued*

Compound name	Structure	CSPs	100% MeOH k_1	a	R_s
5-(4-Hydroxyphenyl)-5-phenylhydantoin	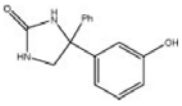	D1	0.51	1.95	2.5
		D2	2.59	4.07	7.0
		T1	0.36	1.08	0.5
		T2	0.68	1.44	1.4
5-(3-Hydroxyphenyl)-5-phenylhydantoin	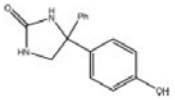	D2	1.51	1.32	1.3
		T1	0.32	1.11	0.6
		T2	0.49	1.23	0.9
Hydrobenzoin		T1	0.09	1.22	0.5
DL-Homocysteine thiolactone hydrochloride	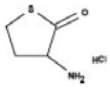	T2	3.06	1.19	1.8
4-Hydroxy-2-pyrrolidinone	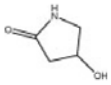	D2	0.60	1.37	1.3
5-(Hydroxymethyl)-2-pyrrolidinone	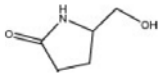	D2	0.68	2.06	2.9
		T1	0.50	1.19	1.4
5-Hydroxymethyl-2(5H)-furanone	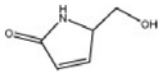	D2	0.42	1.54	1.4
		T1	0.29	1.08	0.5
Iopanoic acid or (3-[3-amino-2,4,6-triiodophenyl]-2-ethyl-propanoic acid	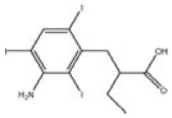	D1	0.26	1.23	0.9
Methoxyphenamine	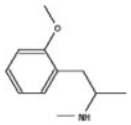	D2	0.50	1.78	2.2
		T1	0.31	1.27	1.2
		T2	0.34	1.23	0.8
Mephenesin	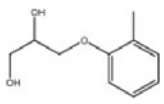	T1	0.09	1.32	0.6

Table 9.2 *Continued*

Compound name	Structure	CSPs	100% MeOH k_1	a	R_s
Metanephrine hydrochloride	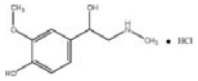	T2	1.83	1.29	1.0
2-Phenoxypropionic acid	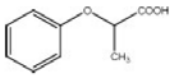	T2	0.02	6.80	1.2
5-Phenyl-2-(2-propynyl-amino)-2-oxazolin-4-one	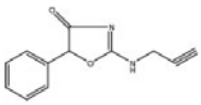	D1 D2 T1	0.27 0.46 0.31	1.88 3.81 1.46	1.3 3.0 0.9
3a,4,5,6-Tetrahydro-succininido[3,4-b]-acenaphthen-10-one	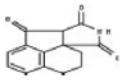	D1 D2 T1 T2	0.30 0.81 0.31 0.33	1.14 1.24 1.16 1.19	0.7 0.9 1.0 0.7

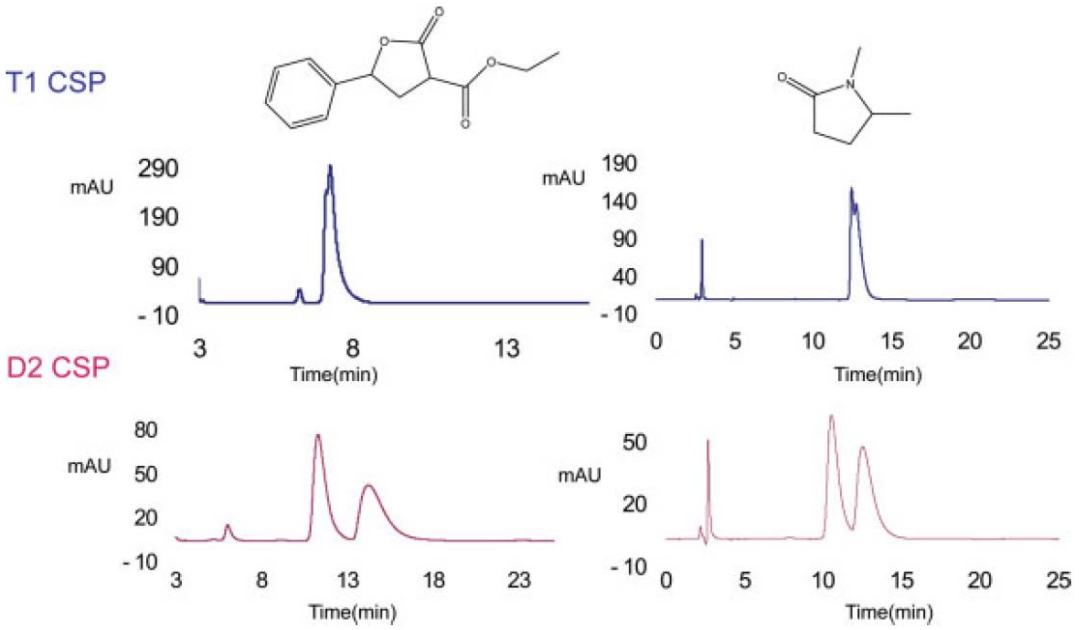

Figure 9.3 Representative chromatograms of two analytes on the T1 and D2 CSPs in the normal phase mode: heptane/ethanol 80/20 v/v; flow rate 1ml/min.

Table 9.3 Chromatographic data for the reversed phase resolution of racemic compounds on D1, D2, T1 and T2 columns.

Compound name	Structure	CSPs	NH_4OAc Buffer 50%/ MeOH 50%		
			K_1	A	R_s
Benzoin methyl ether	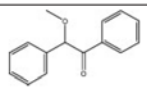	2	6.25	1.29	1.4
2,6-Bis(4-isopropyl-2-oxazolin-2-yl)pyridine	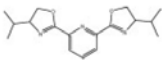	D2 T2	1.74 0.79	1.58 1.94	2.3 3.0
Chlorthalidone	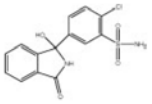	D2 T1 T2	1.86 0.45 0.93	1.41 1.12 1.06	1.3 0.8 0.5
2-Carbethoxy-gamma-phenyl-gamma-butyrolactone	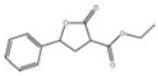	D2	5.21	1.11	0.8
1,5-Dimethyl-4-phenyl-2-imidazolidinone	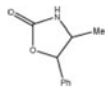	D2 T1 T2	2.80 0.57 2.06	1.21 1.05 1.10	1.4 0.5 0.9
1,5-Dimethyl-4-phenyl-2-imidazolidinone	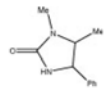	D2 T1 T2	2.80 0.57 2.06	1.21 1.05 1.10	1.4 0.5 0.9
3,4-Dihydroxyphenyl-2-propylacetamide	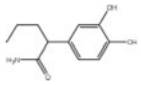	D2	2.19	0.90	0.6
2,3-Dibenzoyl-α-tartaric acid	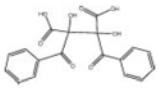	D2	3.01	1.10	0.5
5,5-Dimethyl-4-phenyl-2-oxazolidinone	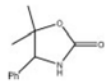	D1	0.75	1.84	1.2
5-Methoxy-1-indanone-3-acetic acid	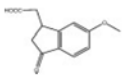	D2	1.41	1.10	0.6

Table 9.3 *Continued*

Compound name	Structure	CSPs	NH_4OAc Buffer 50%/ MeOH 50%		
			K_1	A	R_s
alpha-Methyl-alpha-phenyl-succinimide	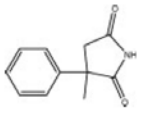	D2 T1 T2	1.20 0.49 0.69	1.23 1.13 1.12	1.2 1.0 0.8
3,3a,8,8a-Tetrahydro-2H-indeno[1,2-d]-oxazol-2-one	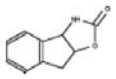	D1	1.52	1.61	1.5
(1-Phenethyl)phthalimide	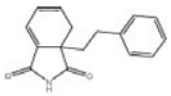	D2 T1 T2	4.81 0.89 2.38	1.10 1.07 1.06	0.8 0.8 0.5
2-(4-Nitrophenyl)propionic acid	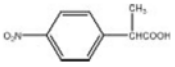	D1 D2	1.29 3.33	1.30 1.17	1.4 1.0
Methyl trans-3-(4-methoxyphenyl)glycidate	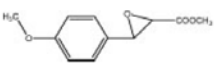	D2	1.49	1.10	0.6
dl-alpha-Aminophenyl-acetic acid	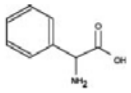	T2	0.50	5.05	4.6
Atrolactic acid hemihydrate	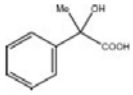	D1 D2	0.80 0.59	1.82 5.05	2.4 4.9
4-Benzyl-2-oxazolidinone	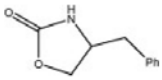	T1 T2	8.50 1.29	1.03 1.30	0.9 1.5
(−/+)-4-Benzyl-5, 5-dimethyl-2-oxazolidinone	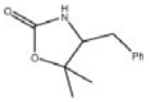	D1 T1	1.46 1.00	1.31 3.57	1.5 5.9
2-(2-Chlorophenoxy)-propionic acid	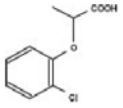	D1 D2 T2	1.00 1.10 0.04	1.42 2.43 0.62	1.2 2.4 0.4

Table 9.3 *Continued*

Compound name	Structure	CSPs	NH_4OAc Buffer 50%/ MeOH 50% K_1	A	R_s
2-(4-Chloro-2-methyl-phenoxy)propionic acid	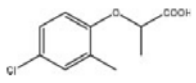	D1 D2	1.21 1.63	1.33 1.64	1.2 2.0
2-(3-Chlorophenoxy)propionamide	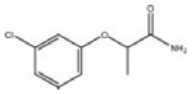	D2 T2	1.42 0.77	1.18 1.04	1.0 0.4
(±)Camphor *p*-tosyl hydrazon	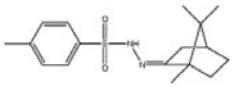	T1	0.97	1.14	1.0
cis-4,5-Diphenyl-2-oxazolidinone	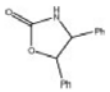	D1 T1 T2	1.63 0.87 1.94	1.23 1.42 1.44	1.3 2.9 2.7
4-(Diphenylmethyl)-2-oxazolidinone	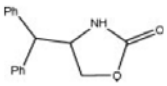	D1 T1 T2	2.28 1.31 2.06	1.20 1.59 1.22	1.2 1.8 1.3
2,2′-Diamino-1,1′-binaphthalene	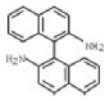	T1	1.01	1.11	1.0
1,5-Dimethyl-2-pyrrolidinone	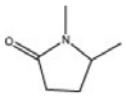	D2	0.35	1.16	0.6
alpha,alpha-Dimethyl-beta-methylsuccinimide	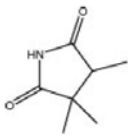	D2 T1 T2	0.37 0.30 0.29	1.52 1.07 1.14	1.4 0.5 0.6
Europium tris[3-(trifluoromethylhydroxy-methylene)]-(−) camphorate	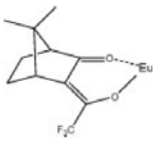	D2	2.09	1.33	0.8

Table 9.3 *Continued*

Compound name	Structure	CSPs	NH_4OAc Buffer 50%/ MeOH 50% K_1	A	R_s
Ethyl 11-cyano-9,10-dihydro-endo-9,10-ethanoanthracene-11-carboxylate	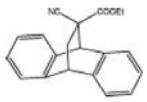	D2 T2	4.66 2.07	1.04 1.07	0.5 0.6
Furoin	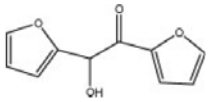	D2 T2	0.73 0.42	1.09 1.07	0.5 0.4
Ftorafur	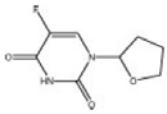	T1	0.94	1.08	0.9
DL-Homocysteine thiolactone hydrochloride	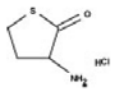	D2 T2	0.67 1.40	1.15 1.04	0.8 0.5
5-(Hydroxymethyl)-2-pyrrolidinone	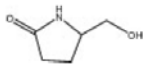	D2	0.24	1.99	1.4
5-Hydroxymethyl-2(5H)-furanone	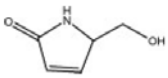	D2 T2	0.31 0.15	1.79 1.20	1.4 0.5
5-(4-Hydroxyphenyl)-5-phenylhydantoin	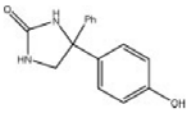	D1 T1	3.00 1.27	1.48 1.17	1.8 1.2
5-(3-Hydroxyphenyl)-5-phenylhydantoin	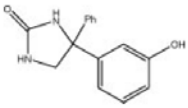	D1 T1 T2	2.36 1.15 4.11	1.18 1.15 1.36	1.2 1.2 1.5
Iopanoic acid or (3-[3-amino-2,4,6-triiodophenyl]-2-ethyl-propanoic acid	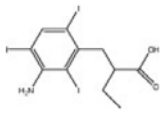	D1	1.94	1.16	0.9

Table 9.3 *Continued*

Compound name	Structure	CSPs	NH_4OAc Buffer 50%/ MeOH 50% K_1	A	R_s
4-Isobutyl-alpha-methylphenylacetic acid	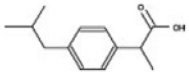	D1	1.91	1.08	0.7
(±)2,3-O-Isopropylidene 2,3-dihydroxy-1,4-bis-(disphenylphosphino)butane	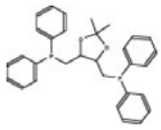	D2	4.67	1.21	1.0
Methoxyphenamine	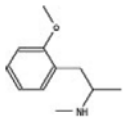	D2 T2	1.68 9.30	2.00 1.03	1.2 0.4
N-(alpha-Methylbenzyl)phthalic acid monoamide	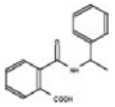	D1	0.71	1.66	2.0
alpha-Methoxyphenylacetic acid	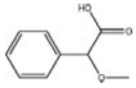	D1	0.66	1.07	0.5
3-Oxo-1-indancarboxylic acid	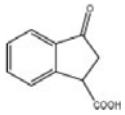	D2	1.64	1.50	1.5
2-Phenoxypropionic acid	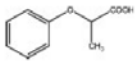	D2	0.57	2.73	3.3
2-Phenylpropionic acid	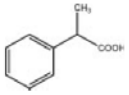	D2	1.10	1.10	0.5
5-Phenyl-2-(2-propynyl-amino)-2-oxazolin-4-one	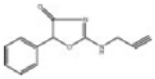	D1	0.86	1.69	1.5

Table 9.3 *Continued*

Compound name	Structure	CSPs	NH_4OAc Buffer 50%/ MeOH 50% K_1	A	R_s
Phenyl vinyl sulfoxide	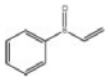	D2	1.08	1.25	1.3
		T1	0.52	1.13	1.0
		T2	0.56	1.27	1.4
DL-beta-Phenyllactic acid	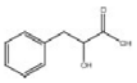	D1	0.41	1.14	0.6
(±)-5-(alpha-Phenethyl)semioxamazide	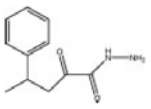	D2	0.70	1.07	0.5
		T2	0.50	1.13	0.7
Phensuximide	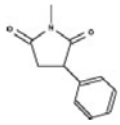	D2	1.01	1.31	1.4
		T2	1.00	1.31	1.4
1,2,3,4-Tetrahydro-3-isoquinolinecarboxylic acid hydrochloride	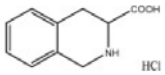	D1	0.73	1.65	1.5
Terbutaline hemisulfate salt	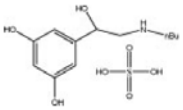	T2	5.63	1.22	3.1
3a,4,5,6-Tetrahydro-succininido[3,4-b]acenaphthen-10-one	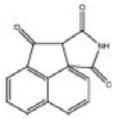	D1	1.06	1.30	1.2
		T1	0.93	1.42	5.0

Comparison of CSPs in the polar organic mode. Methanol is used as mobile phase for the polar organic mode because it can elute analytes faster than acetonitrile for teicoplanin type CSPs [4]. A total of 13, 17, 18 and 18 racemates have been separated on D1, D2, T1 and T2 respectively. These analytes include carboxylic acids, amine, alcohol and neutral compounds. The results are listed in Table 9.2 and representative chromatograms are shown in Figure 8.4. According to the enantioselectivity factors, three enantiomers are best separated on the D1

CSP, including one that was separated only on this CSP, 12 solutes were best separated by the D2 CSP including 4 that were separated only on this stationary phase, ten racemates were best separated by the T1 column including 4 that were separated only by this CSP, ten analytes were best separated by the T2 CSP including 9 that were separated only by this CSP. There are five compounds can be separated by all of the four CSPs. All of them are neutral molecules containing a hetero-five-member-ring in the structure. For the compound 5-(4-hydroxyphenyl)-5-phenylhydantoin, both the D1 and D2 CSPs gave much higher enantioselectivities and resolutions than those of T1 and T2 CSPs. The enantioselectivity factors for D1 and D2 are 1.95 and 4.07 respectively, and their resolutions correspond to 2.5 and 7.0 respectively, which indicates the excellent chiral resolving capabilities of Dalbavancin. Interestingly, the separation results changed significantly if a small alteration is made to the analyte's structure. For example, the only structural difference between 5-(3-hydroxyphenyl)-5-phenylhydantoin and 5-(4-hydroxyphenyl)-5-phenylhydantoin is position of the phenolic group. However, the previous baseline separation (Rs 7.0) achieved on D2 for 5-(4-hydroxyphenyl)-5-phenylhydantoin was downgraded to a partial separation (Rs 1.3) on D2 for 5-(3-hydroxyphenyl)-5-phenylhydantoin. The substantial decline in the enantiomeric selectivity and resolution indicates that the position of phenol group is very important for chiral recognition. Some of the compounds separated in the polar organic mode can also be separated in the normal phase mode. For example, enantiomers of 2-carbethoxy- gamma-phenyl-gamma-butyrolactone can be separated on all of the four CSPs and was baseline separated by D2. However, it was only partially separated on D2 in the polar organic mode (Rs=0.7). This is because the analyte does not retain long enough to interact with the chiral selectors in the polar organic mode.

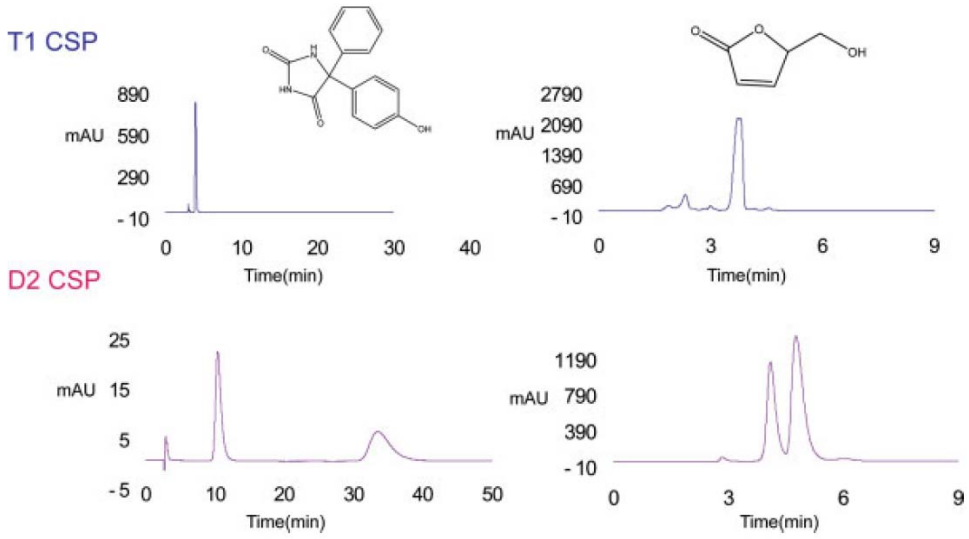

Figure 9.4. Representative chromatograms of two analytes on the T1 and D2 CSPs in the polar organic phase mode: 100% methanol; flow rate 1ml/min.

Comparison of CSPs in the reversed phase mode. Previous studies have revealed that reversed phase separations are among the most successful for the glycopeptide CSPs. Clearly, dalbavancin and teicoplanin CSPs follow this trend (see Figure 9.5). 54 racemates have been separated by these four columns together. The results are listed in Table 9.3. Twenty three racemic solutes can be separated on both dalbavancin and teicoplanin CSPs. This suggests that these two chiral selectors have somewhat analogous chiral recognition capabilities due to their similar structures. Fourteen racemates were only separated on the dalbavancin columns. This also demonstrates that these two classes of CSPs are complimentary to each other. Atrolactic acid hemihydrate was baseline separated by D1(α=1.82, Rs=2.4) and D2(α=5.05, Rs=4.9) CSPs, but it was not separated on either of the teicoplanin based columns. These differences in enantioselective Gibbs energy correspond to 0.3 kcal/mol for D1, 0.9 kcal/mol for D2 and 0 kcal/mol for T1 and T2. In this particular example, the dalbavancin columns are much more effective. Interestingly, many of the analytes that are only separated on dalbavancin based CSPs have a free carboxylic group in their structure, such as N-(alpha-methylbenzyl)phthalic acid monoamide, alpha-methoxyphenylacetic acid, 3-oxo-1-

indancarboxylic acid, 2-phenoxypropionic acid, 2-phenylpropionic acid, beta-phenyllactic acid and 1,2,3,4-tetrahydro-3-isoquinolinecarboxylic acid hydrochloride. This improved enantioselectivity towards carboxylic acids may be partly attributed to the tertiary amino group coupled to dalbavancin via an amide linkage (Figure 9.1). In aqueous solution at pH 4.2, this group is protonated and carries a positive charge. This cationic site can interact with deprotonated carboxylic anions through charge-charge interactions which is an important process in chiral recognition. In contrast, the teicoplanin based CSPs (i.e. T2) only separated one of the tested amino acids, DL-alpha-aminophenyl-acetic acid and one of the tested carboxylic acids, 2-(2-chlorophenoxy)-propionic acid (Rs=0.4). Although there is one cationic site on native teicoplanin, it can be converted to a carbamate group when bonded to silica gel. Thus, the teicoplanin chiral selector only has one anionic site after linked to silica gel. The poor enantioselectivity of teicoplanin to some of the carboxylic acids in this study should be partially due to the lack of cationic sites on the teicoplanin molecule.

9.5 Conclusions

Two dalbavancin based CSPs were made using two different linkages to silica gel. Their enantiomeric separation capabilities have been investigated by comparison of the separations achieved on Chirolbiotic T1 and T2 commercial columns. The structural differences in the chiral selectors and linkages between the four CSPs presented in this work do not make one superior to another. All of them can separate some racemic solutes that can not be separated by the other CSPs tested. It is as expected that they show similar enantiomeric separation abilities to many analytes since their structures are very closely related. However, dalbavancin based CSPs exhibits enhanced enantioselectivities to carboxylic acids, where the additional cationic site of the chiral selector may play an important role during the chiral recognition process. Thus, it is obvious that these four CSPs are complementary to one another. If a racemate is poorly separated on one CSP, it is possible the other related CSPs will produce an enhanced separation. This is the principal of complementary separation that was model for the class of

chiral selectors. Future work will involve the study of elution order of enantiomers and binding linkage effects on dalbavancin based CSPs.

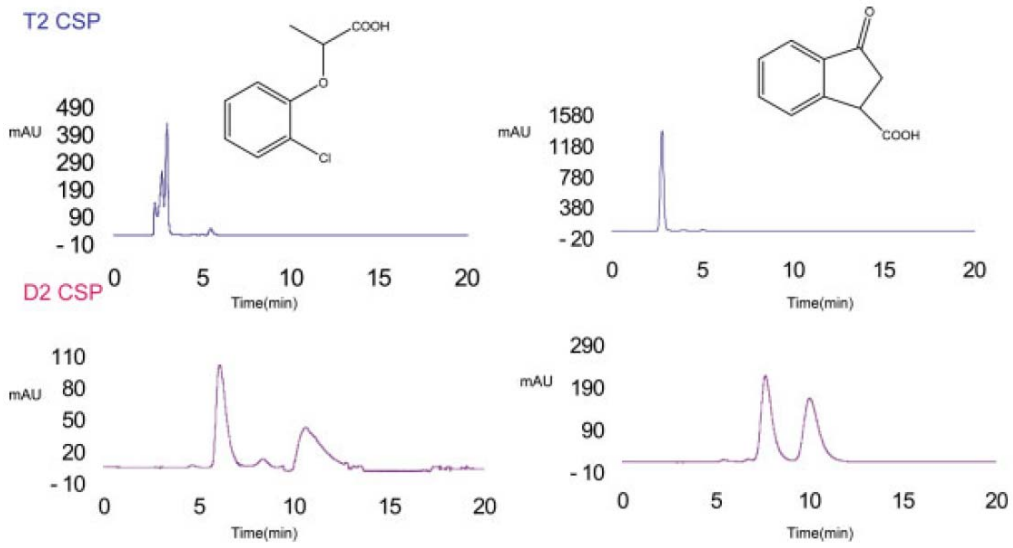

Figure 9.5 Representative chromatograms of two analytes on the T2 and D2 CSPs in the reversed phase mode: 20mM NH_4NO_3 Buffer/Methanol 1/1 v/v; flow rate 1ml/min.

CHAPTER 10

GENERAL CONCLUSIONS

10.1 Part one (Chapter 1-4)

The enantiomeric purity of chiral molecules is important not only in the pharmaceutical, biotechnology and agrochemical industries, but also in asymmetric syntheses in which the enantiomeric impurities can directly affect the reaction selectivity and product purity. Eighty-four commercially available chiral compounds were evaluated to determine their actual enantiomeric composition. The majority of the tested reagents were determined to have enantiomeric contaminants over 0.01%, and two of them were found to contain optical impurity levels exceeding 10%. The Chiraldex GTA chiral stationary phase was found to be to the most effective for separation of these kinds of small molecules. In another study, greater than baseline separations were achieved for 19 *β*-lactams on the Chiraldex column series. The overall best results were obtained also using the Chiraldex G-TA stationary phase. The dimethylated Chiraldex B-DM stationary phase produced the fastest separations for most of the sample compounds investigated albeit with lower resolutions.

The first fast and effective baseline separation of crocetane from phytane, as well as chromatographic separation of some of their stereoisomers, was achieved using derivatized cyclodextrin GC stationary phases. The Chiraldex B-PH cyclodextrin stationary phase proved to be the most applicable. It was used successfully for the analysis of authentic geological samples (i.e., crude oils).

10.2 Part two (Chapter 5-7)

Ionic liquids have favorable physicochemical properties for use as GC stationary phases. A fundamental linear solvation energy study of PEG functionalized dicationic RTILs shows how their structure affect their solvation properties. Compared to commercial INNOWAX and Rtx-5

columns, the PEG functionalized dicationic RTILs possess somewhat better separation powers and distinct selectivities for components within complex samples. The examination of volatile herbal essence oils on PEG coupled RTIL stationary phases demonstrated their comparable separation power to the most successful IL-polysiloxane-mixture stationary phase reported previously.

10.3 Part three (Chapter 8-9)

The development of a superior IL-based cyclodextrin GC-CSP was realized by dissolving charged cyclodextrins in a dicationic ionic liquid stationary phase matrix. High efficiencies and enantioselectivities were achieved on this stationary phase. The ionic nature of these cationic cyclodextrin chiral selectors makes a crucial contribution to the significantly enhanced column performance. When evaluated against the commercial stationary phase, the IL-based stationary phase showed comparable and complementary separation powers for the 70 compounds tested. Furthermore, the IL-based column provides improved peak shapes and peak efficiencies for compounds with higher polarities.

Two dalbavancin based HPLC-CSPs were developed using two different linkages to silica gel. Their enantiomeric separation capabilities were complementary to those achieved on Chirobiotic T1 and T2 commercial columns. Enhanced enantioselectivities were observed for carboxylic acids on the dalbavancin stationary phases probably due to the additional cationic site on the chiral selector.

APPENDIX A

PUBLICATION INFORMATION

Chapter 2: A manuscript published in Tetrahedron Asymmetry. K. Huang, Z. Breitbach, D.W. Armstrong, 2006, 17, 2821-2832. Copyright ©2006 with permission from Elsevier.

Technologies. P. Sun, C. Wang, D.W. Armstrong, 2006, 29, 1847-1860. Taylor & Francis

Chapter 3: A manuscript published in Chromatographia. K. Huang, D.W. Armstrong, E. Forro, F. Fulop, A. Peter, 2009, 69, 331-337. Copyright @2008 with permission

from SpringerLink.

Chapter 4: A manuscript published in Oganic Geochemistry. K. Huang, D.W. Armstrong, 2009, 40, 283-286. Copyright ©2009 with permission from Elsevier.

Chapter 6: A manuscript published in Analytical Bioanalytical Chemistry. K. Huang, X. Han, X. Zhang, D.W. Armstrong, 2007, 389, 2265-2275. Copyright ©2007 with permission from SpringerLink.

Chapter 9: A manuscript published in Chirality, 2009. X. Zhang, Y. Bao, K. Huang, K.L. Rundlett, D.W. Armstrong, Copyright ©2009 with permission from Interscience.

.

REFERENCES

1 C.-M. Jin, C. Ye, B. S. Phillips, J. S. Zabinski, X. Liu, W. Liu, J. n. M. Shreeve, *J. Mater. Chem.* **2006**, *16*, 1529-1535.
2 J. R. A. Powel, J. J.; Rug, T. I., *Drug stereochemistry:analytical methods and pharmacology*. Editor, CRC Press, New York, **1988**.
3 D. E. Drayer, *Clin. Pharmacol. Ther.* **1986**, *40*, 125-133.
4 D. E. Drayer, *Drug stereochemistry:analytical methods and pharmacology*. Editor, CRC Press, New York, **1988**.
5 A. R. Cushny, *J. Physiol.* **1904**, *30*, 176-194.
6 F. a. D. Administration, *Fed. Reg.* **1992**, *22*, 249.
7 E. Gil-Av, B. Feibush, R. Charles-Sigler, *Tetrahedron Lett.* **1966**, 1009-15.
8 H. Frank, G. J. Nicholson, E. Bayer, *J. Chromatogr. Sci.* **1977**, *15*, 174-6.
9 H. Frank, G. J. Nicholson, E. Bayer, *J. Chromatogr., Biomed. Appl.* **1978**, *146*, 197-206.
10 V. Schurig, W. Buerkle, *J. Am. Chem. Soc.* **1982**, *104*, 7573-80.
11 V. Schurig, W. Buerkle, *Angew. Chem.* **1978**, *90*, 132-3.
12 V. Schurig, B. Koppenhoefer, W. Buerkle, *Angew. Chem.* **1978**, *90*, 993-5.
13 V. Schurig, R. Weber, *J. Chromatogr.* **1981**, *217*, 51-70.
14 V. Schurig, D. Schmalzing, M. Schleimer, *Angew. Chem.* **1991**, *103*, 994-6 (See also Angew Chem , Int Ed Engl , 1991, 30(8), 987-9).
15 S. Allenmark, V. Schurig, *J. Mater. Chem.* **1997**, *7*, 1955-1963.
16 E. Smolkova-Keulemansova, *J. Chromatogr.* **1982**, *251*, 17-34.
17 W. A. L. König, S.; Wenz, G., *Angew. Chem., Int. Ed.* **1988**, *100*, 989-990.
18 W. A. L. König, S.; Mischnick-Luebbecke, P.; Brassat, B.; Wenz, G., *J. Chromatogr.* **1988**, *447*, 193-197.
19 R. M.-L. König W.; Krebber, P., *J. High Resolut. Chromatogr.* **1989**, *12*, 732-738.
20 D. W. Armstrong, W. Li, J. Pitha, *Anal. Chem.* **1990**, *62*, 214-17.
21 D. W. Armstrong, W. Li, C. D. Chang, J. Pitha, *Anal. Chem.* **1990**, *62*, 914-23.
22 A. Berthod, W. Li, D. W. Armstrong, *Anal. Chem.* **1992**, *64*, 873-9.
23 D. W. Armstrong, Y. Tang, T. Ward, M. Nichols, *Anal. Chem.* **1993**, *65*, 1114-17.
24 C. Handbook, **2002**.
25 V. Schurig, M. Jung, S. Mayer, M. Fluck, S. Negura, H. Jakubetz, *J. Chromatogr., A* **1995**, *694*, 119-28.
26 Y. Tang, Y. Zhou, D. W. Armstrong, *J. Chromatogr., A* **1994**, *666*, 147-59.
27 J. Ding, T. Welton, D. W. Armstrong, *Anal. Chem.* **2004**, *76*, 6819-6822.
28 X.-C. Zhou, H. Yan, Y.-Y. Chen, C.-Y. Wu, X.-R. Lu, *J. Chromatogr., A* **1996**, *753*, 269-277.
29 J. Pfeiffer, V. Schurig, *J. Chromatogr., A* **1999**, *840*, 145-150.
30 F. Mikes, G. Boshart, E. Gil-Av, *J. Chromatogr.* **1976**, *122*, 205-21.
31 F. Mikes, G. Boshart, *J. Chem. Soc., Chem. Commun.* **1978**, 173-5.
32 F. Mikes, G. Boshart, *J. Chromatogr.* **1978**, *149*, 455-64.
33 W. H. Pirkle, C. J. Welch, *J. Liq. Chromatogr.* **1992**, *15*, 1947-55.
34 R. C. Helgeson, J. M. Timko, P. Moreau, S. C. Peacock, J. M. Mayer, D. J. Cram, *J. Am. Chem. Soc.* **1974**, *96*, 6762-3.
35 c. handbook, **2003**.
36 D. W. Armstrong, Y. Tang, S. Chen, Y. Zhou, C. Bagwill, J.-R. Chen, *Analytical Chemistry* **1994**, *66*, 1473-1484 10.1021/ac00081a019.

37 S. Chen, Y. Liu, D. W. Armstrong, J. I. Borrell, B. Martinez-Teipel, J. L. Matallana, *J. Liq. Chromatogr.* **1995**, *18*, 1495-507.
38 D. W. Armstrong, Y. Liu, K. H. Ekborgott, *Chirality* **1995**, *7*, 474-497.
39 A. Berthod, Y. Liu, C. Bagwill, D. W. Armstrong, *J. Chromatogr., A* **1996**, *731*, 123-37.
40 Chirobiotic, **2004**.
41 S. Allenmark, B. Bomgren, H. Boren, *J. Chromatogr.* **1983**, *264*, 63-8.
42 K. R. Lindner, A. Mannschreck, *J. Chromatogr.* **1980**, *193*, 308-10.
43 Y. Okamoto, M. Kawashima, K. Yamamoto, K. Hatada, *Chem. Lett.* **1984**, 739-42.
44 Y. Okamoto, R. Aburatani, T. Fukumoto, K. Hatada, *Chem. Lett.* **1987**, 1857-60.
45 D. W. Armstrong, J. T. Lee, L. W. Chang, *Tetrahedron Asymmetry* **1998**, *9*, 2043-2064.
46 D. W. Armstrong, L. He, T. Yu, J. T. Lee, Y.-s. Liu, *Tetrahedron Asymmetry* **1999**, *10*, 37-60.
47 A. L. Jenkins, W. A. Hedgepeth, *Chirality* **2005**, *17*, S24-S29.
48 X. Han, L. He, Q. Zhong, T. E. Beesley, D. W. Armstrong, *Chromatographia* **2006**, *63*, 13-23.
49 D. W. Armstrong, H. L. Jin, *J. Chromatogr.* **1990**, *502*, 154-9.
50 Y. Ding, Q. Habib, S. Z. Shaw, D. Y. Li, J. W. Abt, Z. Hong, H. An, *J. Comb. Chem.* **2003**, *5*, 851-859.
51 B. F. Thomas, M. E. Y. Francisco, H. H. Seltzman, J. B. Thomas, S. E. Fix, A.-K. Schulz, A. F. Gilliam, R. G. Pertwee, L. A. Stevenson, *Bioorg. Med. Chem.* **2005**, *13*, 5463-5474.
52 C. Karapire, C. Zafer, S. Icli, *Synth. Met.* **2004**, *145*, 51-60.
53 S. Ueda, H. Terauchi, A. Yano, M. Matsumoto, T. Kubo, Y. Kyoya, K. Suzuki, M. Ido, M. Kawasaki, *Bioorg. Med. Chem.* **2004**, *12*, 4101-4116.
54 K. Shankaran, K. L. Donnelly, S. K. Shah, R. N. Guthikonda, M. MacCoss, J. L. Humes, S. G. Pacholok, S. K. Grant, T. M. Kelly, K. K. Wong, *Bioorg. Med. Chem. Lett.* **2004**, *14*, 4539-4544.
55 S. Fernandez, R. Brieva, F. Rebolledo, V. Gotor, *J. Chem. Soc., Perkin Trans. 1* **1992**, 2885-9.
56 S. Ueda, H. Terauchi, A. Yano, M. Ido, M. Matsumoto, M. Kawasaki, *Bioorg. Med. Chem. Lett.* **2004**, *14*, 313-316.
57 H. C. Brown, J. V. N. V. Prasad, *J. Org. Chem.* **1986**, *51*, 4526-30.
58 P. Raboisson, B. Mekonnen, N. P. Peet, *Tetrahedron Lett.* **2003**, *44*, 2919-2921.
59 J. F. Gerster, K. J. Lindstrom, R. L. Miller, M. A. Tomai, W. Birmachu, S. N. Bomersine, S. J. Gibson, L. M. Imbertson, J. R. Jacobson, R. T. Knafla, P. V. Maye, N. Nikolaides, F. Y. Oneyemi, G. J. Parkhurst, S. E. Pecore, M. J. Reiter, L. S. Scribner, T. L. Testerman, N. J. Thompson, T. L. Wagner, C. E. Weeks, J.-D. Andre, D. Lagain, Y. Bastard, M. Lupu, *J. Med. Chem.* **2005**, *48*, 3481-3491.
60 E. M. Zubin, D. A. Stetsenko, T. S. Zatsepin, M. J. Gait, T. S. Oretskaya, *Bioorg. Med. Chem.* **2005**, *13*, 4912-4920.
61 K. Tomita, Y. Tsuzuki, K.-i. Shibamori, M. Tashima, F. Kajikawa, Y. Sato, S. Kashimoto, K. Chiba, K. Hino, *J. Med. Chem.* **2002**, *45*, 5564-5575.
62 Y. Tsuzuki, K. Tomita, K. Shibamori, Y. Sato, S. Kashimoto, K. Chiba, *J. Med. Chem.* **2004**, *47*, 2097-2109.
63 I. Egle, N. Barriault, M. Bordeleau, J. Drage, L. Dube, J. Peragine, L. Mazzocco, J. Arora, K. Jarvie, A. Tehim, *Bioorg. Med. Chem. Lett.* **2004**, *14*, 4847-4850.
64 C. Neri, J. M. J. Williams, *Tetrahedron Lett.* **2002**, *43*, 4257-4260.
65 C. Neri, J. M. J. Williams, *Adv. Synth. Catal.* **2003**, *345*, 835-848.
66 C. C. Aldrich, L. Venkatraman, D. H. Sherman, R. A. Fecik, *J. Am. Chem. Soc.* **2005**, *127*, 8910-8911.
67 C. Gaul, J. T. Njardarson, D. Shan, D. C. Dorn, K.-D. Wu, W. P. Tong, X.-Y. Huang, M. A. S. Moore, S. J. Danishefsky, *J. Am. Chem. Soc.* **2004**, *126*, 11326-11337.

68 J. M. Dougherty, D. A. Probst, R. E. Robinson, J. D. Moore, T. A. Klein, K. A. Snelgrove, P. R. Hanson, *Tetrahedron* **2000**, *56*, 9781-9790.
69 A. M. Arink, C. M. P. Kronenburg, J. T. B. H. Jastrzebski, M. Lutz, A. L. Spek, R. A. Gossage, G. Van Koten, *J. Am. Chem. Soc.* **2004**, *126*, 16249-16258.
70 T. I. Richardson, P. L. Ornstein, K. Briner, M. J. Fisher, R. T. Backer, C. K. Biggers, M. P. Clay, P. J. Emmerson, L. W. Hertel, H. M. Hsiung, S. Husain, S. D. Kahl, J. A. Lee, T. D. Lindstrom, M. J. Martinelli, J. P. Mayer, J. T. Mullaney, T. P. O'Brien, J. M. Pawlak, K. D. Revell, J. Shah, J. M. Zgombick, R. J. Herr, A. Melekhov, P. B. Sampson, C.-H. R. King, *J. Med. Chem.* **2004**, *47*, 744-755.
71 X. Wu, A. K. Mahalingam, Y. Wan, M. Alterman, *Tetrahedron Lett.* **2004**, *45*, 4635-4638.
72 D.-M. Feng, J. M. Wai, S. D. Kuduk, C. Ng, K. L. Murphy, R. W. Ransom, D. Reiss, R. S. L. Chang, C. M. Harrell, T. MacNeil, C. Tang, T. Prueksaritanont, R. M. Freidinger, D. J. Pettibone, M. G. Bock, *Bioorg. Med. Chem. Lett.* **2005**, *15*, 2385-2388.
73 S. Kim, W. S. Powell, J. A. Lawson, S. H. Jacobo, D. Pratico, G. A. FitzGerald, K. Maxey, J. Rokach, *Bioorg. Med. Chem. Lett.* **2005**, *15*, 1613-1617.
74 K. Suzuki, N. Suzuki, M. Yamaura, T. Yoshizawa, *J. Carbohydr. Chem.* **2005**, *24*, 73-84.
75 M. Aepkers, B. Wuensch, *Synthesis* **2004**, 1033-1036.
76 E. Canpolat, M. Kaya, *J. Coord. Chem.* **2002**, *55*, 961-968.
77 D. Isaksson, M. Lindmark-Henriksson, T. Manoranjan, K. Sjoedin, H. E. Hoegberg, *J. Mol. Catal. B Enzym.* **2004**, *31*, 31-37.
78 A. L. Handlon, Y. Guo, *Synlett* **2005**, 111-114.
79 R. Palin, D. R. Barn, J. K. Clark, J. E. Cottney, P. M. Cowley, M. Crockatt, L. Evans, H. Feilden, R. R. Goodwin, F. Griekspoor, S. J. A. Grove, A. K. Houghton, P. S. Jones, R. J. Morphy, A. R. C. Smith, H. Sundaram, D. Vrolijk, M. A. Weston, G. Wishart, P. Wren, *Bioorg. Med. Chem. Lett.* **2005**, *15*, 589-593.
80 R. Silvestri, M. Artico, G. La Regina, A. Di Pasquali, G. De Martino, F. D. D'Auria, L. Nencioni, A. T. Palamara, *J. Med. Chem.* **2004**, *47*, 3924-3926.
81 G. Zhao, T. Yu, R. Wang, X. Wang, Y. Jing, *Bioorg. Med. Chem.* **2005**, *13*, 4056-4062.
82 J. A. Aikins, M. Haurez, J. R. Rizzo, J.-P. Van Hoeck, W. Brione, J.-P. Kestemont, C. Stevens, X. Lemair, G. A. Stephenson, E. Marlot, M. Forst, I. N. Houpis, *J. Org. Chem.* **2005**, *70*, 4695-4705.
83 E. Queron, R. Lett, *Tetrahedron Lett.* **2004**, *45*, 4527-4531.
84 C. Satge, J. Le Bras, F. Henin, J. Muzart, *Tetrahedron* **2005**, *61*, 8405-8409.
85 I. K. Mangion, D. W. C. MacMillan, *J. Am. Chem. Soc.* **2005**, *127*, 3696-3697.
86 S. P. Romeril, V. Lee, J. E. Baldwin, *Tetrahedron Lett.* **2004**, *45*, 3273-3277.
87 L. T. Burke, D. J. Dixon, S. V. Ley, F. Rodriguez, *Org. Biomol. Chem.* **2005**, *3*, 274-280.
88 M. Prashad, Y. Lu, H.-Y. Kim, B. Hu, O. Repic, T. J. Blacklock, *Synth. Commun.* **1999**, *29*, 2937-2942.
89 M. Besson, P. Gallezot, S. Neto, C. Pinel, *Tetrahedron Asymmetry* **2000**, *11*, 1809-1818.
90 A. G. Schultz, M. Macielag, P. Sundararaman, A. G. Taveras, M. Welch, *J. Am. Chem. Soc.* **1988**, *110*, 7828-41.
91 J. Gerencser, N. Bathori, M. Czugler, P. Huszthy, M. Nogradi, *Tetrahedron Asymmetry* **2003**, *14*, 2803-2811.
92 A. V. Lobach, O. N. Leus, N. Y. Titova, N. G. Luk'yanenko, *Russ. J. Org. Chem.* **2003**, *39*, 1037-1041.
93 N. G. Luk'yanenko, A. V. Lobach, O. N. Leus, N. Y. Titova, *Russ. J. Org. Chem.* **2002**, *38*, 895-899.
94 O. Meyer, C. Grosdemange-Billiard, D. Tritsch, M. Rohmer, *Org. Biomol. Chem.* **2003**, *1*, 4367-4372.
95 D. T. Gryko, P. Piatek, P. Salanski, J. Jurczak, *Tetrahedron Asymmetry* **1998**, *9*, 1771-1778.

96 E. Garcia-Urdiales, F. Rebolledo, V. Gotor, *Tetrahedron Asymmetry* **1999**, *10*, 721-726.
97 H. Nemoto, H. Tsutsumi, S. Yuzawa, X. Peng, W. Zhong, J. Xie, N. Miyoshi, I. Suzuki, M. Shibuya, *Tetrahedron Lett.* **2004**, *45*, 1667-1670.
98 C. S. Cho, B. T. Kim, H.-J. Choi, T.-J. Kim, S. C. Shim, *Tetrahedron* **2003**, *59*, 7997-8002.
99 H.-U. Blaser, M. Diggelmann, H. Meier, F. Naud, E. Scheppach, A. Schnyder, M. Studer, *J. Org. Chem.* **2003**, *68*, 3725-3728.
100 C. S. Cho, D. K. Lim, T.-J. Kim, S. C. Shim, *J. Chem. Res., Synop.* **2002**, 550-551.
101 N. Kadi, L. Belloy, P. Chalier, J. C. Crouzet, *J. Agric. Food Chem.* **2002**, *50*, 5552-5557.
102 S. T. Hazeldine, L. Polin, J. Kushner, K. White, N. M. Bouregeois, B. Crantz, E. Palomino, T. H. Corbett, J. P. Horwitz, *J. Med. Chem.* **2002**, *45*, 3130-3137.
103 S. T. Hazeldine, L. Polin, J. Kushner, K. White, T. H. Corbett, J. Biehl, J. P. Horwitz, *Bioorg. Med. Chem.* **2005**, *13*, 1069-1081.
104 C. Cena, D. Boschi, G. C. Tron, K. Chegaev, L. Lazzarato, A. Di Stilo, M. Aragno, R. Fruttero, A. Gasco, *Bioorg. Med. Chem. Lett.* **2004**, *14*, 5971-5974.
105 M. Koufaki, T. Calogeropoulou, A. Detsi, A. Roditis, A. P. Kourounakis, P. Papazafiri, K. Tsiakitzis, C. Gaitanaki, I. Beis, P. N. Kourounakis, *J. Med. Chem.* **2001**, *44*, 4300-4303.
106 M. Tobe, Y. Isobe, Y. Goto, F. Obara, M. Tsuchiya, J. Matsui, K. Hirota, H. Hayashi, *Bioorg. Med. Chem.* **2000**, *8*, 2037-2047.
107 H. Yoda, K. Takabe, *Chem. Lett.* **1989**, 465-6.
108 S. Wang, M. M. Kayser, V. Jurkauskas, *J. Org. Chem.* **2003**, *68*, 6222-6228.
109 R. Bernini, A. Coratti, G. Fabrizi, A. Goggiamani, *Tetrahedron Lett.* **2003**, *44*, 8991-8994.
110 W. Zhang, Y. Henry, *Synlett* **2001**, 1129-1130.
111 A. Cappelli, G. Giuliani, A. Gallelli, S. Valenti, M. Anzini, L. Mennuni, F. Makovec, A. Cupello, S. Vomero, *Bioorg. Med. Chem.* **2005**, *13*, 3455-3460.
112 C. P. Butts, M. D. S. Jazdzyk, *Org. Biomol. Chem.* **2005**, *3*, 1209-1216.
113 R. Fringuelli, F. Schiaffella, M. P. Utrilla Navarro, L. Milanese, C. Santini, M. Rapucci, C. Marchetti, C. Riccardi, *Bioorg. Med. Chem.* **2003**, *11*, 3245-3254.
114 P. A. Zoretic, F. Barcelos, *Tetrahedron Lett.* **1977**, 529-32.
115 L. Zhang, S. Wang, *J. Am. Chem. Soc.* **2006**, *128*, 1442-1443.
116 K. S. Dunne, F. Bisaro, B. Odell, J.-M. Paris, V. Gouverneur, *J. Org. Chem.* **2005**, *70*, 10803-10809.
117 H. Ohno, M. Okumura, S.-I. Maeda, H. Iwasaki, R. Wakayama, T. Tanaka, *J. Org. Chem.* **2003**, *68*, 7722-7732.
118 F. C. Tucci, Y.-F. Zhu, Z. Guo, T. D. Gross, P. J. Connors, R. S. Struthers, G. J. Reinhart, J. Saunders, C. Chen, *Bioorg. Med. Chem. Lett.* **2003**, *13*, 3317-3322.
119 E. Bridgeman, J. L. Cavill, D. J. Schofield, D. S. Wilkins, N. C. O. Tomkinson, *Tetrahedron Lett.* **2005**, *46*, 8521-8524.
120 S. K. Mandal, D. R. Jensen, J. S. Pugsley, M. S. Sigman, *J. Org. Chem.* **2003**, *68*, 4600-4603.
121 R. M. Trend, B. M. Stoltz, *J. Am. Chem. Soc.* **2004**, *126*, 4482-4483.
122 H. Hamada, M. Shiromoto, M. Funahashi, T. Itoh, K. Nakamura, *J. Org. Chem.* **1996**, *61*, 2332-6.
123 O. Lavastre, J. P. Morken, *New J. Chem.* **2002**, *26*, 745-749.
124 J.-B. Sortais, V. Ritleng, A. Voelklin, A. Holuigue, H. Smail, L. Barloy, C. Sirlin, G. K. M. Verzijl, J. A. F. Boogers, A. H. M. de Vries, J. G. de Vries, M. Pfeffer, *Org. Lett.* **2005**, *7*, 1247-1250.
125 H. Koide, T. Hata, M. Uemura, *J. Org. Chem.* **2002**, *67*, 1929-1935.
126 H. Yamada, T. Kawate, A. Nishida, M. Nakagawa, *J. Org. Chem.* **1999**, *64*, 8821-8828.
127 K. Itoh, H. Yamada, A. Sera, *Bull. Chem. Soc. Jpn.* **1984**, *57*, 2140-3.
128 A. D. Malievskii, O. I. Gorbunova, *Izv. Akad. Nauk SSSR, Ser. Khim.* **1981**, 2307-9.

129 H. M. Bank, G. T. Decker, Application: US
US 94-363800
5449802, **1995**.
130 L. Liu, Y.-f. Kang, R. Wang, Y.-f. Zhou, C. Chen, M. Ni, M.-z. Gong, *Tetrahedron Asymmetry* **2004**, *15*, 3757-3761.
131 Y. Sakito, T. Mukaiyama, *Chem. Lett.* **1979**, 1027-8.
132 Y. Sakito, S. Tanaka, M. Asami, T. Mukaiyama, *Chem. Lett.* **1980**, 1223-6.
133 H. Takayanagi, Y. Kitano, Y. Morinaka, *J. Org. Chem.* **1994**, *59*, 2700-6.
134 J. Chen, S. P. Corbin, N. J. Holman, *Org. Process Res. Dev.* **2005**, *9*, 185-187.
135 G. Cremonesi, P. Dalla Croce, C. La Rosa, E. Pizzatti, *Heterocycles* **2003**, *61*, 563-567.
136 B. Moller, K. Undheim, *Tetrahedron* **1998**, *54*, 5789-5804.
137 K. Hammer, K. Undheim, *Tetrahedron* **1997**, *53*, 10603-10614.
138 S. Kotha, N. Sreenivasachary, S. Ilalder, *Bioorg. Med. Chem. Lett.* **1999**, *9*, 2565-2568.
139 J. Gilmore, W. Prowse, D. Steggles, M. Urquhart, J. Olkowski, *J. Chem. Soc., Perkin Trans. 1* **1996**, 2845-2850.
140 J.-l. Jiang, A.-H. Li, S.-Y. Jang, L. Chang, N. Melman, S. Moro, X.-d. Ji, E. B. Lobkovsky, J. C. Clardy, K. A. Jacobson, *J. Med. Chem.* **1999**, *42*, 3055-3065.
141 M. J. Ferreiro, S. K. Latypov, E. Quinoa, R. Riguera, *J. Org. Chem.* **2000**, *65*, 2658-2666.
142 A. Ammazzalorso, R. Amoroso, G. Bettoni, B. De Filippis, L. Giampietro, C. Maccallini, M. L. Tricca, *ARKIVOC (Gainesville, FL, U. S.)* **2004**, 375-381.
143 R. M. Moreno, M. Rosol, A. Moyano, *Tetrahedron Asymmetry* **2006**, *17*, 1089-1103.
144 V. Dimitrov, K. Kostova, *Lett. Org. Chem.* **2006**, *3*, 176-182.
145 Y.-H. Cho, A. Fayol, M. Lautens, *Tetrahedron Asymmetry* **2006**, *17*, 416-427.
146 R. Tokuda, H. Matsunaga, T. Ishizuka, M. Nakajima, T. Kunieda, *Heterocycles* **2005**, *66*, 135-141.
147 T. Hayashi, *Shokubai* **2005**, *47*, 533-538.
148 M. Sedlak, P. Drabina, I. Cisarova, A. Ruzicka, J. Hanusek, V. Machacek, *Tetrahedron Lett.* **2004**, *45*, 7723-7726.
149 V. V. Nesterov, O. I. Kolodiazhnyi, *Tetrahedron Asymmetry* **2006**, *17*, 1023-1026.
150 D. Enders, L. Tedeschi, D. Foerster, *Synthesis* **2006**, 1447-1460.
151 Y.-T. Wu, T. Hayama, K. K. Baldridge, A. Linden, J. S. Siegel, *J. Am. Chem. Soc.* **2006**, *128*, 6870-6884.
152 N. Mateus, L. Routaboul, J.-C. Daran, E. Manoury, *J. Organomet. Chem.* **2006**, *691*, 2297-2310.
153 Y. Ichikawa, Y. Matsukawa, M. Isobe, *J. Am. Chem. Soc.* **2006**, *128*, 3934-3938.
154 M. Penhoat, P. Bohn, G. Dupas, C. Papamicael, F. Marsais, V. Levacher, *Tetrahedron Asymmetry* **2006**, *17*, 281-286.
155 I. Larrosa, P. Romea, F. Urpi, *Org. Lett.* **2006**, *8*, 527-530.
156 Z.-Y. Du, R.-T. Xiao, *Yingyong Huaxue* **2005**, *22*, 1372-1374.
157 H. Shi, *Synth. Commun.* **2006**, *36*, 237-248.
158 A. Matagne, J. Lamotte-Brasseur, J.-M. Frere, *Biochem. J.* **1998**, *330*, 581-598.
159 J. Lamotte, G. Dive, J. M. Ghuysen, *Eur. J. Med. Chem.* **1991**, *26*, 43-50.
160 A. Peter, A. Arki, E. Forro, F. Fueloep, D. W. Armstrong, *Chirality* **2005**, *17*, 193-200.
161 C. Palomo, J. M. Aizpurua, I. Ganboa, M. Oiarbide, *Synlett* **2001**, 1813-1826.
162 H. H. Wasserman, H. Matsuyama, R. P. Robinson, *Tetrahedron* **2002**, *58*, 7177-7190.
163 S. M. Allin, J. S. Khera, J. Witherington, M. R. J. Elsegood, *Tetrahedron Lett.* **2006**, *47*, 5737-5739.
164 C. Palomo, I. Ganboa, M. Oiarbide, G. T. Sciano, J. I. Miranda, *ARKIVOC (Gainesville, FL, U. S.)* **2002**, 8-16.
165 A. Basak, S. C. Ghosh, A. K. Das, V. Bertolasi, *Org. Biomol. Chem.* **2005**, *3*, 4050-4052.

166 B. Alcaide, P. Almendros, J. M. Alonso, M. F. Aly, C. Pardo, E. Saez, M. R. Torres, *J. Org. Chem.* **2002**, *67*, 7004-7013.
167 K. Huang, Z. S. Breitbach, D. W. Armstrong, *Tetrahedron Asymmetry* **2006**, *17*, 2821-2832.
168 W. H. Pirkle, A. Tsipouras, M. H. Hyun, D. J. Hart, C. S. Lee, *J. Chromatogr.* **1986**, *358*, 377-84.
169 T. Huang, C. Kuang, J. Zhou, D. Gou, *Fenxi Huaxue* **1991**, *19*, 687-9.
170 R. Berkecz, R. Torok, I. Ilisz, E. Forro, F. Fulop, D. W. Armstrong, A. Peter, *Chromatographia* **2006**, *63*, S37-S43.
171 R. Berkecz, I. Ilisz, E. Forro, F. Fulop, D. W. Armstrong, A. Peter, *Chromatographia* **2006**, *63*, S29-S35.
172 I. Ilisz, R. Berkecz, A. Peter, *J. Sep. Sci.* **2006**, *29*, 1305-1321.
173 Y. Okamoto, T. Senoh, H. Nakane, K. Hatada, *Chirality* **1989**, *1*, 216-22.
174 Y. Okamoto, Y. Kaida, *J. Chromatogr., A* **1994**, *666*, 403-19.
175 P. Sun, c. Wang, D. W. Armstrong, A. Peter, E. Forro, *J. Liq. Chromatogr. Relat. Technol.* **2006**, *29*, 1847-1860.
176 C. Jiang, D. W. Armstrong, A. Peter, F. Fulop, *J. Liq. Chromatogr. Relat. Technol.* **2007**, *30*, 1709-1721.
177 E. Forro, F. Fueloep, *Org. Lett.* **2003**, *5*, 1209-1212.
178 E. Forro, F. Fulop, *Tetrahedron Asymmetry* **2004**, *15*, 573-575.
179 E. Forro, F. Fulop, *Tetrahedron Asymmetry* **2004**, *15*, 2875-2880.
180 E. Forro, F. Fulop, *Chem.--Eur. J.* **2006**, *12*, 2587-2592.
181 E. Forro, T. Paal, G. Tasnadi, F. Fulop, *Adv. Synth. Catal.* **2006**, *348*, 917-923.
182 A. L. Berthod, W.; Armstrong, D. W., *Analytical Chemistry* **1992**, *64*, 873-879.
183 W. Y. Li, H. L. Jin, D. W. Armstrong, *J. Chromatogr.* **1990**, *509*, 303-24.
184 G. Eglinton, M. T. J. Murphy, Editors, *Organic Geochemistry; Methods and Results*. Editor, **1969**, pp. 828 pp.
185 J. R. Maxwell, R. E. Cox, R. G. Ackman, S. N. Hooper, *Advan. Org. Geochem., Proc. Int. Meet., 5th* **1972**, 277-91.
186 R. L. Patience, S. J. Rowland, J. R. Maxwell, *Geochim. Cosmochim. Acta* **1978**, *42*, 1871-5.
187 A. S. Mackenzie, R. L. Patience, J. R. Maxwell, M. Vandenbroucke, B. Durand, *Geochim. Cosmochim. Acta* **1980**, *44*, 1709-21.
188 B. Chappe, W. Michaelis, P. Albrecht, G. Ourisson, *Naturwissenschaften* **1979**, *66*, 522-3.
189 D. M. Ward, S. C. Brassell, G. Eglinton, *Nature (London)* **1986**, *318*, 656-9.
190 M. Stefanova, *Fuel* **2000**, *79*, 755-758.
191 R. E. Summons, L. L. Jahnke, Z. Roksandic, *Geochim. Cosmochim. Acta* **1994**, *58*, 2853-63.
192 P. F. Greenwood, R. E. Summons, *Org. Geochem.* **2003**, *34*, 1211-1222.
193 H. L. Ten Haven, J. W. De Leeuw, J. Rullkoetter, J. S. Sinninghe Damste, *Nature (London)* **1987**, *330*, 641-3.
194 V. Thiel, J. Peckmann, R. Seifert, P. Wehrung, J. Reitner, W. Michaelis, *Geochim. Cosmochim. Acta* **1999**, *63*, 3959-3966.
195 R. D. Pancost, J. S. Sinninghe Damste, S. De Lint, M. J. E. C. Van der Maarel, J. C. Gottschal, *Appl. Environ. Microbiol.* **2000**, *66*, 1126-1132.
196 M. Elvert, E. Suess, M. J. Whiticar, *Naturwissenschaften* **1999**, *86*, 295-300.
197 M. Elvert, E. Suess, J. Greinert, M. J. Whiticar, *Org. Geochem.* **2000**, *31*, 1175-1187.
198 S. C. Brassell, A. M. K. Wardroper, I. D. Thomson, J. R. Maxwell, G. Eglinton, *Nature (London)* **1981**, *290*, 693-6.
199 J. B. Risatti, S. J. Rowland, D. A. Yon, J. R. Maxwell, *Org. Geochem.* **1984**, *6*, 93-104.

200 Y. Koga, M. Nishihara, H. Morii, M. Akagawa-Matsushita, *Microbiol. Rev.* **1993**, *57*, 164-82.
201 K.-U. Hinrichs, J. M. Hayes, S. P. Sylva, P. G. Brewer, E. F. DeLong, *Nature (London)* **1999**, *398*, 802-805.
202 K.-U. Hinrichs, R. E. Summons, V. Orphan, S. P. Sylva, J. M. Hayes, *Org. Geochem.* **2000**, *31*, 1685-1701.
203 C. J. Barber, K. Grice, T. P. Bastow, R. Alexander, R. I. Kagi, *Org. Geochem.* **2001**, *32*, 943-947.
204 J. N. Robson, S. J. Rowland, *Org. Geochem.* **1993**, *20*, 1093-8.
205 C. J. Barber, T. P. Bastow, K. Grice, R. Alexander, R. I. Kagi, *Org. Geochem.* **2001**, *32*, 765-769.
206 D. W. Armstrong, Y. Tang, J. Zukowski, *Anal. Chem.* **1991**, *63*, 2858-61.
207 A. Berthod, X. Wang, K. H. Gahm, D. W. Armstrong, *Geochim. Cosmochim. Acta* **1998**, *62*, 1619-1630.
208 D. W. Armstrong, J. Zukowski, *J. Chromatogr., A* **1994**, *666*, 445-48.
209 D. W. Armstrong, E. Y. Zhou, J. Zukowski, B. Kosmowska-Ceranowicz, *Chirality* **1996**, *8*, 39-48.
210 K.-H. Gahm, L. W. Chang, D. W. Armstrong, *J. Chromatogr., A* **1997**, *759*, 149-155.
211 S. W. Gabriel, J, *Ber.* **1988**, *21*, 2669-2679.
212 P. Walden, *Bull. Acad. Imp. Sci. St.-Petersbourg* **1914**, 405-22.
213 J. S. Wilkes, J. A. Levisky, R. A. Wilson, C. L. Hussey, *Inorg. Chem.* **1982**, *21*, 1263-4.
214 J. S. Wilkes, M. J. Zaworotko, *J. Chem. Soc., Chem. Commun.* **1992**, 965-7.
215 T. Welton, *Chem. Rev. (Washington, D. C.)* **1999**, *99*, 2071-2083.
216 J. Ding, V. Desikan, X. Han, T. L. Xiao, R. Ding, W. S. Jenks, D. W. Armstrong, *Org. Lett.* **2005**, *7*, 335-337.
217 K. R. Seddon, *J. Chem. Technol. Biotechnol.* **1997**, *68*, 351-356.
218 A. C. Cole, J. L. Jensen, I. Ntai, K. L. T. Tran, K. J. Weaver, D. C. Forbes, J. H. Davis, Jr., *J. Am. Chem. Soc.* **2002**, *124*, 5962-5963.
219 S. T. Handy, M. Okello, *J. Org. Chem.* **2005**, *70*, 2874-2877.
220 A. R. Khosropour, M. M. Khodaei, M. Beygzadeh, M. Jokar, *Heterocycles* **2005**, *65*, 767-773.
221 X. Han, D. W. Armstrong, *Org. Lett.* **2005**, *7*, 4205-4208.
222 R. A. Sheldon, R. M. Lau, M. J. Sorgedrager, F. van Rantwijk, K. R. Seddon, *Green Chem.* **2002**, *4*, 147-151.
223 C. W. Scheeren, G. Machado, J. Dupont, P. F. P. Fichtner, S. R. Texeira, *Inorg. Chem.* **2003**, *42*, 4738-4742.
224 P. J. Dyson, *Appl. Organomet. Chem.* **2002**, *16*, 495-500.
225 S. Carda-Broch, A. Berthod, D. W. Armstrong, *Anal. Bioanal. Chem.* **2003**, *375*, 191-199.
226 S. Chun, S. V. Dzyuba, R. A. Bartsch, *Anal. Chem.* **2001**, *73*, 3737-3741.
227 C. Li, B. Xin, W. Xu, Q. Zhang, *J. Chem. Technol. Biotechnol.* **2007**, *82*, 196-204.
228 R. Germani, M. V. Mancini, G. Savelli, N. Spreti, *Tetrahedron Lett.* **2007**, *48*, 1767-1769.
229 E. V. Dickinson, M. E. Williams, S. M. Hendrickson, H. Masui, R. W. Murray, *J. Am. Chem. Soc.* **1999**, *121*, 613-616.
230 C. Lagrost, D. Carrie, M. Vaultier, P. Hapiot, *J. Phys. Chem. A* **2003**, *107*, 745-752.
231 M. Ue, M. Takeda, *J. Korean Electrochem. Soc.* **2002**, *5*, 192-196.
232 C. Y. Wang, V. Mottaghitalab, C. O. Too, G. M. Spinks, G. G. Wallace, *J. Power Sources* **2007**, *163*, 1105-1109.
233 K. P. Doyle, C. M. Lang, K. Kim, P. A. Kohl, *J. Electrochem. Soc.* **2006**, *153*, A1353-A1357.
234 Y. Xia, H. Wu, Y. Zhang, Y. Fang, S. Sun, Y. Shi, *Huaxue Jinzhan* **2006**, *18*, 1660-1667.

235 P. U. Naik, S. J. Nara, J. R. Harjani, M. M. Salunkhe, *J. Mol. Catal. B Enzym.* **2007**, *44*, 93-98.
236 V. Rumbau, R. Marcilla, E. Ochoteco, J. A. Pomposo, D. Mecerreyes, *Macromolecules* **2006**, *39*, 8547-8549.
237 M. Paljevac, M. Habulin, Z. Knez, *Chem. Ind. Chem. Eng. Q.* **2006**, *12*, 181-186.
238 D. W. Armstrong, L.-K. Zhang, L. He, M. L. Gross, *Anal. Chem.* **2001**, *73*, 3679-3686.
239 S. Carda-Broch, A. Berthod, D. W. Armstrong, *Rapid Commun. Mass Spectrom.* **2003**, *17*, 553-560.
240 T. N. Laremore, F. Zhang, R. J. Linhardt, *Anal. Chem.* **2007**, *79*, 1604-1610.
241 A. Tholey, E. Heinzle, *Anal. Bioanal. Chem.* **2006**, *386*, 24-37.
242 L. M. Yuan, Y. Han, Y. Zhou, X. Meng, Z. Y. Li, M. Zi, Y. X. Chang, *Anal. Lett.* **2006**, *39*, 1439-1449.
243 C. D. Tran, D. Oliveira, S. Yu, *Anal. Chem.* **2006**, *78*, 1349-1356.
244 A.-E. Jimenez, M.-D. Bermudez, *Tribol. Lett.* **2007**, *26*, 53-60.
245 Y. Xia, S. Sasaki, T. Murakami, M. Nakano, L. Shi, H. Wang, *Wear* **2007**, *262*, 765-771.
246 J. L. Anderson, D. W. Armstrong, *Anal. Chem.* **2003**, *75*, 4851-4858.
247 J. L. Anderson, R. Ding, A. Ellern, D. W. Armstrong, *J. Am. Chem. Soc.* **2005**, *127*, 593-604.
248 I. A. Sumartschenkowa, S. P. Verevkin, T. V. Vasiltsova, E. Bich, A. Heintz, M. P. Shevelyova, G. J. Kabo, *J. Chem. Eng. Data* **2006**, *51*, 2138-2144.
249 A. Heintz, S. P. Verevkin, D. Ondo, *J. Chem. Eng. Data* **2006**, *51*, 434-437.
250 A. Heintz, S. P. Verevkin, *J. Chem. Eng. Data* **2005**, *50*, 1515-1519.
251 D. W. Armstrong, L. He, Y.-S. Liu, *Anal. Chem.* **1999**, *71*, 3873-3876.
252 A. Berthod, L. He, D. W. Armstrong, *Chromatographia* **2001**, *53*, 63-68.
253 J. L. Anderson, J. Ding, T. Welton, D. W. Armstrong, *J. Am. Chem. Soc.* **2002**, *124*, 14247-14254.
254 J. L. Anderson, D. W. Armstrong, *Anal. Chem.* **2005**, *77*, 6453-6462.
255 A. J. Carmichael, K. R. Seddon, *J. Phys. Org. Chem.* **2000**, *13*, 591-595.
256 H. Lu, S. C. Rutan, *Anal. Chem.* **1996**, *68*, 1387-93.
257 M. Petsch, B. X. Mayer-Helm, V. Soellner, *Anal. Bioanal. Chem.* **2005**, *383*, 322-326.
258 A. Berthod, E. Y. Zhou, K. Le, D. W. Armstrong, *Anal. Chem.* **1995**, *67*, 849-57.
259 M. Vitha, P. W. Carr, *J. Chromatogr., A* **2006**, *1126*, 143-194.
260 M. H. Abraham, G. S. Whiting, J. Andonian-Haftvan, J. W. Steed, J. W. Grate, *J. Chromatogr.* **1991**, *588*, 361-4.
261 M. J. Kamlet, P. W. Carr, R. W. Taft, M. H. Abraham, *J. Am. Chem. Soc.* **1981**, *103*, 6062-6.
262 M. H. Abraham, *Chem. Soc. Rev.* **1993**, *22*, 73-83.
263 S. K. Poole, C. F. Poole, *J. Chromatogr., A* **1995**, *697*, 415-27.
264 J. Maria Santiuste, *Anal. Chim. Acta* **1998**, *377*, 71-83.
265 J.-M. Xu, Q. Wu, Q.-Y. Zhang, F. Zhang, X.-F. Lin, *Eur. J. Org. Chem.* **2007**, 1798-1802.
266 J. Durand, E. Teuma, M. Gomez, *C. R. Chim.* **2007**, *10*, 152-177.
267 J. C. Lee, H. J. Park, *Synth. Commun.* **2007**, *37*, 87-90.
268 V. Calo, A. Nacci, A. Monopoli, A. Damascelli, E. Ieva, N. Cioffi, *J. Organomet. Chem.* **2007**, *692*, 4397-4401.
269 S. A. Shamsi, N. D. Danielson, *J. Sep. Sci.* **2007**, *30*, 1729-1750.
270 S. M. Mwongela, N. Siminialayi, K. A. Fletcher, I. M. Warner, *J. Sep. Sci.* **2007**, *30*, 1334-1342.
271 Y. Francois, A. Varenne, E. Juillerat, D. Villemin, P. Gareil, *J. Chromatogr., A* **2007**, *1155*, 134-141.
272 M. Mank, B. Stahl, G. Boehm, *Anal. Chem.* **2004**, *76*, 2938-2950.
273 A. Berthod, *Chirality* **2009**, *21*, 167-175.

274 G. Inoue, Y. Iwai, M. Yasutake, K. Honda, Y. Arai, *Fluid Phase Equilib.* **2007**, *251*, 17-23.
275 M. Qi, W. Armstrong Daniel, *Anal Bioanal Chem* **2007**, *388*, 889-99.
276 K. Huang, X. Han, X. Zhang, W. Armstrong Daniel, *Anal Bioanal Chem* **2007**, *389*, 2265-75.
277 K. Huang, D. W. Armstrong, *Org. Geochem.* **2009**, *40*, 283-286.
278 D. W. Armstrong, W. DeMond, *J. Chromatogr. Sci.* **1984**, *22*, 411-15.
279 S. R. Gratz, A. M. Stalcup, *Anal. Chem.* **1998**, *70*, 5166-5171.
280 Y. Bao, D. Yue, N. Della Ca, R. C. Larock, D. W. Armstrong, *J. Liq. Chromatogr. Relat. Technol.* **2008**, *31*, 2035-2052.
281 A. Dietrich, B. Maas, A. Mosandl, *J. High Resolut. Chromatogr.* **1995**, *18*, 152-6.
282 P. Jing, R. N. Fu, R. J. Dai, J. L. Ge, J. L. Gu, Z. Huang, Y. Chen, *Chromatographia* **1996**, *43*, 546-550.
283 T. Payagala, Y. Zhang, E. Wanigasekara, K. Huang, Z. S. Breitbach, P. S. Sharma, L. M. Sidisky, D. W. Armstrong, *Anal. Chem. (Washington, DC, U. S.)* **2009**, *81*, 160-173.
284 Z. S. Breitbach, D. W. Armstrong, *Anal. Bioanal. Chem.* **2008**, *390*, 1605-1617.
285 C. D. Tran, S. H. De Paoli Lacerda, *Anal. Chem.* **2002**, *74*, 5337-5341.
286 Y. He, Q. Chen, C. Xu, J. Zhang, X. Shen, *J Phys Chem B* **2009**, *113*, 231-8.
287 D. W. Armstrong, L. W. Chang, S. S. C. Chang, *J. Chromatogr., A* **1998**, *793*, 115-134.
288 H. Cai, T. V. Nguyen, G. Vigh, *Anal. Chem.* **1998**, *70*, 580-589.
289 T.-T. Ong, W. Tang, W. Muderawan, S.-C. Ng, H. S. O. Chan, *Electrophoresis* **2005**, *26*, 3839-3848.
290 W. Tang, S.-C. Ng, *Nat. Protoc.* **2007**, *2*, 3195-3200.
291 I. Ciucanu, F. Kerek, *Carbohydr. Res.* **1984**, *131*, 209-17.
292 J.-f. Liu, J. A. Jonsson, G.-b. Jiang, *TrAC, Trends Anal. Chem.* **2005**, *24*, 20-27.
293 D. W. Armstrong, K. Rundlett, G. L. Reid, *Analytical Chemistry* **1994**, *66*, 1690-1695 10.1021/ac00082a015.
294 K. L. Rundlett, D. W. Armstrong, *Analytical Chemistry* **1995**, *67*, 2088-2095 10.1021/ac00109a030.
295 A. L. Berthod, Y.; Bagwill, C.; Armstrong, D. W., *J. Chromatogr. A* **1996**, *731*, 123-137.
296 I. G. D'acquarica, F.; Misiti, D.; Vlillani, D.; Carootti, A.; Cellamare, S.; Muck, S., *J. Chromatogr. A* **1999**, *857*, 145-155.
297 G. D. a. Cancelliere, I.; Gasparrini, F.; Misiti, D.; Villani, C., *Pharm. Sci. Technol. Today* **1999**, *2*, 484-492.
298 D. W. Armstrong, M. P. Gasper, K. L. Rundlett, *J. Chromatogr., A* **1995**, *689*, 285-304.
299 REILLY, #160, J., RISLEY, D. S., *The separation of enantiomers by countercurrent capillary electrophoresis using the macrocyclic antibiotic A82846B*. Editor, Aster, Riverton, NJ, ETATS-UNIS, **1998**, Vol. 16, pp. 5.
300 V. S. Sharp, D. S. Risley, S. McCarthy, B. E. Huff, M. A. Strege, *Journal of Liquid Chromatography & Related Technologies* **1997**, *20*, 887 - 898.
301 K. H. Ekborg-Ott, J. P. Kullman, X. Wang, K. Gahm, L. He, D. W. Armstrong, *Chirality* **1998**, *10*, 627-660.
302 A. Berthod, T. Yu, J. P. Kullman, D. W. Armstrong, F. Gasparrini, I. D'Acquarica, D. Misiti, A. Carotti, *J. Chromatogr., A* **2000**, *897*, 113-129.
303 A. Berthod, X. Chen, J. P. Kullman, D. W. Armstrong, F. Gasparrini, I. D'Acquaric, C. Villani, A. Carotti, *Analytical Chemistry* **2000**, *72*, 1767-1780 10.1021/ac991004t.
304 D. R. Guay, *Expert Review of Anti-infective Therapy* **2004**, *2*, 845-852 doi:10.1586/14789072.2.6.845.
305 V. R. K. Anderson, G. M., *Drugs* **2008**, *68*, 639-648.
306 A. C. Berthod, C. D.; Armstrong, D. W., *Talanta* **1993**, *40*, 1367-1373.
307 P. Franco, M. Lammerhofer, P. M. Klaus, W. Lindner, *J Chromatogr A* **2000**, *869*, 111-27.

308 M. H. Hyun, D. H. Kim, *Chirality* **2004**, *16*, 294-301.
309 Q. Zhong, L. He, T. Beesley, W. Trahanovsky, P. Sun, C. Wang, D. Armstrong, *Chromatographia* **2006**, *64*, 147-155.
310 L. Thunberg, S. Allenmark, A. Friberg, F. Ek, T. Frejd, *Chirality* **2004**, *16*, 614-624.

BIOGRAPHICAL INFORMATION

Ke Huang obtained her Bachelor of Science from Sichuan University in 2004. She joined Dr.Daniel W. Armstrong's group and received her Doctor of Philosophy from the University of Texas at Arlington in May 2010. Her research focused on development of new chiral and non-chiral stationary phases for gas chromatography.